Population Pharmacokinetic Analysis for the Therapeutic anti-EGFR Humanised Monoclonal Antibody Matuzumab

Dissertation

zur Erlangung des akademischen Grades
doctor rerum naturalium (Dr.rer.nat.)

Vorgelegt der
Naturwissenschaftlichen Fakultät I
Biowissenschaften

der Martin-Luther-Universität Halle-Wittenberg

von

Frau Katharina Küster
geb. am 16.01.1979 in Bremen

Für meine Familie.

Abstract

This thesis aims to contribute to a comprehensive characterisation of the pharmacokinetics (PK) of the novel humanised monoclonal antibody (mAb) matuzumab, targeting the epidermal growth factor receptor, and to a general understanding of mAbs. Concentration-time profiles from 3 clinical studies including 90 study patients (IDs) were analysed simultaneously using the population modelling software NONMEM^{TM}. The data was best described by a final 2-compartment PK model, including the parameters central and peripheral volume of distribution, inter-compartmental clearance, linear clearance (CLL), an additional non-linear elimination pathway and the covariate relation fat-free mass (FFM) on CLL. Three types of variability were identified in the model: interindividual on 4 parameters, interoccasion (IOV) on CLL and residual variability. The model was evaluated by various evaluation techniques for its precision, robustness and predictivity. External evaluation with a second dataset including 81 IDs from 3 additional studies refined the model, as an earlier incorporated covariate relation was not supported and was for this purpose omitted. For internal evaluation the bootstrap (BS) method, case deletion diagnostics (CDD, deletion of either 10% or of 1 ID and reestimation of the parameters with the reduced datasets) and visual predictive checks (VPC) were performed. Calculated BS medians of the parameter estimates from 200 BS runs were similar to the original values; relative bias ranged from -1.2% to +4.3%. CDD showed an influence of one ID on the IOV. Closer examination revealed that the influence was due to one observation from this ID (omitting this observation led to a reduction of 19% in IOV). The 90% prediction interval of 1000 simulated concentration-time profiles by VPCs included most of the observed concentrations. The calculated medians and variances were in accordance with the original data. Simulations were perfomed to analyse the impact of different dosing regimens and of the covariate relation on the concentration-time profiles. The variability in simulated steady-state concentrations could be reduced by a developed and proposed adapted dosing regimen. The analysis of different body size descriptors (body weight, body surface area and FFM) suggested that FFM should be used in covariate relations in population PK models for mAbs. These results were confirmed in a covariate analysis of another mAb (sibrotuzumab). In future, the developed population PK model for matuzumab combined with pharmacodynamic data could serve as a tool to guide selection of optimal dose regimens for matuzumab, a highly promising 'targeted' cancer therapy.

Zusammenfassung

Ziel dieser Arbeit war, die Pharmakokinetik (PK) des humanisierten, monoklonalen, gegen den epidermalen Wachstumsfaktor gerichteten Antikörpers (AK) Matuzumab, umfassend zu charakterisieren. Die Konzentrations-Zeitverläufe von 90 Patienten (IDs) aus 3 klinischen Studien wurden mit der Populations-Pharmakokinetik-Software NONMEM^{TM} simultan ausgewertet und am besten durch das finale 2-Kompartiment Modell mit den Parametern zentrales und peripheres Verteilungsvolumen, inter-kompartimenteller und linearer (CLL) Clearance, eines zusätzlichen nicht-linearen Eliminationsweges und einer Covariatenbeziehung zwischen Fett-freiem Gewicht (FFM) und CLL beschrieben. Das Modell beinhaltete drei Arten von Variabilität: die interindividuelle (auf 4 Parametern), die interoccasion (IOV) und die Residual-Variabilität. Das Modell wurde durch verschiedene Evaluationstechniken auf Präzision, Robustheit und Vorhersagekraft untersucht. Die externe Evaluation mit einem zweiten Datensatz (81 IDs von 3 weiteren Studien) verbesserte das Modell, nachdem eine zuvor eingeschlossene Covariate nicht unterstützt und damit ausgeschlossen wurde. Interne Evaluation waren die Bootstrap (BS)-Methode, Case-Deletion-Diagnostics (CDD, Entfernung von entweder 10% oder eines einzelnen IDs und erneute Parameterabschätzung mit den reduzierten Datensätzen) und Visual-Predictive-Checks (VPC). Berechnete BS-Mediane von 200 BS-Untersuchungen waren den Originalwerten ähnlich: relative Fehler lagen zwischen -1.2% und +4.3%. Das 90%-Vorhersageintervall von 1000 durch VPC simulierten Konzentrations-Zeitverläufen beinhaltete größtenteils die gemessenen Konzentrationen und die zentrale Tendenz spiegelte die Originaldaten wider. CDD ermittelte 1 ID, bzw. präziser 1 Konzentration, mit einem Einfluss auf die IOV (ohne diese war die IOV um 19% vermindert). Für die Analyse des Einflusses von verschiedenen Dosierungen und der Covariaten wurden Simulationen durchgeführt. Durch eine angepasste Dosierung wurde die Variabilität in Steady-State-Konzentrationen vermindert. Die Analyse von Körpermaßen (Gewicht, Oberfläche, FFM) ermittelte FFM als bestes Maß in Covariatenbeziehungen für monoklonale AKs. Um die Ergebnisse zu bestätigen, wurde eine weitere Covariatenanalyse für ein entwickeltes Modell für den monoklonalen AK Sibrotuzumab durchgeführt. Das entwickelte PK Modell, kombiniert mit Pharmako-dynamik-Daten, könnte zukünftig bei der Ermittlung der optimalen Dosierung für diese vielversprechende zielgerichtete Tumortherapie mit Matuzumab helfen.

Original papers discussed in this thesis

This thesis is based on the following papers:

I   Population pharmacokinetic data analysis of three phase I studies of matuzumab, a humanised anti-EGFR monoclonal antibody in clinical cancer development.
Katharina **Kuester**, Andreas Kovar, Christian Lüpfert, Brigitte Brockhaus, Charlotte Kloft
Br J Cancer, 98: 900-906 (2008)

II   Refinement of the population pharmacokinetic model for the monoclonal antibody matuzumab: external model evaluation and simulations.
Katharina **Kuester**, Andreas Kovar, Christian Lüpfert, Brigitte Brockhaus, Charlotte Kloft
Clin Pharmacokinet., accepted 2008.

III   Nonlinear pharmacokinetics of therapeutic proteins resulting from receptor mediated endocytosis.
Ben-Fillippo Krippendorff, Katharina **Kuester**, Charlotte Kloft, Wilhelm Huisinga
J Pharmacokinet Pharmacodyn., submitted 2008.

IV   Population pharmacokinetic evaluation techniques for a therapeutic monoclonal antibody in cancer therapy.
Katharina **Kuester**, Andreas Kovar, Christian Lüpfert, Brigitte Brockhaus, Charlotte Kloft
In manuscript.

V   Body size descriptors in population pharmacokinetic analyses for monoclonal antibodies.
Katharina **Kuester** and Charlotte Kloft
In preparation.

TABLE OF CONTENTS

Abbreviations

AGE	age of study patient at the day of inclusion into the study (years)
AIC	Akaike information criterion
ALT	alanine aminotransferase (U/L)
AMT	amount of drug administered (mg)
AP	alkaline phosphatase (U/L)
APC	antigen-presenting cell
AST	aspartete aminotransferase (U/L)
BIL	bilirubin (µmol/L)
BMI	body mass index (kg/m²)
BS	bootstrap
BSA	body surface area (m²)
BOV	between occasion variability, same as IOV
CDD	case deletion diagnostics
CDR	complementarity determing regions (antibody structure)
C_H	constant part of H-chain (antibody structure)
C_L	constant part of L-chain (antibody structure)
CLL	linear clearance (mL/h)
CLCR	creatinine clearance (mL/min)
CLNL	non-linear clerance
CLTD	decimal 24 h clock time during study
CLTI	24 h clock time during study
CMT	number of compartment in model
COME	concomitant chemotherapy
COV	covariate
CREA	creatinine (µmol/L)
$C_{ss, min}$	minimum steady-state concentration
$C_{ss, max}$	maximum steady-state concentration
CV	coefficient of variation in percent
DATE	date
df	degree of freedom

DD	development dataset
DGR	dose group
DOSE	dose (mg)
DV	dependent variable
ED	evaluation dataset
EGFR, HER1, c-Erb-1	epidermal growth factor receptor
ELISA	enzyme-linked immunosorbent essay
EMEA	European Medicines Agency
EVID	event identification
Fab	antigen binding fragment (antibody structure)
Fc	crystallisable fragment (antibody structure)
Fc-Rn	Fc receptor of neonates
FDA	Food and Drug Administration
FFM	fat-free mass (kg)
FLAG	identifier for different records
FLAM	flag for analytical record
FM	fat mass (kg)
FO	first-order
FOCE	first-order conditional estimation
Fv	variable part of Fab (antibody structure)
GAM	generalised additive modelling
GGT	gamma-glutamyl transpeptidase (U/L)
HACA	human anti-chimeric antibody
HAHA	human anti-human antibody
HAMA	human anti-murine antibody
HAxA	anti-idiotype antibodies against therapeutic monoclonal antibodies
H-chain	heavy chain (antibody structure)
HT	body height (cm)
i.v.	intravenous
ID	individual subject, study patient
IgG, IgA, IgD, IgM, IgE	immunoglobulin G, immunoglobulin A, immunoglobulin D, immunoglobulin M, immunoglobulin E
IIV	interindividual variability

IND	indicator variable
IOV	interoccasion variability, same as BOV
KARN	Karnofsky performance index (%)
Km	Michaelis Menten constant (mg/L)
LBW	lean body weight (kg)
L-chain	light chain (antibody structure)
LDH	lactate dehydrogenase (U/L)
mAb	monoclonal antibody
NLME	non-linear mixed effect(s)
NONMEM^{TM}	non-linear mixed effects modelling software program
OCC	number of occasion
O_{els}	extended least squares objective function
OFV	objective function value
OID	original study subject number
PBPK	physiologically based pharmacokinetic(s)
P	percentile
PD	pharmacodynamic(s)
PK	pharmacokinetic(s)
PPC	posterior predictive check
PROD	production procedure
Q	inter-compartmental clearance (L/h)
R_0	infusion rate
RACE	ethnic origin of study subject
RATE	dosing input. i.e. amount/infusion duration normalised to 1 h
REC	record
RSE	relative standard error in percent
s^2	variance
SD	standard deviation
SEX	sex of study subject
SID	study site
SIM-ID	simulated study patient
-SS-	disulfide bridge
STDY	study number
T	infusion duration

$t_{1/2}$	half-life (days)
TALD	time elapsed from start of most recent administration
TIME	time elapsed from start of first administration
TIM1	time elapsed from start of first study event
TIPL	time planned from start of first administration
TGF-α	transforming growth factor-alpha
V	total volume of distribution (L)
V_H	variable part of H-chain (antibody structure)
VISI	number of study visit
V_L	variable part of L-chain (antibody structure)
V_{max}	maximum elimination rate (mg/h)
VPC	visual predictive check
WBC	white blood cell count
WT	body weight (kg)
$\tilde{x}$	median
$\bar{x}$	arithmetic mean
ε	random deviation between the individual prediction and the observed measurement ('random effects')
η	difference between the individual parameter and the population parameter estimate ('random effects')
θ	typical value of a population parameter ('fixed effects')
κ	difference between individual parameters of different study occasions ('random effects')
ξ	any additional model parameter
π^2	variance of κ
σ^2	variance of ε
υ	variance function
ϕ	vector of model parameters
ω	standard deviation of η
ω^2	variance of η

1   Introduction

1.1   Current perspectives on cancer disease and tumour therapy

Currently, cancer diseases caused about 13% of all deaths worldwide in 2007 and, according to the American Cancer Society, 6.7 million people died from cancer in the world in 2002 and this number is expected to rise up to 10.2 million in 2020 [1, 2]. In Germany, cancer incidence data is collected by population-based cancer registries. The Federal Cancer Surveillance Unit at the Robert Koch Institute (RKI) estimates the total number of new cancer cases per year on the basis of the data from the cancer registries. The Robert Koch Institute's current estimate indicated a total of 436,500 new cases of cancer in Germany in 2004 [3]. Cancer mortality data is based on death certificates submitted by law to the Federal Statistical Office of Germany. In 2003, one in four deaths in Germany (21.5 % of deaths among women and 27.9 % of deaths among men) was due to cancer [4]. Better prevention, early detection and advances in treatment have especially supported developed nations to decrease incidences and mortality rates. But in most parts of the world and for an older growing population cancer is an increasing problem [2]. Due to continuous cancer research, patients can nowadays be offered highly effective antineoplastic therapies. With new therapy options more cancer entities become curable. However, this is also accompanied by a change in patient needs such as an increasing information need about diagnosis, future conditions or needs for psychological support and economic aid [5].

In the haematological and oncological clinical practice tumour therapy is still often based on surgery, therapeutic radiology and chemotherapy. Large attempts to discover new and more effective therapy options have been made. A significant impact in the treatment of some types of cancer is the so-called 'targeted' therapy, which became available in the late 1980s. The general principle is to use agents, which are specific for deregulated cell properties, e.g. proteins, of cancer cells. Tyrosine kinase inhibitors such as imatinib or gefitinib are examples for small molecule targeted therapy drugs, which are, in general, inhibitors of enzymatic domains on mutated, overexpressed or

otherwise critical proteins within cancer cells [6-8]. Another strategy is the therapy with monoclonal antibodies (mAbs). The first report of the treatment of a tumour patient with a monoclonal antibody was published in 1980 [9]. An antibody (therapeutic agent or therapeutic carrier) specifically binds to a target, e.g. a protein on the surface of cancer cells. Trastuzumab, an anti-HER2/neu antibody against breast cancer, and the anti-CD20 antibody rituximab against B-cell malignancies are approved therapeutic examples [10, 11]. Monoclonal antibodies, as members of the biotech drugs, are currently a very active research area and also approvals have increased over the last few years (e.g. last approval of panitumumab by the EMEA, the European Medicines Agency, in December 2007). The next sections will focuss on physiological antibodies (section 1.2), the structure of antibodies (section 1.3) and the promising new class of therapeutic monoclonal antibodies (section 1.4) because matuzumab (section 1.5), the compound for the population pharmacokinetic (PK) analysis of this thesis, is a new monoclonal antibody currently in clinical cancer development.

1.2 Physiological antibodies

Under physiological conditions, the immune system is capable of generating its own antibodies against invading material with antigenic determinants. These antibodies are called immunoglobulins (Ig), and are glycoproteins produced by B lymphocytes. As part of the specific humoral immune system they are secreted into the blood or lymph system to identify and neutralise foreign invading objects such as microorganisms (bacteria, parasites, or viruses) or their products, or other non-endogenous substances and objects. In Table 1 an overview of the human immune system including the production of antibodies is presented.

Table 1 Humane immune system [12].

	Different immune response types	
	specific	**nonspecific**
humoral	antibodies	complement system
cellular	T lymphocytes, APC[§], (B lymphocytes)	macrophages, natural killer cells, granulocytes, monocytes

[§] APC: antigen-presenting cell

2

Antibodies can be classified according to the GADME system based on their configuration and function. The five different classes (also referred to as isotypes) are presented, along with their function, in Table 2. Also integrated in this overview are the molecular mass, half-life and the proportion of each class. In general, immunoglobulins - as proteins with hydrophilic and glycosylated moieties - have a high molecular weight of approximately 150-200 kD. The only exception is the tentameric IgM, which has a larger molecular mass of 970 kD. Immunoglobulin G (IgG) represents the most important class of immunoglobulins, with a serum concentration of approximately 12 mg/mL. IgG molecules have the lowest molecular mass and are the predominant antibody for immunochemistry.

Table 2 Immunoglobulins [12].

Class	Sub-classes	Function	Molecular mass [kD]	Proportion of total Ig [%]	$t_{1/2}$ [days]
IgG	IgG1 IgG2 IgG3 IgG4	- main Ig in blood and extravascular region - binds to antigen and toxins	150	75	21 21 7 21
IgA	IgA1 IgA2	- main Ig in seromucous excretion - surface protection	monomer: 160 dimer: 390 secretoric dimer: 385 [§]	15	6 6
IgD	IgD	- mainly in humans - on B lymphocytes	180	0.5	3
IgM	IgM	- first Ig on B lymphocytes - favors agglutination	970	7	10
IgE	IgE	- main role in allergies - surface protection	190	0.002	2

§ heterogeneous distribution; also larger polymers

1.3   Structure of antibodies

In Figure 1, the typical structure of antibodies is shown. Antibodies have as a monomer a typical common chemical structure of several structural elements, two identical heavy and long chains (H-chains), and two identical light chains (L-chains). These chains are held together by a number of disulfide bridges and may be glycosylated. The L-chain consists of 220 amino acids and appears in two different configurations, the λ- and κ-chains. Any individual of a species produces both types of L-chains. The ratio of κ- to

λ-chains varies with the species, e.g. humans have 60% and mice 95% κ-chains. In any Ig molecule, however, the L-chains are always either both κ-chains or both λ-chains.
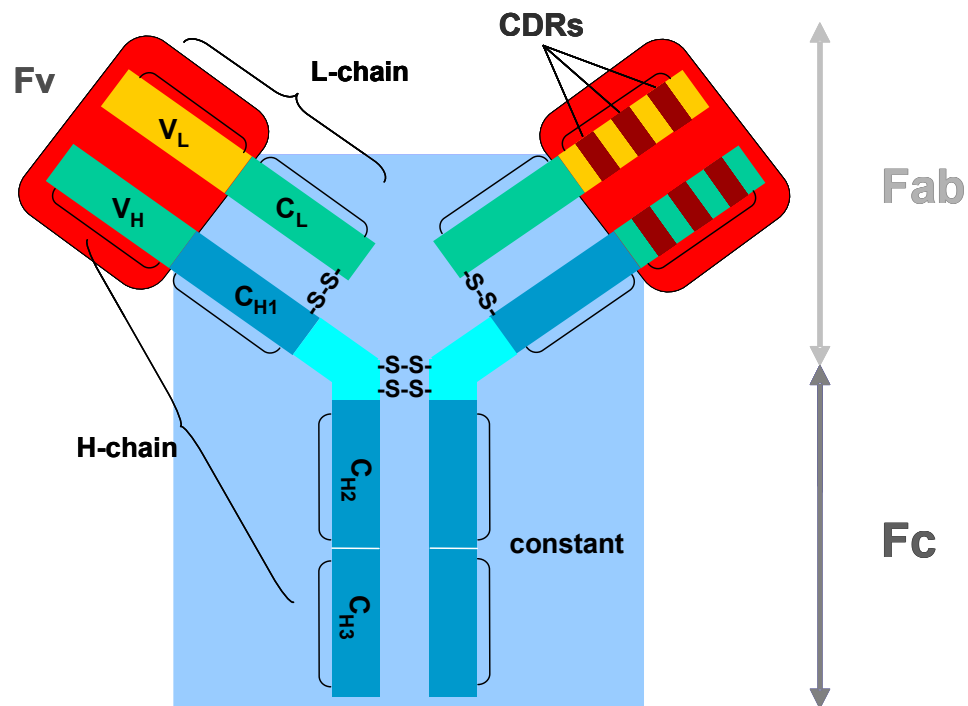

Figure 1 Structure of antibodies [12].

        H-chain: heavy chain, consisting of V_H, C_{H1}, C_{H2} and C_{H3}; **L-chain:** light chain, consisting of V_L and C_L; **V_H:** variable part of H-chain; **V_L:** variable part of L-chain; **C_L:** constant part of L-chain; **C_{H1-3}:** constant part 1, 2 or 3 of H-chain; **-SS-:** disulfide bridges; **Fc:** crystallisable fragment; **Fab:** antigen binding fragment; **Fv:** variable part of Fab; **CDR:** complementarity determining regions, special hypervariable sequences of amino acids

The type of H-chain of about 450-550 amino acids determines the GADME classification (see section 1.2 and Table 2). There are five different types of H-chains: type γ in the IgG molecule, type α in the IgA molecule, type δ in the IgD molecule, type μ in the IgM molecule and type ε in the IgE molecule. Thus, the different classes and subclasses of human immunoglobulins differ in the structure of the heavy chain, the number and localisation of the disulfide bridges, and the glycosylation pattern.

The shape of antibodies resembles the letter 'Y', which is due to the disulfide bridges between the two H-chains and between each H-chain with one L-chain. These endings

tend to crystallise, and for this reason the region is referred to as 'fragment crystallisable' (Fc). The antigen-binding fragment (Fab) is located where H- and L-chains are linked by both covalent bindings (disulfide bridge) and non-covalent bindings. At the end of this part there is a region in both L-chains, which is variable, the so-called Fv region. Within the Fv region special hypervariable sequences of amino acids, the complementarity-determining regions (CDR), are responsible for the huge differentiation of antibodies as they vary in each immunoglobulin in both length and sequence. The steric structure of the summary of only six CDRs builds a contact surface, the counterpart to the epitope, also referred to as the antigenic determinant, which binds to the antibody. The area between these CDRs, called the framework region, provides the basis for the stability of the frame. Based on these structural features, antibodies show very specific recognition of highly diverse antigenic determinants, despite their generally uniform structure [12].

1.4   Therapeutic monoclonal antibodies

During the late 1970s the first mAbs were developed and reached clinical trials for therapeutic use. Generally, these protein drugs are macromolecules (molecular weight for macromolecules: > 1000 Dalton, molecular weight for immunoglobulin G, i.e. antibodies: ~150 kD, see Table 2), which are diverse as well as complex. The interest in antibody products (antibodies, antibody-fusion proteins, antibody fragments, conjugated antibodies, bispecific antibodies, monoclonal intrabodies) has been rapidly increased over the last decades, especially after the Nobel price - winning research of Milstein and Köhler (Medicine 1984) about the principle of mAb production by the hybridoma technique [13]. Using this method, the first extracted mAbs were produced and emanated from murine B cells. The biotechnological steps involved in the hybridoma technique are initiated by the immunisation of a mouse with a specific antigen. The subsequent immune reaction results in an increase of B lymphocytes that produce and secrete antibodies. These antibodies react with the antigen and accumulate in the spleen. After removal of the spleen, the B lymphocytes are isolated and an antibody-producing B lymphocyte is fused with a malignant myeloma cell (an 'immortal' cancer cell capable of replicating indefinitely). The result is a so-called 'hybridoma cell' or cell line, which produces only a single type antibody targeted against a particular antigen. The major advantage of the fusion of the two cell types

(myeloma cell and B lymphocyte) is the unification of their original characteristics, the capability of the myeloma cell for unlimited growth, and the ability of the B lymphocyte to produce a specific antibody. For the production of mAbs, the cell line with the best binding to the targeted epitope of the antigen is chosen from several engineered hybridoma cell lines. The obtained species of antibodies is referred to as 'monoclonal antibodies' because they derive from one original B lymphocyte and thus, they are all identical (clones) [12].

Each year multiple approvals of therapeutic mAbs are documented from the administration agencies [12]. At the moment, approximately thirty approved mAbs are available for human disease therapy, hundreds of mAbs are in clinical development in all clinical phase studies and new approvals are assumed to increase in the future [14].

There are four different types, i.e. classes, of mAbs: murine, chimeric, humanised and human. Examples of these types, together with the year of their first approval and manufacturer, are listed in Table 3. Figure 2 illustrates the different classes of mAbs with their declining immunogenicity by decreasing murine fractions.

Table 3 Overview of monoclonal antibody classes [12].

Class of antibody	Suffix (or prefix)	Example compound	Approval year	Manufacturer
murine	'muro-…ab'	muromonab-CD3	1986 (first approval)	Ortho Biotech
chimeric	'-ximab'	rituximab	1997	Biogen Idec / Genentech
humanised	'-xumab, -zumab'	alemtuzumab	2001	Millennium / ILEX
human	'-mumab'	adalimumab	2002	Abbott

Because of their ability to bind to specific structures with high specificity mAbs show a high potential as therapeutic agents. This also called principle of 'targeted therapy' is often connected with high efficacy and, compared with small molecule therapeutics, mAbs have a lower incidence of adverse events [15]. Main mAb research and therapeutic areas are focussed on immunological and oncological targets and diseases such as transplant rejection, auto-immun reactions, e.g. multiple sclerosis, or cancer
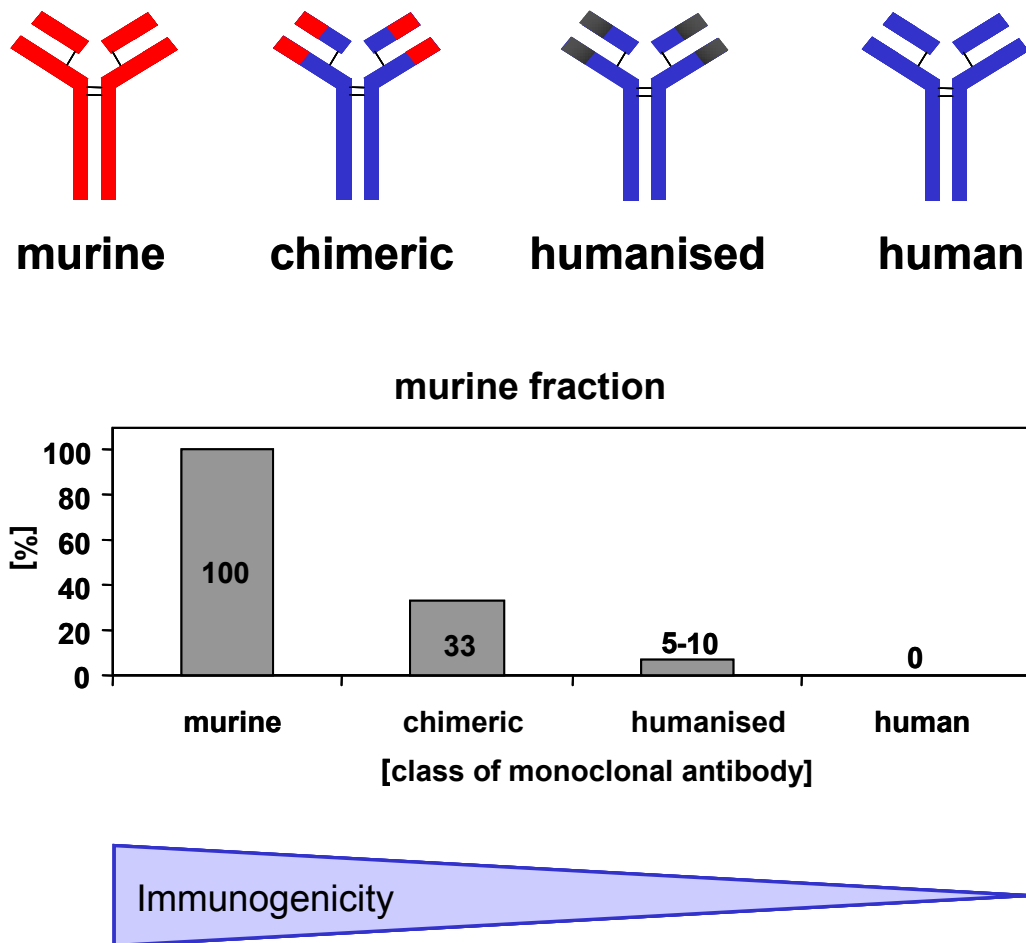
Figure 2 Classes of monoclonal antibodies. Upper panel: different classes of monoclonal antibodies (murine, chimeric, humanised and human; colours: red = fraction of murine origin, blue = fraction of human origin). Lower panel: murine fractions of different classes are illustrated, with declining immunogenicity of the decreasing murine fractions [12].

therapy. Many of the improvements in the treatment of certain cancer entities are due to the incorporation of mAbs in existing therapy schedules, e.g. for metastatic colorectal cancer: the combination of the traditional dosing schemes FOLFOX (folinic acid, 5-fluorouracil, oxaliplatin) and FOLFIRI (folinic acid, 5-fluorouracil, irinotecan) with the mAb bevacizumab showed a high clinical benefit for patients, followed by the inclusion of bevacizumab in the first line chemotherapy guidelines [16]. The addition of bevacizumab was generally associated with a survival advantage: in phase III clinical studies (first- and second-line treatment of metastatic colorectal cancer) the

increases in median overall survival attributable to bevacizumab were 4.7 months with first-line therapy and 2.1 months with second-line therapy [17].

In general, mAbs display several different modes of action as part of their function. The four most important and best-understood effector functions/modes of action of therapeutic mAbs or antibody-derived products (e.g. antibody fragments) for cancer therapy are:

- antibody-dependent cellular cytotoxicity

- complement-dependent cytotoxicity

- blockage of interaction between (patho-) physiological substance and antigen

- conjugated unlabeled mAbs or radioactively labeled mAbs.

Compared with traditional small molecule therapeutics mAbs show several different and partly unique characteristics (e.g. negligible renal clearance and often non-linear pharmacokinetics at therapeutic concentrations) [18]. For a summarised comparison between small molecules and therapeutic mAbs see Table 4. For mAb development and clinical research a thorough understanding of the complex processes after mAb administration including the PK, the pharmacodynamics (PD) and relations between these divisions is nonetheless essential and currently under profound investigation.

Table 4 Comparison of characteristics between traditional small molecule drugs and therapeutic monoclonal antibodies [12].

Characteristic	Small molecule drugs	Monoclonal antibodies
Tissue penetration	often good	usually poor
Binding	usually implies distribution	usually implies clearance
Degradation	metabolic degradation	proteolytic degradation
Renal clearance	often important	uncommon
Unbound concentration	considered to exert effect	considered to exert effect + may cause immunogenicity
Pharmacokinetics	usually linear usually independent from pharmacodynamics	often non-linear often dependent on pharmaco-dynamics and HAxA [§]

[§] HAxA: anti-idiotype antibodies against therapeutic monoclonal antibodies, such as HAMA (human anti-murine antibody); HACA (human anti-chimeric antibody); HAHA (human anti-human antibody)

1.5 Matuzumab

Matuzumab is a humanised recombinant monoclonal antibody of the immunoglobulin subclass IgG1 (κ-chain), which targets the epidermal growth factor receptor (EGFR, HER1, c-ErbB-1) [19, 20]. This physiological transmembrane receptor with protein tyrosine kinase activity is targeted by its natural ligands such as epidermal growth factor and transforming growth factor-alpha (TGF-α) [21-23]. Matuzumab also binds with a high affinity to the ligand-binding domain of the EGFR. The EGFR is constitutively expressed in many healthy epithelial tissues, including skin and hair follicle, and it is overexpressed or up-regulated in a variety of tumour entities (e.g. colon, mamma and bronchial carcinoma) [24-29]. The receptor can be used as a target molecule for therapies based on blockade of receptor-ligand interactions and inhibition of downstream signaling pathways (cell proliferation, angiogenesis, invasion) as well as an increase of apoptosis [2, 30-33]. In general, EGFR expression in tumours is often correlated with a high metastatic rate and advanced disease progression and is accompanied by poor prognosis [34-36].

To overcome the disadvantages of an existing murine (mAb 425) [37, 38] and an approved chimeric antibody (cetuximab) against EGFR [39-41] (i.e. skin toxicity, immune response by the production of autoantibodies), matuzumab was developed by the humanisation of the murine mAb 425. The humanisation was performed according to the method of Winter and described by Kettleborough et al [42].

Matuzumab is currently in clinical development and has already shown promising results [43]. The antibody has indicated potential benefit in several clinical trials within the treatment of different tumour entities such as lung [44], colorectal [45] and gastric [46] cancer. However, a thorough understanding of its PK characteristics, i.e. by population pharmacokinetic modelling, is lacking.

1.6 Population pharmacokinetic modelling

1.6.1 Overview

Pharmacokinetics is the study of a drug in the body, including the processes of ADME (adsorption, distribution, metabolism and excretion). In clinical research, it is used to

analyse and to predict the concentration-time curve of a drug and to support decision making for dosing recommendations [47]. Population pharmacokinetic modelling is a technique that can be used to analyse the variability in drug concentration-time data between individuals when standard dosage regimens are administered (for more details see sections 1.6.2 and 1.6.3) [48].

Regulatory official agencies, such as the U.S. Food and Drug Administration (FDA) or the EMEA, increasingly demand for population pharmacokinetic, pharmacodynamic and combined (PK/PD) approaches for new therapeutics and their evaluation [49, 50].

1.6.2   History

Population PK, PD and combined PK/PD analyses have shown their usefulness and beneficial input for decision making in the therapeutic use and in drug development from their beginning in the early 1980s up to date in a large number of approaches [51-58]. They are performed to identify differences in population subgroups concerning pharmacokinetics, efficacy or toxicity characteristics, to analyse dose-concentration-effect relations or to simulate clinical trials [59-62].

To obtain population PK and PD parameters, three different approaches can be used (because of simplification only the PK will be considered in the following):

- the **naïve pooling procedure** (a method of estimating mean – population – pharmacokinetic parameters by first averaging the concentration at each time point and fitting a model to the averaged data or by pooling all data under the assumption that they belong to one individual and fitting a model to this data) [51]

- the **standard two-stage method** (a method, in which the pharmacokinetic parameters of each individual are estimated in a first step and in a second step the empirical means and variances of the individual parameter estimates are computed) [52]

- the **non-linear mixed effects (NLME) approach** which has been used in this thesis and will be explained in more detail in the following section [52].

1.6.3   Non-linear mixed effects modelling

The NLME approach, a method, in which a non-linear regression method accounts for both fixed and random effects, has several advantages over the other methods (in section 1.6.2). The approach was first introduced by Beal and Sheiner and provides typical population parameters as well as variability parameters [63, 64]. The method estimates all parameters simultaneously and considers the population as a whole, but without ignoring individual subject information [65]. The characteristical mixture of fixed effects (i.e. population parameter estimates and measurable factors, e.g. dose or age) and random effects (i.e. parameter variability) is the source of the term 'mixed effects modelling'.

In NONMEM^{TM} V, a parametric maximum likelihood regression procedure is used as estimation method (in NONMEM^{TM} VI a nonparametric population parameter estimation method is also implemented). The used method seeks for the combination of model parameter values that maximises the probability of observing the data given the specific model by iteratively adjusting the model parameters [66]. The aim is the minimisation of the extended least squares objective function value (OFV; proportional to -2 times the log of the likelihood of the data) [51]. Within NONMEM^{TM} the minimisation routine is a derivative-free quasi-Newton-type of algorithm [67]. The optimisation procedure invariably proceeds by iteration, starting from an approximated solution. A useful estimation method (e.g. the first-order estimation method, see section 2.3.1) will gradually refine the parameter estimates until a predetermined level of precision (convergence criteria: 0.001) has been reached. In NONMEM^{TM}, nested models (e.g. two models with and without covariate relation) are compared by calculating the difference between their OFV referred to as likelihood ratio, which is assumed to be χ^2 distributed [68]. A difference in the OFV of +/-3.84 is considered to be significant at p<0.05 with one degree of freedom (df).

The extended least square objective function (O_{ELS}) is given by the following equation (equation 1.1):

$$O_{ELS} = \sum_{i=1}^{n} \left[\frac{(y_i - f(\theta, x_i))^2}{\upsilon(\theta, \xi, x_i)} + \ln(\upsilon(\theta, \xi, x_i)) \right] [51] \qquad \text{(equation 1.1)}$$

where $f(\theta,x_i)$ represents the structural model part and a respective expected value of y_i (vector of observations belonging to the individual i). ξ and $\upsilon(\theta,\ \xi,\ x_i)$ correspond to any additional parameter and to the variance model, respectively. The logarithm term is included as a penalty in order to counteract the decrease in the sum of squares term as otherwise the OFV would be driven to zero under any circumstances as ξ takes values that increase υ.

One of the main benefits of the NLME method is the simultaneous estimation of mean and variance parameters using merged data from all study individuals as metaanalysis while the individuality of each subject is maintained and accounted for. This method can handle data situations, which are usually complicated for the two other methods (e.g. sparse, rich and unbalanced data and timepoints) [52]. It is possible to use only sparse data from each individual, but then a large enough number of individuals is required [65]. Different studies, including different dosage regimens and administration routes, can be pooled, which enables the incorporation of a large number of study subjects. This method can minimise the need to exclude patient groups and also allows analysis of a variety of unbalanced designs that frequently arise in the evaluation of the relations between dose or concentration on the one hand and efficacy or safety on the other [69]. Another important advantage is the ability to identify and to quantify different types of variability [65]. Additionally, by the analysis of covariate relations, part of the variability, e.g the variability among individuals, the interindividual variability, can be explainable.

Nowadays, several software packages provide non-linear mixed effects capabilities but the most widely used software program for these modelling research activities is NONMEM[TM] [70].

1.7   Objectives

Since the beginning of clinical monoclonal antibody research, the importance to determine the special pharmacokinetics of this new group of therapeutic drugs has increased continuously. In contrast to small molecules, monoclonal antibodies have different characteristics, which have to be taken into account for pharmacokinetic considerations. The objectives of this thesis can be separated into the following parts:

Part I:

With the available data from six clinical studies of the new monoclonal antibody matuzumab,

- one aim of this thesis was to comprehensively characterise the PK of this biological and to develop an accurate, precise, robust and predictive population pharmacokinetic model. This model was to include patient-specific characteristics, which should attempt to explain part of the variability of the PK parameters.

- Moreover, the developed model was to be evaluated and, if necessary, to be refined.

- For model evaluation, different techniques, i.e. internal and external evaluation methods, were to be used.

- Hence, it was aimed to assess, whether in general these internal evaluation techniques are suitable to confirm the precision, robustness and predictivity of population pharmacokinetic models for monoclonal antibodies.

Part II:

- A further objective was to use the developed model for simulations in order to analyse the impact of possible covariate relations and of different dosing regimens on the concentration-time profiles.

- Finally, to evaluate, which body size descriptor is in general best capable to characterise covariate relations including body size for monoclonal antibodies, different body size descriptors were to be analysed for the developed model for matuzumab. To confirm results of this body size descriptor analysis, an additional covariate investigation for an already developed population PK model for sibrotuzumab was to be performed [71]. For this purpose, data from three clinical studies of sibrotuzumab were analysed.

2 Patients and Methods

Part I

2.1 Patient population, treatment and data description

This thesis includes data from i) matuzumab of six clinical studies from patients with different types of advanced carcinomas (e.g. pancreatic, colon, gastric) and ii) sibrotuzumab of three clinical studies from patients with advanced or metastatic cancer (this data will not further be described here, but in section 2.6). Patient and study characteristics of the matuzumab data with descriptive statistics are presented in Table 5. Patients received matuzumab as multiple 1 h i.v. infusions in constant dosing regimens ranging from 100 mg weekly up to 2000 mg in the first week followed by 1600 mg weekly. Serum samples were taken pre- and post-infusions and matuzumab concentrations were determined using a validated sandwich enzyme-linked immunosorbent assay (ELISA) at the Institute of Drug Metabolism and Pharmacokinetics, Merck KGaA, Grafing, Germany [43]. Precision and accuracy of the ELISA method met the international recommendations for bioanalytical immunoassays [72].

2.2 Dataset for modelling and simulation

2.2.1 Building of the matuzumab dataset and derived covariates

To perform a population pharmacokinetic analysis different data sources, including information concerning i) demographics, ii) vital functions, iii) concentration-time data, iv) laboratory values, v) administration data and vi) study specific parameters were merged into a single datafile according to the requirements provided by NONMEM^{TM} and a dataset specification table (Table 6). The development dataset (DD) was built from three studies (studies 1-3) and included 1256 serum mAb concentrations. The evaluation dataset (ED) comprised studies 4 to 6 with 1124 serum concentrations. Derived covariates (body mass index, body surface area, fat-free mass, creatinine clearance) were obtained according to published equations [73-75].

Table 5 Population and study characteristics from the development dataset (study 1-3) and from the evaluation dataset (study 4-6).

		Study 1	Study 2	Study 3	Total	Missings (**) (Study 1-3)	Study 4	Study 5	Study 6	Total	Missings (Study 4-6)
tumour entity	-	advanced pancreatic cancer	various advanced cancer (mainly colon/rectum cancer)	various advanced cancer (mainly colon/rectum cancer)	-	-	advanced/ metastatic pancreatic	advanced oesophago-gastric cancer	various advanced cancer	-	-
dose regimens	-	400 mg q1w, 800 mg q2w, 800 mg q1w	1200 mg q1w, q2w, q3w, 400 mg q3w, 800 mg q3w, 1600 mg q3w	400 mg q1w, 800 mg q1w, 1200 mg q1w, 1600 mg q1w, 2000 mg q1w (from week2: 1600 mg)	-	-	200 mg q1w	400 mg q1w, 800 mg q1w, 1200 mg q3w	100 mg q1w, 200 mg q1w, 400 mg q1w, 800 mg q1w	-	-
patients	(male/female)	17 (9/8)	51 (33/18)	22 (11/11)	**90** (53/37)	-	35 (23/12)	21 (16/5)	25 (17/8)	**81** (56/25)	-
age (years)	median	65	57	58	**60**	0	61	59	59	**60**	0
	(min.-max.)	(40-82)	(29-78)	(30-71)	(29-82)		(47-79)	(51-77)	(29-71)	(29-79)	
height (cm)	median	168	169	170	**169**	3	172	173	176	**173**	0
	(min.-max.)	(156-183)	(143-198)	(150-184)	(143-198)		(159-184)	(158-184)	(159-193)	(158-193)	
weight (kg)	median	68	71	72	**71**	3	67	69	80	**69**	0
	(min.-max.)	(48-81)	(47-125)	(44-98)	(44-125)		(43-101)	(48-101)	(55-120)	(43-120)	
body mass index (kg/m²)	median	24.7	25.8	24.3	**24.9**	4	24.7	23.1	24.4	**23.8**	0
	(min.-max.)	(17.0-30.7)	(20.1-37.0)	(15.9-33.9)	(15.9-37.0)		(16.2-32.6)	(19.2-30.9)	(19.0-32.2)	(16.2-32.6)	
body surface area (m²)	median	1.77	1.82	1.85	**1.82**	4	1.79	1.85	1.95	**1.85**	0
	(min.-max.)	(1.51-2.01)	(1.34-2.59)	(1.44-2.16)	(1.34-2.59)		(1.43-2.17)	(1.46-2.21)	(1.56-2.50)	(1.43-2.50)	
fat-free mass (kg*)	median	51.5	53.2	49.7	**52.7**	4	52.1	55.8	58.9	**54.5**	0
	(min.-max.)	(34.4-62.5)	(30.1-85.4)	(31.7-68.4)	(30.1-85.4)		(31.6-68.2)	(33.0-70.2)	(36.4-81.6)	(31.6-81.6)	

(*) calculated as: male: $(9.27 * 10^3 * weight)/(6.68 * 10^3 + 216 * body\ mass\ index)$; female: $(9.27 * 10^3 * weight)/(8.78 * 10^3 + 244 * body\ mass\ index)$

(**) Missing values in the individual dataset were replaced by the median value of the population.

15

Table 6 Dataset specifications for the matuzumab NONMEM^{TM} file.

Data label	Unit	Data name
ID	---	subject identification
TIME	h	time
TIPL	h	time planned
TIM1	h	time 1
TALD	h	time after last dose
AMT	mg	amount
RATE	mg/h	infusion rate
DV	if PK e.g. µg/mL if PD variable	dependent variable
CMT	---	compartment
EVID	---	event identification
FLAG	---	flag
VISI	---	visit
OCC	---	occasion
DGR	---	dose group
DOSE	mg	administered dose
AGE	year	age
HT	m	body height
WT	kg	body weight
BMI	kg/m²	body mass index
FFM	kg	fat-free mass
FM	kg	fat mass
BSA	m²	body surface area

Table 6 Dataset specifications for the matuzumab NONMEM^{TM} file (continued).

Data label	Unit	Data name
SEX	---	sex
RACE	---	race
WBC	---	white blood cell count
ALT	U/L	alanine aminotransferase
AST	U/L	aspartate aminotransferase
GGT	U/L	gamma-glutamyl transpeptidase
AP	U/L	alkaline phosphatase
LDH	U/L	lactate dehydrogenase
BIL	µmol/L	bilirubin
CREA	µmol/L	creatinine
CLCR	mL/min	creatinine clearance
COME	---	co-medication
DATE	dd.mm.yyyy	date
CLTI	hh:mm	24 h clock time
CLTD	---	decimal 24 h clock time
OID	---	original subjct identification
SID	---	site identification
STDY	---	study
KARN	%	Karnofsky Performance Index
FLAM	---	flag for analytical method
REC	---	record

2.2.2   Missing data

For the model-building process missing individual data of study population characteristics were replaced by the median value of the study population. In the development dataset for the continuous covariates height (HT) and weight (WT) were replaced by the median values for three individuals (3.3% of the study population) and body mass index (BMI), body surface area (BSA), fat-free mass (FFM) and fat mass (FM) for four individuals (4.4% of the study population). The 'last observation carried forward' procedure was used for time changing covariates within study individuals [76].

2.3   Pharmacokinetic model development

2.3.1   Non-linear mixed effects modelling

In this thesis the NLME method implemented in NONMEM^{TM} was used for all population pharmacokinetic analyses of clinical data of matuzumab and sibrotuzmab.

For PK, PD and PK/PD analyses there are different estimation methods implemented in NONMEM^{TM} that are described in the literature [77]. In this thesis, the following methods have been used:

- the first-order method (**FO**)

- the first-order conditional estimation method (**FOCE**)

- the first-order conditional estimation with interaction method (**FOCE with INTERACTION**).

The **FO** method estimates population parameters by a first-order Taylor series expansion with respect to random variables, where it is assumed that these random-effects parameters are independently multivariately normally distributed with means of zero. Using the POSTHOC option in NONMEM^{TM}, individual parameters can be obtained *a posteriori* based on the fixed and the random effects and the individual observations [77].

The improved **FOCE** method uses a first-order Taylor series expansion around the conditional estimates of the differences between the population and the individual parameters. With this method, population parameters and random-effects parameters are estimated at each iteration step.

The advanced **FOCE with INTERACTION** method additionally allows the dependence of random deviations between the individual predictions and the observed measurements.

The analyses for this thesis were performed using the mentioned different estimation methods (FO, FOCE with or without INTERACTION). For the final model and all evaluation and simulation analyses for matuzumab FOCE with INTERACTION was used. All models were parameterised in terms of clearance(s) and volume(s) using the subroutine ADVAN6 TRANS1 TOL5 in NONMEM^{TM}. For the sibrotuzumab analyses and simulations the FO method and the POSTHOC option and the subroutine ADVAN6 TRANS1 TOL5 were used.

2.3.2   Structure of a NLME model

The population model in the NLME approach is typically divided into three submodels (see Figure 3, left panel), which will be discussed in the respective sections:

- the **structural** submodel (section 2.3.2.1)

- the **pharmacostatistical** submodel (section 2.3.2.2)
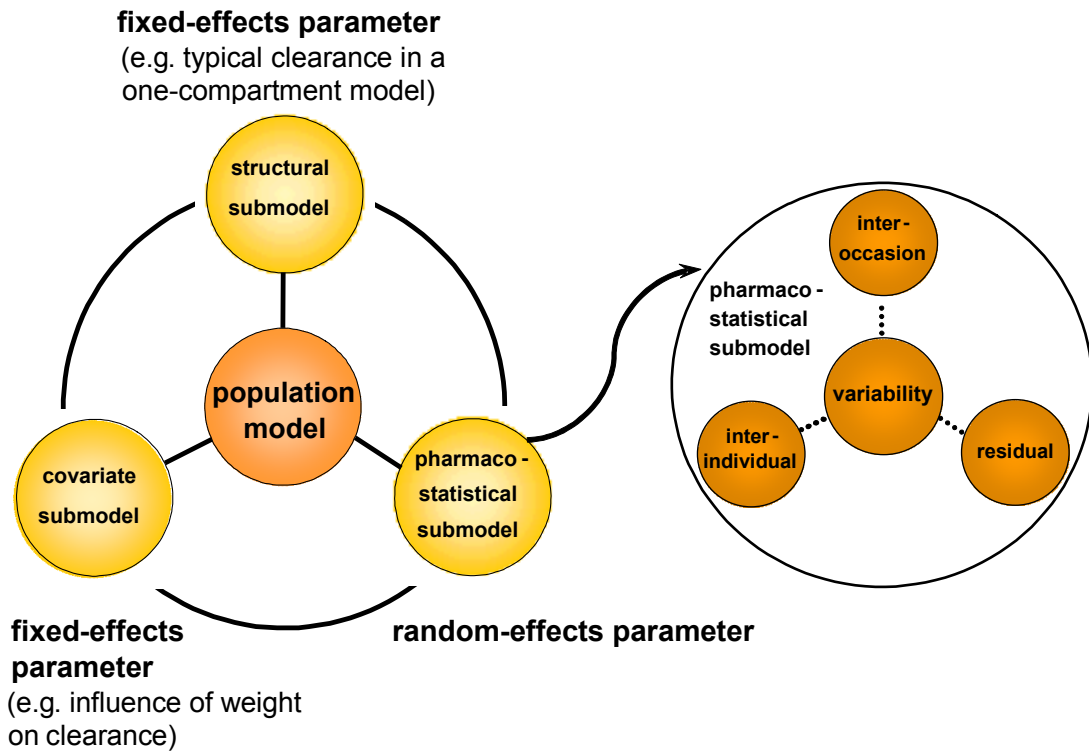
- the **covariate** submodel (section 2.3.2.3).

Figure 3 Schematic structure of a population pharmacokinetic model.

2.3.2.1 Structural submodel

The first step in the population pharmacokinetic analysis was to develop the structural submodel. This model structure should describe the central tendency of the measured data best, generally in the absence of covariates. It should characterise the typical time profile of the data by the following function (equation 2.2):

$$f(\phi_i, X_{ij})$$ (equation 2.2)

where $f()$ is the function describing the structural model that relates the independent variables X_{ij} (e.g. time and dose) to the response given the i-th individual's vector of model parameters ϕ (e.g. typical clearance, typical volume of distribution).

2.3.2.2   Pharmacostatistical submodel

The pharmacostatistical submodel characterised the variability between and within individuals and quantifies the influence of the random effects. The population model was influenced by three types of variability (see Figure 3, right panel):

-   the **interindividual** variability (variability among individuals)

-   the **interoccasion** variability (variability within individuals between occasions)

-   the **residual** variability (non-measurable and non-controllable factors, e.g. uncertainty in measurements or dicrepancies in sampling time points)

During model development and all other analyses the **interindividual** variability (IIV), which quantifies the non-explainable difference of a model parameter among the different individuals, was modelled with an exponential random-effects term (equation 2.2):

$$P_{ki} = \theta_k \cdot e^{\eta_{ki}} \qquad \text{(equation 2.2)}$$

where P_{ki} represents the parameter value k from the individual i and θ_k describes the population value of the parameter k. η_{ki} denotes the ln-difference between P_{ki} and θ_k. There are two additional models, which are sometimes used to describe individual parameter distribution, the additive and the proportional model [78]. However, the exponential model is the most physiological one, because it ensures that all individual parameters are strictly positive. For this purpose, this model was used in this thesis.

The **interoccasion** variability (IOV) or between occasion variability (BOV), i.e. the variability within one individual between study occasions, was (in addition to the IIV) also examined with an exponential random-effects term (equation 2.3):

$$P_{kiq} = \theta_k \cdot e^{\eta_{ki} + \kappa_{kiq}} \qquad \text{(equation 2.3)}$$

where P_{kiq} is the individual parameter value k from the individual i at the occasion q. P_{kiq} differs from the typical individual value by an additional random effect κ_{kiq}. η_{ki} and κ_{kiq} were assumed to be symmetrically distributed with a zero mean and a variance of ω^2 and π^2, respectively.

The definition of one occasion has to be defined by the modeller. In this thesis, the inclusion of IOV was limited to eight infusions due to insufficient data later-on and implemented by different ways of assigning the eight infusions to a varying number of occasions:

- definition 1: IOV on CLL; infusion 1 and infusions 2-7 (2 occasions)

- definition 2: IOV on CLL; every 8 infusions corresponded to one occasion (8 occasions)

- definition 3: IOV on CLL; infusions 1-3 and infusions 4-8 (2 occasions)

- definition 4: IOV on V1 (different occasion duration for each dosing regimen depending on data rich time points).

Residual variability represents the discrepancy between the observed and the model-predicted concentrations after incorporation of IIV and IOV. During model development, this type of variability was modelled using additive, proportional or combined error models [79]. After the base model (structural submodel + pharmacostatistical submodel) had been developed, the combined error model was used for all further analyses. The combined error model uses an additive and a proportional component (equation 2.4):

$$Y_{ij} = f(\Phi_i, X_{ij}) \cdot (1 + \varepsilon_{1,ij}) + \varepsilon_{2,ij} \qquad \text{(equation 2.4)}$$

where Y_{ij} corresponds to the measured observation from the individual i at a certain time point j. The function $f(\Phi_i, X_{ij})$ denotes the structural part of the model, this time including IIV and IOV and therefore, estimating the individual prediction of the model. $\varepsilon_{1,ij}$ and $\varepsilon_{2,ij}$ denote the random deviation between the individual prediction and the observed measurement for each individual i at a certain time point j. The term $(1 + \varepsilon_{1,ij})$ corresponds to deviations, which increase proportionally with higher observations and $\varepsilon_{2,ij}$ denotes the additional constant additive deviation over the whole measurement range.

For the determination of the residual variability model it is assumed that ε_{ij} is a zero mean random variable with a multivariately symmetrically distributed variance σ^2. The

variance σ^2 represents the diagonal element of the Σ matrix and is estimated as a population PK parameter, which reflects the extent of the residual variability.

2.3.2.3   Covariate submodel

The covariate submodel as part of the population model was included to explain part of the IIV, IOV and the residual error on the PK parameters originally included in the base model. The model denotes the relations between covariates and model parameters by using fixed-effects parameters [80]. Covariates describe individual- or study-specific characteristics: patient demographics (e.g. age, weight), disease status (e.g. laboratory values, disease indices such as the Karnofsky index for cancer patients) or environmental factors (e.g. smoking status or alcohol consumption). Covariates can also be classified into categorical (e.g. dose group [DGR]), dichotomous (specific categorical classification, e.g. sex) or continuous (e.g. age).

Two sequential methods are widely used to investigate covariates: the **GAM analysis** ('generalized additive modelling', implemented in the software Xpose®), using the Akaike´s Information Criterion, AIC [81, 82], and a **covariate analysis investigating the covariate relations within the NLME model in NONMEM**[TM].

The **GAM analysis** was first proposed by Mandema et al. and allows a fast initial screening of potentially important covariates [80]. The method includes three different possibilities to implement a covariate: (1) inclusion in a linear relation, (2) inclusion in a spline (non-linear) relation or (3) no inclusion [83]. Each covariate was analysed by a stepwise addition and deletion procedure and the covariate that reduced the AIC to the largest extent was retained in the model. When no further reduction in AIC was achievable the procedure was finished.

The **covariate analysis within the NLME model** was performed in NONMEM[TM] on the basis of the developed base model with respect to the statistical significance of the influence of a covariate on a model parameter. Different implementation strategies have been described to investigate covariate relations in NONMEM[TM] [80, 84-86], but none of them has shown its superiority towards the other. For this purpose, in this thesis all covariates were analysed by the often used stepwise procedure of forward inclusion and backward deletion [84]. In each step, all possible/remaining parameter-covariate relations were assessed. The included covariate relation, which led to the largest

decrease in the OFV, was kept in the model. In the next steps, the remaining covariate relations were investigated. All covariate relations, which caused a ΔOFV>-3.84 (p<0.05, df=1), formed the full covariate model. From the full model the covariate relations were then deleted one at a time using a stricter significance criterion (ΔOFV<10.83, p<0.001, df=1). The final covariate model was the one in which deletion of any of the covariate relations led to an increase in OFV (ΔOFV>10.83).

Covariates investigated for their influence on PK parameters included continuous characteristics such as demographics (weight, height, age [AGE], body surface area, body mass index, fat-free mass, fat mass; for ranges and quantities see Table 5), laboratory values (creatinine clearance [CLCR], lactate dehydrogenase [LDH], alkaline phosphatase [AP], white blood cell count [WBC]) and additional: Karnofsky index ([KARN], range: 40-100%), dose group ([DGR], in DD: 11 DGRs, in ED: 5 DGRs). Categorical/dichotomous characteristics were sex ([SEX], 64% male and 36% female), study number ([STDY], original study number), study site ([SID], in DD: 4, in ED: 6) and concomitant chemotherapy ([COME]; in studies 1 and 4 matuzumab was combined with a fixed dosing of gemcitabine, in study 5 with a fixed ECX - epirubicin, cisplatin and capecitabine – dosing).

Continuous covariates were investigated with a linear covariate model (equation 2.5):

$$TVP_k = \theta_k \cdot (1 + \theta_{COV} \cdot (COV - COV_{median})) \qquad \text{(equation 2.5)}$$

where TVP_k is the population value of the parameter P_k for a specific covariate value (COV) and θ_k is the population value of the parameter P_k with the covariate value being the median value (COV_{median}). θ_{COV} is the fractional change in the population parameter value with each covariate unit deviation from the median covariate value. If graphical inspection suggested non-linear relations, they were investigated by a power model, an Emax model or an exponential model [87].

The categorical covariates SEX and COME were given as dichotomous variables (sex: male/female, concomitant chemotherapy: yes/no). The coding for this covariate type is illustrated using an indicator variable (IND), being 0 or 1 (e.g. male or female) (equation 2.6):

$$TVP_k = \theta_k \cdot (1 + \theta_{COV} \cdot (IND)) \qquad \text{(equation 2.6)}$$

where θ_k is the typical value of the parameter P_k when IND=0. θ_{COV} represents the fractional increase or decrease of the parameter P_k caused by IND=1.

If the categorical covariate had multiple categories each category had an own indicator variable (e.g. study site: site 1 = (IND) 1, etc.) (equation 2.7):

$$TVP_{k1} = \theta_{k1} \quad if\,(IND) = 1,\ etc. \hspace{3cm} \text{(equation 2.7)}$$

where θ_{kx} is the typical value of the parameter P_k for each category$_x$.

Visual exploratory analysis of the covariate relations revealed that for the laboratory parameters aspartate aminotransferase, alanine aminotransferase, gamma glutamyltransferase and bilirubin a 'suspected relation' by the GAM analysis was driven by very few individuals. Neglecting these individuals did not support the relation anymore. Consequently, these relations were not considered for further covariate analysis.

In general, the modelling strategy for the population PK analysis for matuzumab in this thesis was a bottom up approach based on the data situation including the following steps:

- development of the structural and the pharmacostatistical submodels (i.e. base model)

- development of the covariate submodel

- refinement of the model (see sections 2.4.1, 3.2 and 3.3).

2.4 Model evaluation

The aim of model evaluation methods is to qualify the developed model for its appropriateness. In general, the evaluation procedures can be divided into external and internal evaluation techniques, wich can be used to show the reliability and the prediction performance of the developed model and will be presented in detail in the following sections 2.4.1 and 2.4.2 [88].

It has to be pointed out, that the first evaluation of the developed population PK model for matuzumab was performed by the visual inspection of goodness of fit plots. The

inspection of respective goodness of fit plots was also used as continuous diagnostic method during model development. However, this technique is part of the basic internal evaluation and will be described in section 2.4.2.

2.4.1   External evaluation

The external evaluation was based on a second dataset, which had not been used to develop the model. The procedure was used in this thesis to analyse whether the investigated population pharmacokinetic model for matuzumab was able to describe the concentration-time profiles of a new study population (i.e. the observations of the population of the evaluation dataset introduced in sections 2.1 and 2.2). The obtained population parameters from the evaluation dataset were compared with the original parameter values from the development dataset. Additionally, the parameters were reestimated on the basis of a combined dataset (DD + ED). The external evaluation is presented as the first evaluation method, because the internal evaluation was performed based on the obtained results from the external evaluation.

2.4.2   Internal evaluation

In general, the internal evaluation can be devided into basic and advanced evaluation techniques. Basic internal evaluation, usually performed during model development and for the evaluation of the final model, included the graphical inspection (presentation of goodness of fit plots) of the obtained results and the analysis of the uncertainty of model parameter estimates (relative standard errors, RSE). Additionally, the following advanced internal evaluation techniques were performed in this thesis: the **bootstrap method** [87, 89, 90], **case deletion diagnostics** (CDD) and **visual predictive checks** (VPC) [91, 92], described in detail in the following sections 2.4.2.1, 2.4.2.2 and 2.4.2.3.

2.4.2.1   Bootstrap method

The developed model (Final Model, see Table 9) was evaluated by the bootstrap technique, a resampling method, which was first presented by Efron in the late 1970s as a tool for modern statistical data analysis, i.e. the assessment of bias and precision [90, 93]. The nonparametric bootstrap is the most common approach. By 'sampling with

replacement' from the original dataset, a series of new datasets with equal size to the original dataset is obtained [89].

The bootstrap analysis was performed with the software program 'Wings for NONMEM' [94]. The new datasets were estimated based on the final population pharmacokinetic model for matuzumab. The bootstrap median, the bias, the relative bias and the 95% confidence interval (calculated by the determination of the 2.5[th] and the 97.5[th] percentiles) of each PK parameter from 200 successful (i.e. converged runs with an objective function value estimation) bootstrap runs were assessed.

2.4.2.2   Case deletion diagnostics

To assess the robustness of the developed model CDD were performed. This standard method detects individuals, groups of individuals or observations that have a substantial influence on the estimation of the model parameters [95, 96].

For the matuzumab model, all 90 study subjects from the development dataset were randomly allocated to 10 new groups of 81 subjects each (i.e. 10% of the original study population was excluded in each group), so that each subject was excluded only once (scenario 1). Additionally, each study subject was removed individually from the original dataset, resulting in 90 new datasets with 89 subjects each (scenario 2). For all new datasets the model was fitted to the data (based on the final population PK model for matuzumab). The estimated new parameters were compared with the original model parameters and with the original 95% confidence intervals obtained from the NONMEM[TM] run report (estimated parameter value +/- 1.96 * standard error). Secondary, for nine model parameters (56% of 16 parameters) with original relative standard errors (RSE) > 15%, and consequently large confidence intervals, new confidence intervals were calculated according to assumed RSEs of 15% (based on bioanalytical requirements from the FDA [97]) for these nine parameters (scenarios 3 and 4, respectively). The parameter estimates of scenario 1 and 2 were scrutinised for their value still being inside these 'stricter' confidence intervals.

2.4.2.3   Visual predictive check

The visual predictive check method is a technique, which originates from the 'posterior predictive check' (PPC) and which has a strong potential to demonstrate the predictivity of a developed model [88, 98]. A VPC graphically compares the observations with model based simulated data. The aim of the VPC is to demonstrate, whether a developed model is able i) to reproduce the variability in the observed data, from which it arises, and ii) to simulate the central tendency of the observed data [91].

For this internal evaluation procedure 1000 new individual concentration-time profiles were simulated based on the final parameter estimates of the population PK model for matuzumab. From these simulated profiles the median, the 5th and the 95th percentiles were calculated for each time point. VPCs for single and multiple dosing were graphically presented and the observed matuzumab serum concentrations from the original dataset were included into the plots. Single dosing VPCs included for each single dosing (400, 800, 1200 and 1600 mg) the original concentrations of the first occasion (e.g. for 400 mg single dose: first occasion concentrations from the following dosing regimens: 400 mg weekly, 400 mg every two weeks and 400 mg every three weeks). For multiple dosing VPCs were performed for each dosing regimen separately (11 multiple dosing VPCs).

Part II

2.5   Simulations

Compared to the modelling approach, which is directed retrospectively, simulation scenarios are directed prospectively [87]. Clinical trial simulations are often used to gain additional knowledge for decision making and to save costs, which otherwise have to be spent for traditional experiments [86, 99]. In simulation scenarios, the model is fixed, but inputs (e.g. dosing regimen, administration pathway) can vary.

In this thesis different simulation scenarios were performed based on the final PK model for matuzumab in order to demonstrate the influence of dosing on the PK profiles and to visualise the impact of covariates on the concentration-time profiles. To analyse the effect of dosing, different dosing regimens with the same dose amount per

week (400 mg weekly, 800 mg biweekly and 1200 mg every three weeks) were simulated in the central (scenario 1a) and in the peripheral (scenario 1b) compartment. Covariate influences were determined by the simulation of study subjects representing the 5th, 50th and 95th covariate percentiles of the original study population (scenario 2). Finally, it was analysed, whether a reduction of observed variability in the PK profiles might be achieved (scenario 3) and whether these investigations might result in a recommendation of a 'new dosing regimen'.

2.6   Body size descriptors in population analyses

In general and in population pharmacokinetic analyses, a number of investigations have been performed to determine, which body size descriptor should be used to best describe body size covariate relations [100-102]. In this thesis, the analysis of body size descriptors in covariate relations had to consider the new and specific conditions of hydrophilic macromolecules (i.e. monoclonal antibodies). For this purpose, body weight, body surface area and fat-free mass were selected and analysed as body size descriptors for covariate relations in population PK analyses for monoclonal antibodies.

1) Firstly, their influence on changes in the OFV was compared for the model of matuzumab. The precision of the obtained model parameters and in particular the precision of the covariate relation parameters were analysed.

2) Secondly, simulations were performed for each body size descriptor separately to visualise and to compare the impact of the different covariates. The dosing regimen of 1200 mg weekly was chosen for three simulated subjects representing the 5th, 50th and 95th body size percentiles of the original matuzumab study population (development dataset + evaluation dataset, n = 171).

3) Thirdly, for deriving generic conclusions and to infer whether FFM is the most recommendable body size descriptor for population pharmacokinetic analyses for monoclonal antibodies, further investigations were performed. For this purpose, the results from a developed population PK model from the literature for the monoclonal antibody sibrotuzumab was used [71]. For the development of this population PK model data from 1844 serum concentrations from 60 patients in three Phase I and Phase II clinical studies (administration of

sibrotuzumab as once weekly 1 h i.v. infusion) had been available. The developed model included the covariate relations WT on CLL, V1, V2 and Vmax. Apart from that, the model was similar to the model developed for matuzumab (two-compartment model, one linear and one non-linear elimination pathway from the central compartment, IIV on CLL, V1/V2 [combined] and Vmax, IOV on the bioavailability F1 in the central compartment). To analyse FFM covariate relations in this model, FFM values for all sibrotuzumab study subjects and a FFM median for this study population were calculated. To evaluate the original model parameters, they were compared with new results, obtained from parameter estimation based on the original model modified by the substitution of FFM for WT (for all covariate relations).

General methods

2.7   Statistical methods

According to standard statistical methods, described in the following part, statistical analyses and evaluations were performed.

For the descriptive statistics different localisation and dispersion parameters were used to characterise the analysed data and obtained results from the population analyses, the evaluation methods and the simulation scenarios. A distribution or a central tendency were described by localisation parameters (Table 7) and the variability of a distribution was denoted by dispersion parameters (Table 8).

Table 7 Localisation parameters.

median ($\tilde{x}$)	value that separates the upper half of a sample or a population from the lower half; corresponds to the 50th percentile
arithmetic mean ($\bar{x}$)	sum of all the items of the set divided by the number of items in the set
5th and 95th percentile (5th and 95th P)	values cutting off the lowest and the highest 5% of the data

Table 8 Dispersion parameters.

range (R)	length of the smallest interval, which contains the highest and the lowest value
standard deviation (SD)	measure of statistical dispersion, defined as the square root of the variance
variance (s²)	measure of the statistical dispersion of a variable, indicating how far from the expected value its values typically are
coefficient of variation (CV%)	measure of dispersion of a distribution defined as the ratio of the standard deviation to the mean*100

2.8 Software

Raw datafiles were merged using SAS® (SAS Institute Inc., Version 9.1, 2003). Calculation of statistics and derived covariates and figure presentations were performed using Microsoft® Excel (Microsoft Corporation, Version 2003 SP2, 2003) or SPSS® (SPSS Inc., Version 15.0.1, 2006).

All population pharmacokinetic model analyses were carried out using the software NONMEM™ (Version V, level 1.1; Icon Development Solutions, Ellicott City, Maryland). The free software management program PROPHET™ was used (Version: v 1.0.1 - 05.05.2004).

For data check-out and graphical analysis Xpose® (Niclas Jonsson and Mats Karlsson, Version 3.104) in connection with S-Plus® (Insightful Corporation, Version 6, 2001) was used.

Datasets generated from NONMEM™ were modified using Microsoft® Excel (Microsoft Corporation, Version 2003 SP2, 2003).

Bootstrap runs were investigated with the free software program 'Wings for NONMEM' [94].

Simulations were carried out using NONMEM™ and WinNonlin® (Pharsight Corporation, Version 5.2, 2007).

3 Results

Part I

3.1 Base/primary model

For the development of the base/primary population model the development dataset (for data details see Table 5 and sections 2.1 and 2.2), which included 1256 serum concentration values of matuzumab, was analysed. The observed PK profiles were best described by a two-compartment model. In addition to a linear clearance (CLL), a second elimination pathway as a non-linear process (implemented as Michaelis-Menten kinetics, CLNL) with the additional parameters Vmax (maximum elimination rate) and Km (the concentration with half-maximal elimination rate) from the central compartment was included. The structural model for matuzumab is presented in Figure 4 including i.v. administration, two volumes of distribution (V1: central compartment, V2: peripheral compartment), linked via the inter-compartmental clearance Q, and the two elimination pathways (CLL and CLNL). As random effects, interindividual variability on four parameters (V1, V2, Vmax and CLL) and interoccasion variability on CLL were implemented. For the incorporation of IOV in the population pharmacokinetic model of matuzumab, one occasion was characterised as the time period from the start of an infusion until the start of the next infusion (see section 2.3.2.2, IOV definition 2).

A need to incorporate non-linearity might already be concluded from the semilogarithmic plots in Figure 5, showing the geometric mean and the standard deviation of the observed concentration–time profiles of four weekly dose regimens of 400–1600 mg, after the first and the fourth infusion. In the terminal phase, the slope of the curve was steeper at lower concentrations.

In the covariate analysis, fourteen relations were identified by the GAM procedure:

- Vmax ~ BSA, SEX, CLCR

- V1 ~ BSA, COME, SEX

- V2 ~ COME, SEX, LDH, SID

- CLL ~ BSA, COME, AP, SEX.

Four relations (DGR and WT on V1, COME and WT on CLL) were identified by the forward inclusion and backward elimination method. After additional graphical inspections and simulations to assess the plausibility and relevance of the found relations, the influence of WT on V1 and WT on CLL remained in the model.
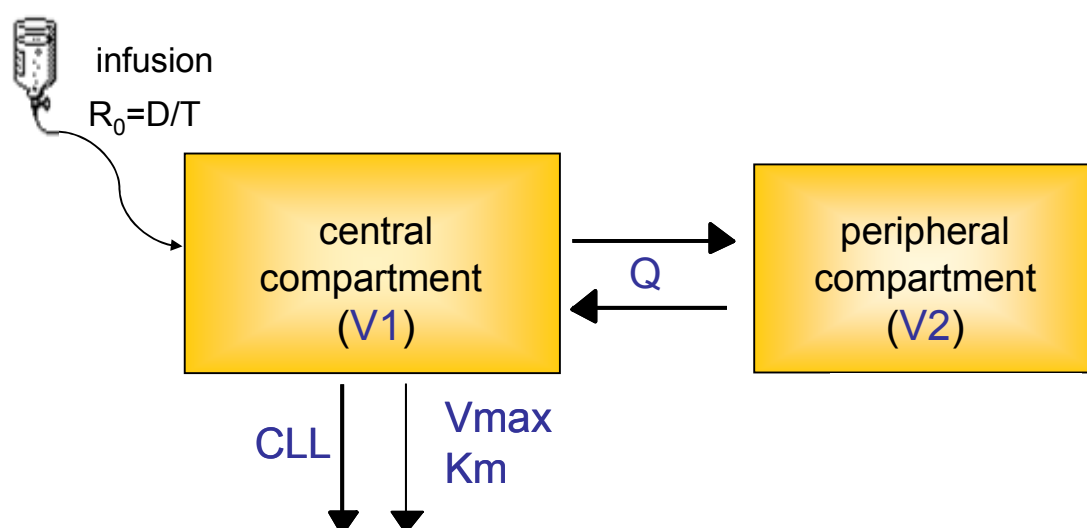

Figure 4 Schematic structural pharmacokinetic model for matuzumab.

R_0: infusion rate; **D**: dose; **T**: infusion duration; **V1**: volume of the central compartment, **Q**: inter-compartmental clearance; **V2**: volume of the peripheral compartment; **CLL**: linear clearance part; **Vmax**: maximum elimination rate; **Km**: concentration, at which the elimination rate is 50% of the maximum value
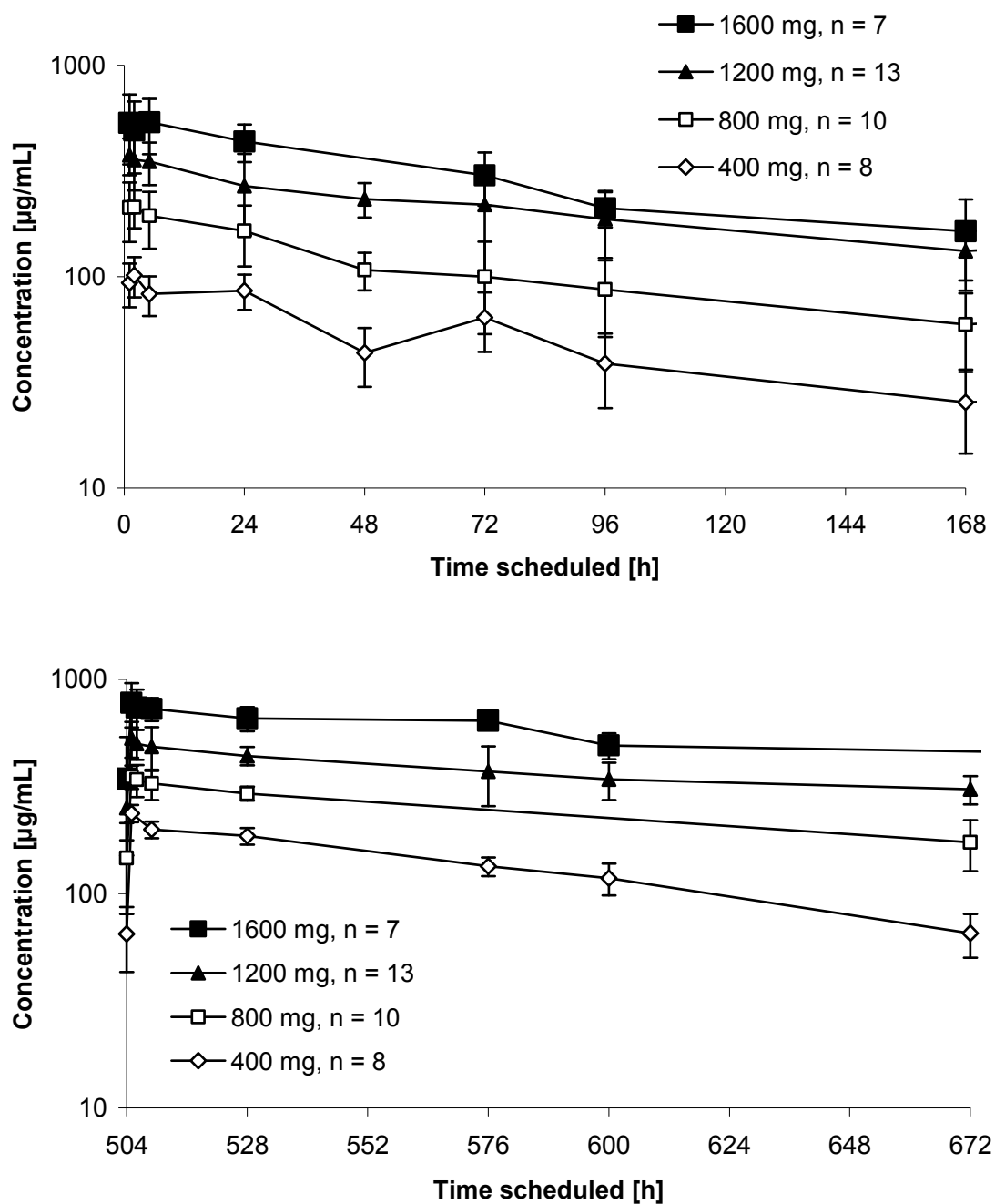
Figure 5 Semilogarithmic plot of the geometric mean and the standard deviation of the observed concentration–time profiles of the four weekly dose regimens (400, 800, 1200 and 1600 mg matuzumab per week) after the first (upper panel) and fourth (lower panel) infusion. n = number of patients in the dose group. Last time point for the 1600 mg dose group was after 1008 h and is not shown.

On the basis of the analysis, which body size descriptor should be used to best describe the covariate relations in population PK analysis for monoclonal antibodies (see sections 2.6 and 3.6) and literature recommendations, WT was exchanged for FFM in both covariate relations [73]. All model parameter estimates including the respective relative standard errors (RSE = standard error divided by population estimate*100) for this primary model are presented in Table 9, column: Primary Model. CLL was estimated to be 15.3 mL/h and CLNL, calculated from the parameter values of Km (3.9 mg/L) and Vmax (0.451 mg/h) at mAb concentrations << Km, was 115.6 mL/h. RSEs for the fixed-effects parameters were ≤14.2%, except for Km (31.0%) and the covariate relations with RSEs ≤ 28.6%. IIV was between 20% CV (IIV on V1) and 62% CV (IIV on V2) and IOV was estimated to be 22.6% CV.

Residual variability was implemented with a proportional error of 13% CV and the additive error was fixed to 0.312 mg/L for reasons of model stability. Random effects were estimated with RSEs ≤ 39.9% (RSEs for random effects were related to the corresponding variance scale).

3.2 External evaluation of the primary model

The primary model was evaluated by external evaluation with the evaluation dataset presented in sections 2.1 and 2.2. On the basis of the primary PK model all population PK parameters of the evaluation dataset were estimated and compared with the primary estimates (Table 9, column: Evaluation 1). In general, the population estimates were very close to the primary estimates, but no support for the covariate FFM on the central volume of distribution was observed (estimated value: 0.0019 with a RSE of 238%). Additionally, the IIV on the peripheral volume of distribution showed a high imprecision (RSE: 112%) as well as the correlation coefficient between V2 and Vmax (RSE: 105%). Further, the IOV had a much higher population estimate (55% CV) than expected from the development dataset (IOV: 23% CV).

The model was changed by the deletion of the unsupported covariate FFM on V1, to investigate whether a refined model could describe the observations from the development dataset and especially those from the evaluation dataset better, including more precise estimates. Model parameters were reestimated for DD and ED. The

Table 9 Parameter estimates from the different models and datasets.

Model Parameter	Unit	Primary Model Population estimate	RSE, %[a]	Evaluation 1 Population estimate	RSE, %[a]	Final Model Population estimate	RSE, %[a]	Evaluation 2 Population estimate	RSE, %[a]	Evaluation 3 Population estimate	RSE, %[a]
Fixed effects											
CLL[b]	[mL/h]	15.3	4.6	12.1	9.6	15.2	4.4	12.0	9.8	13.7	3.8
V1	[L]	3.79	3.1	3.89	6.4	3.73	3.2	3.88	6.4	3.81	3.2
Q	[mL/h]	38.1	7.9	20.8	12.9	37.7	7.7	21.1	12.8	27.9	6.7
V2	[L]	1.83	9.1	2.69	15.6	1.84	9.0	2.67	16.1	2.15	6.6
Vmax	[mg/h]	0.451	14.2	0.565	20.2	0.453	13.4	0.563	21.5	0.509	10.5
Km	[mg/L]	3.9	31.0	5.3	40.0	4.1	30.2	5.1	52.2	3.6	22.7
Covariate influence											
V1_FFM[b,c]		0.0077	28.6	0.0019	237.6	-	-	-	-	-	-
CLL_FFM[b,c]		0.0138	18.6	0.0157	34.1	0.0119	21.6	0.0150	32.3	0.0138	15.9
Random effects											
Interindividual variability											
ωCLL[b]	[%CV]	22.9	20.6	30.2	51.7	22.7	19.5	29.9	49.8	23.8	21.4
ωV1	[%CV]	20.3	18.8	39.9	28.9	24.1	17.1	40.4	26.9	32.7	12.9
ωV2	[%CV]	61.7	29.7	29.8	111.9	60.7	27.0	29.9	78.1	47.0	28.9
ωVmax	[%CV]	52.1	39.9	54.3	47.1	47.6	41.7	53.9	47.1	50.1	23.3
Correlation V1_V2		0.781	23.2	0.977	51.2	0.780	26.6	0.986	41.8	0.806	18.0
Correlation V2_Vmax		0.868	34.5	0.560	104.9	0.862	34.7	0.626	74.9	0.870	22.1
Correlation V1_Vmax		0.821	26.8	0.706	48.2	0.940	26.9	0.725	51.0	0.769	18.3
Interoccasion variability											
πCLL[b]	[%CV]	22.6	12.9	55.0	21.2	22.5	12.1	55.0	21.8	41.5	9.4
Residual error											
σ proportional	[%CV]	13.4	1.6	18.9	2.5	13.4	1.6	18.9	2.5	16.3	1.3
σ additive	[mg/L]	0.312 FIX	-	0.312 FIX	-	0.312 FIX	-	0.312 FIX	-	0.312 FIX	-

[a] relative standard error (standard error divided by population estimate*100; for the random effects parameters RSE is related to the corresponding variance scale)

[b] CLL: linear clearance part; CLNL: non-linear clearance part (at concentrations<<Km); FFM: fat-free mass

[c] $V1\_FFM_{individual} = V1 * [1+ V1\_FFM * (FFM_{individual} - FFM_{median})] * EXP(\eta V1_{individual})$;
$CLL\_FFM_{individual} = CLL * [1 + CLL\_FFM * (FFM_{individual} - FFM_{median})] * EXP(\eta CLL_{individual} + \kappa CLL_{individual})$

reduced primary model for matuzumab obtained equally precise results for DD and better results for ED (RSE < 79%) despite one less covariate, being thus considered as the 'final model' (results are presented in Table 9, columns: Final Model and Evaluation 2).

3.3 Final model

For DD the new estimated population parameters for the fixed effects were almost the same as the primary values (e.g. CLL changed from 15.3 mL/h to 15.2 mL/h). Matuzumab was initially distributed to a restricted central volume of distribution of 3.7 L and a peripheral volume of distribution of 1.8 L. The inter-compartmental clearance Q (37.7 mL/h) indicated a limited distribution. RSEs for the fixed-effects parameters were in the same range compared to the RSEs of the primary model (between 3.2% for V1 and 30.2% for Km). The same behaviour was observed for the random-effects parameters with maximum differences between +3.8% to -4.5% points in CV and, in general, lower RSEs (highest RSE for the IIV on Vmax: 41.7%). Total clearance as the sum of CLL (15.2 mL/h) and CLNL (110.5 mL/h; calculated from Vmax, 0.453 mg/h, and Km, 4.1 mg/L) was 125.7 mL/h (at mAb concentrations <<Km). In Figure 6 upper panel, the dependence of total clearance on the concentration of the mAb is presented. At low mAb concentrations, until approximately 1 µg/mL, total clearance (blue line) was mainly influenced by the non-linear clearance part (lavendel line). At higher mAb concentrations, the impact of the non-linear part on the total clearance decreased and the linear part (red line) was dominating. In accordance with the non-linear behaviour, the half-life ranged between 4.7 and 10.3 days at concentrations of 20 and 1000 µg/mL, respectively (Figure 6, lower panel).

After reestimation of all parameter estimates for the evaluation dataset based on the final model, the population parameters for the fixed effects and respective RSEs were similar to those from the first estimation, except the RSE for Km (change from 40.0% to 52.2%; Table 9, columns: Evaluation 1 and 2). The remaining covariate influence was supported with a comparable value and the improvement of the new model was demonstrated by the random-effects parameters: the IIV on V2 and the correlation coefficient between V2 and Vmax were estimated with a higher precision (RSEs decreased from 112% to 78% and from 105% to 75%).
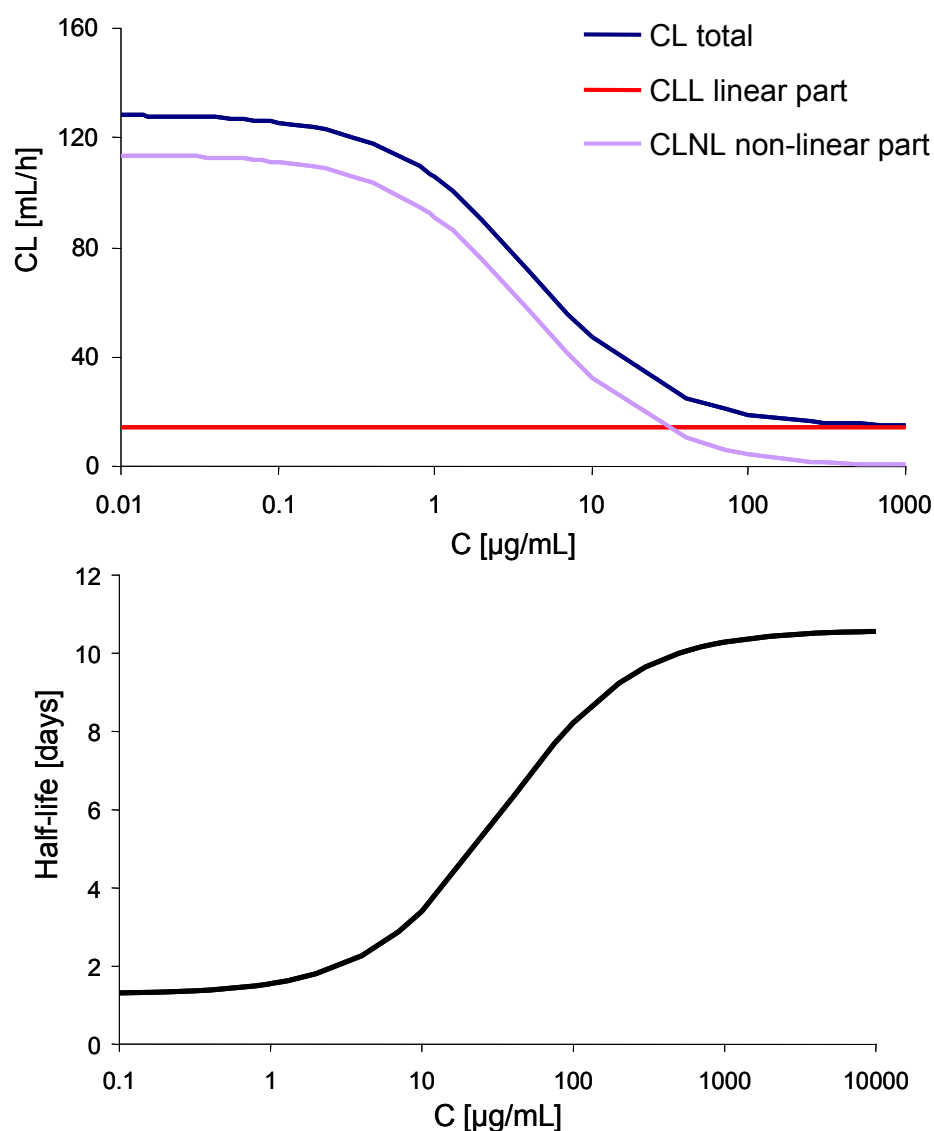
Figure 6 Upper panel: dependence of clearance on the concentration (C) of matuzumab; lower panel: dependence of half-life (in days) on C.

Overall, goodness of fit plots confirmed that the model performed well. Goodness of fit plots of the final model for the development and the evaluation dataset, respectively, are presented, on linear and log scale (for a better visualisation of the higher and lower concentration range), in Figure 7 (plots in A for DD and plots in B for ED), including population predictions *vs* observed concentrations and individual predictions *vs* observed concentrations. Population values for higher concentrations in the ED were underpredicted. However, individual values were adequately estimated. Additionally, to compare individual predicted and observed maximum concentrations (Cmax), concentrations at times equally or - due to the sparse data situation- less than one hour after the end of each administration (corresponding to Cmax after each administration) were analysed (see Figure 8).

In addition, the parameter values for the combined dataset were estimated (Table 9, column: Evaluation 3). In general, the estimates were obtained with higher precision than the estimates from the separate datasets (RSEs $\leq$ 28.9%).
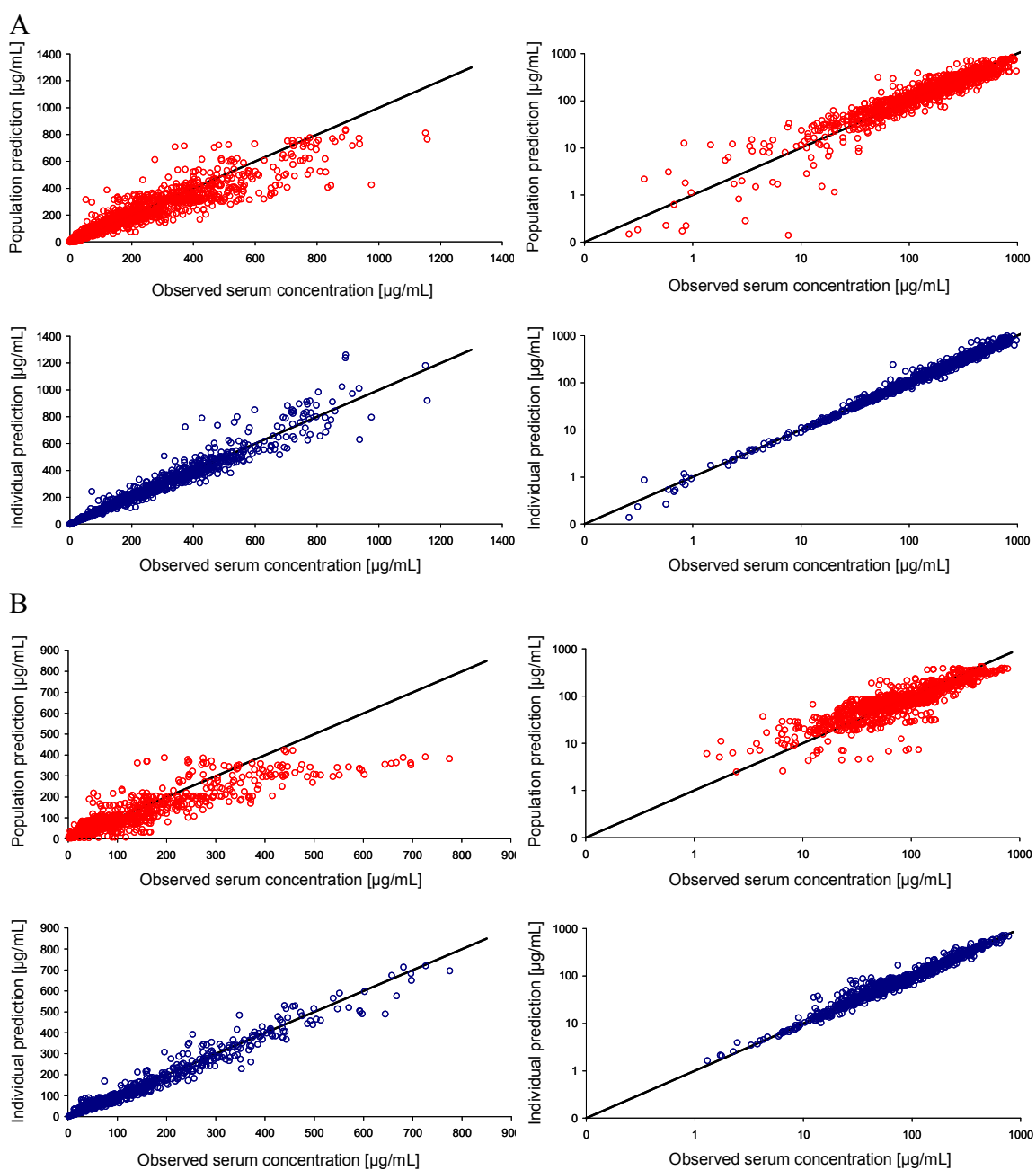

Figure 7 Goodness of fit plots for the final model for the development (A) and the evaluation (B) dataset on linear scale (left panel) and on logarithmic scale (right panel). Red: population predictions *vs* observed concentrations, blue: individual predictions *vs* observed concentrations.
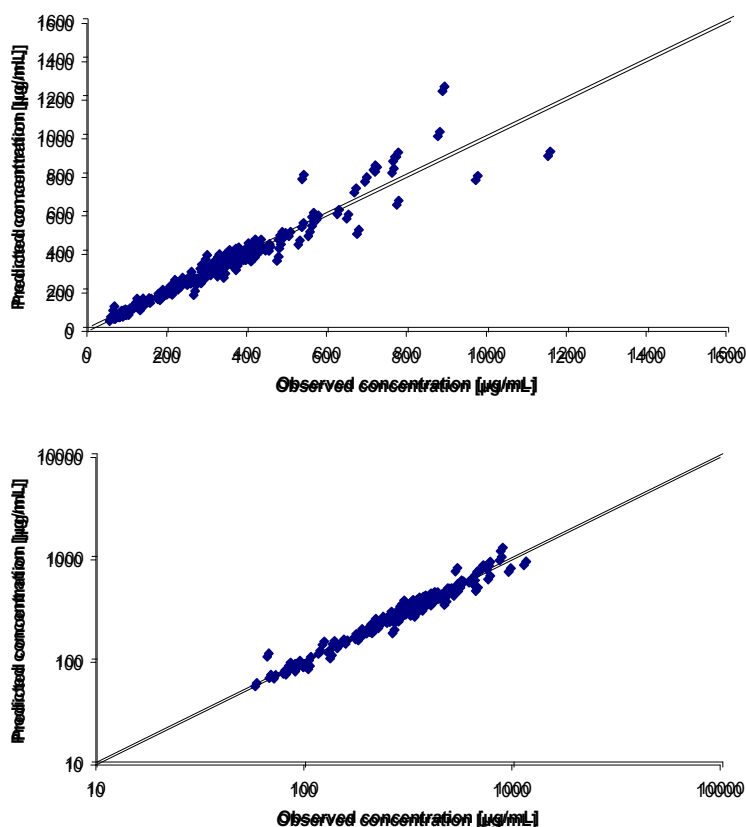
Figure 8 Individual predicted *vs* observed maximum concentrations from the development dataset on linear (upper panel) and log scale (lower panel).

3.4 Internal evaluation of the final model

The final model was profoundly analysed and evaluated by basic and advanced internal evaluation techniques. Basic internal evaluation included the presentation of goodness of fit plots and RSEs for all model parameters (see Figure 7 and Table 9). The bootstrap method, case deletion diagnostics and visual predictive checks were utilised as advanced internal evaluation techniques. The results are presented in the next sections 3.4.1, 3.4.2 and 3.4.3.

3.4.1 Model evaluation by the bootstrap method

From 200 successful bootstrap runs the values for the calculated bootstrap median, the bias and the relative bias compared to the original estimate values are presented in Table 10. For the fixed-effects parameters, the bootstrap medians were very similar to the original model values, and the relative bias for these parameters ranged from -1.2%

(for Vmax) to +4.2% (for the covariate relation FFM on CLL). Hence, the description of the structural model was accurate and precise. The bootstrap medians for the random-effects parameters were also in the same range of the original values with only small bias (relative bias from -1.2% for the correlations between V1/V2 and V2/Vmax up to +4.3% for IIV on CLL).

All original model estimates from the final model were in the 95% confidence intervals, which were calculated by the 2.5[th] and 97.5[th] percentiles of the 200 values for each parameter. Histograms (including respective curves for Gaussian distribution) were visually inspected. In general, it can be anticipated, that the distributions of the obtained values seemed to follow the Gaussian distribution. Additionally, the box-and-whisker plots visualised the normal distribution, including the lower and upper quartile (box), the median (horizontal line in the box, generally situated in the middle of the box, except for IOV on CLL), the almost similar spread of the whiskers (the ends of the whiskers representing the largest and the smallest values that are not outliers) and the low number of outliers (dots, values that are smaller or larger than 1.5 box-lengths from the lower or upper quartile). For the important clearance parameters CLL, IIV on CLL, IOV on CLL and the covariate relation FFM on CLL the histograms (left panel) and box-and-whisker plots (right panel) are exemplarily presented in Figure 9.

Table 10 Results from 200 bootstrap runs in comparison to the final model.

Model parameter	Unit	Final Model estimate	Bootstrap median[a]	Bias[a]	Relative bias, %[a]	95% Confidence interval (2.5[th] and 97.5[th] percentile)
Fixed effects						
CLL[b]	[mL/h]	15.2	15.0	+0.2	+1.3	13.6 – 16.7
V1	[L]	3.73	3.74	-0.01	-0.3	3.55 – 3.88
Q	[mL/h]	37.7	37.6	+0.01	+0.4	30.0 – 47.6
V2	[L]	1.84	1.84	0	0	1.59 – 2.15
Vmax	[mg/h]	0.453	0.459	-0.006	-1.2	0.371 – 0.565
Km	[mg/L]	4.1	4.1	-0.03	-0.6	3.5 – 6.2
Covariate influence						
CLL_FFM[b]		0.0119	0.0114	+0.0005	+4.2	0.0070 – 0.0166
Random effects						
Interindividual variability						
ω CLL[b]	[%CV]	22.7	21.7	+1.0	+4.3	14.2 – 28.8
ω V1	[%CV]	24.1	23.8	+0.3	+1.3	20.3 – 27.5
ω V2	[%CV]	60.7	59.0	+1.7	+2.8	45.1 – 74.0
ω Vmax	[%CV]	47.6	47.2	+0.4	+0.8	34.8 – 61.4
Correlation V1_V2		0.780	0.790	-0.01	-1.2	0.654 – 0.923
Correlation V2_Vmax		0.862	0.872	-0.01	-1.2	0.722 – 0.970
Correlation V1_Vmax		0.940	0.950	-0.01	-1.1	0.785 – 1.002
Interoccasion variability						
π CLL[b]	[%CV]	22.5	22.6	-0.1	-0.7	13.8 – 30.9
Residual error						
σ proportional	[%CV]	13.4	13.5	-0.1	-0.6	11.9 – 14.8
σ additive	[mg/L]	0.312 FIX	0.312 FIX	-	-	-

[a] obtained from 200 bootstrap runs; bias = (final model estimate – bootstrap median); relative bias = 100 * ((final model estimate - bootstrap median) / final model estimate)
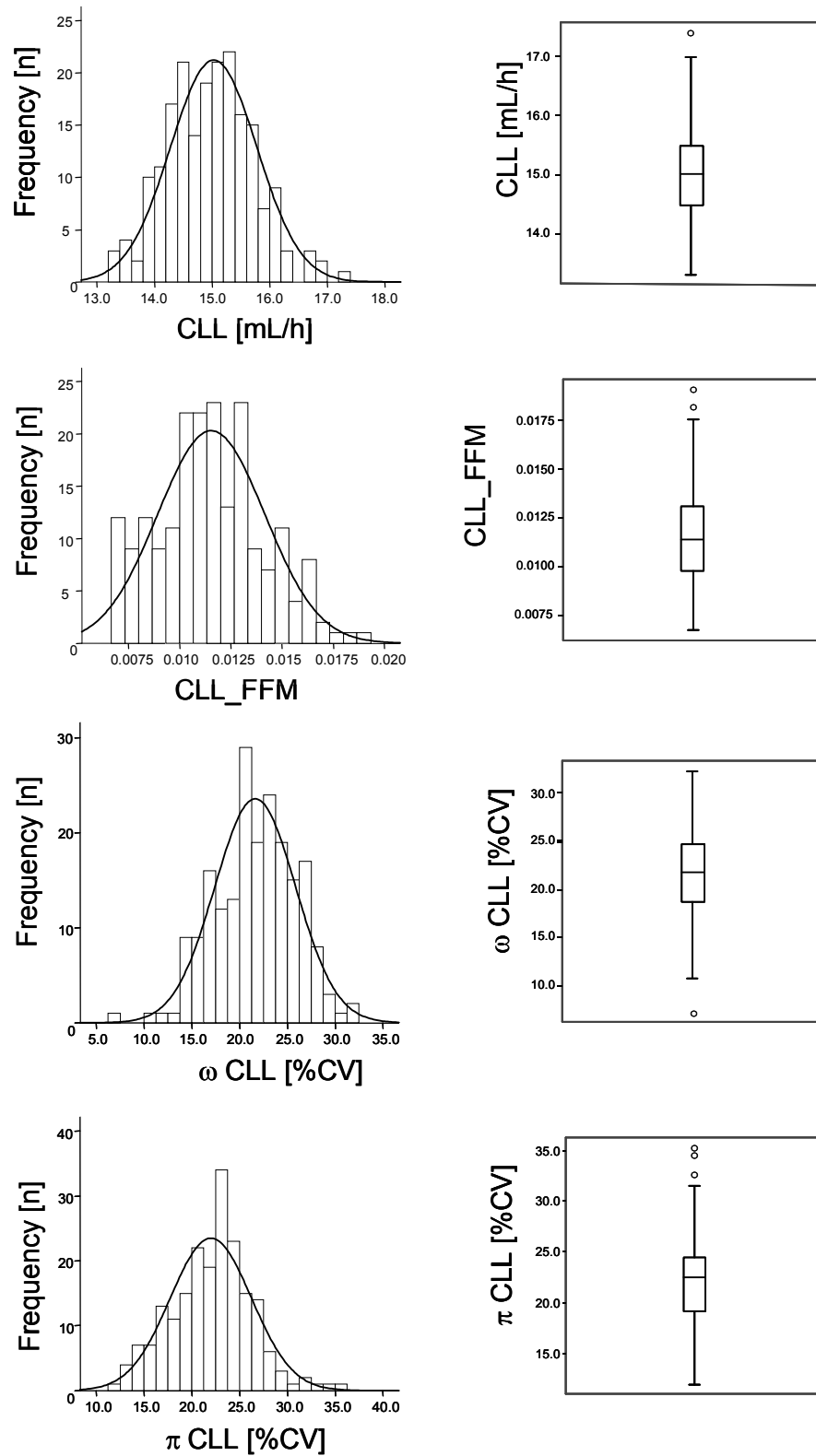[b] CLL: linear clearance part; FFM: fat-free mass

Figure 9 Histograms (left panel) and box-and-whisker plots (right panel) of the distribution of the clearance parameters (from the 200 bootstrap runs). Respective curves incorporated into the histograms indicate Gaussian distribution.

3.4.2   Model evaluation by case deletion diagnostics

The results from the four performed case deletion scenarios (see section 2.4.2.2) were analysed graphically. In general, all new estimates from all scenarios were estimated close to and uniformly distributed around the respective original estimate value.

In the scenarios 1 (deletion of 10% of the study population, see Figure 10) and 2 (deletion of one study subject, see Figure 11) three new parameter estimates were outside the 95% confidence interval (based on calculated standard errors) after reestimation of all model parameters on the basis of the new reduced datasets. In the scenarios 3 (Figure 12) and 4 (Figure 13) the new parameter estimates (parameter values from scenarios 1 and 2) for nine model parameters (Km, IIV on CLL, Vmax, V1 and V2, covariate relation FFM on CLL, correlation parameter between V1 and V2, V1 and Vmax, V2 and Vmax) were analysed with new confidence intervals (according to assumed RSEs of 15%). In scenario 1, two of the estimates for IOV on CLL (dataset 2 and dataset 10) reached a value less than the lower boundary of the 95% confidence interval. In scenario 2, one study subject (ID 4) showed an influence on the IOV on CLL. In the scenarios 3 and 4 no additional estimate obtained a value outside the new confidence intervals (two estimates in scenario 3 [one for IIV on CLL and one for the covariate relation FFM on CLL] and one estimate in scenario 4 [for IIV on CLL] reached a value close to the confidence interval boundaries).

After the results from scenario 2 and closer examination of ID 4 one specific observation from this ID (338 hours after the second administration) was responsible for the IOV value being outside the 95% confidence interval. The concentration of this observation was far too high for the time that has passed after the last administration. To correctly incorporate this concentration into the model, the IOV for this ID and observation had to be very high. Prior to further investigations, the outlier concentration was rechecked in the corresponding study report, but the value was confirmed. Additionally, the sample had been analysed twice at the bioanalysis institute. Hence, the influence on parameter estimation by the deletion of both, the whole subject and only the responsible high concentration, was analysed (see Table 11).

The dataset excluding ID 4 led to a reduction of the IOV from an original value of 22.5% CV to a value of 18.7% CV (decrease of ~ 17%). All other model parameter
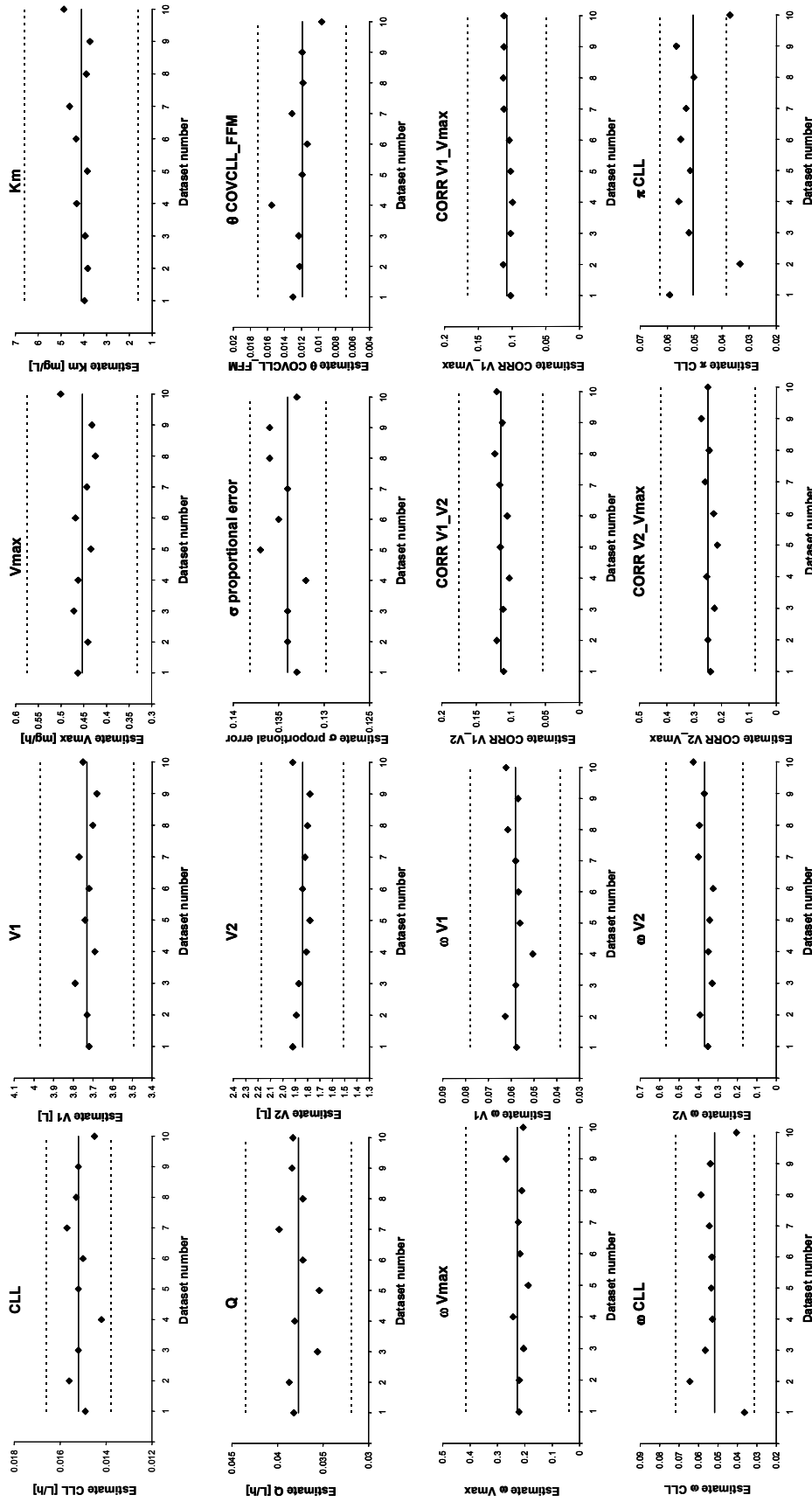
Figure 10 Case deletion diagnostics (scenario 1): deletion of 10% of the study population; confidence intervals (dashed lines), original estimates from final model (solid lines), new parameter estimates (diamonds).
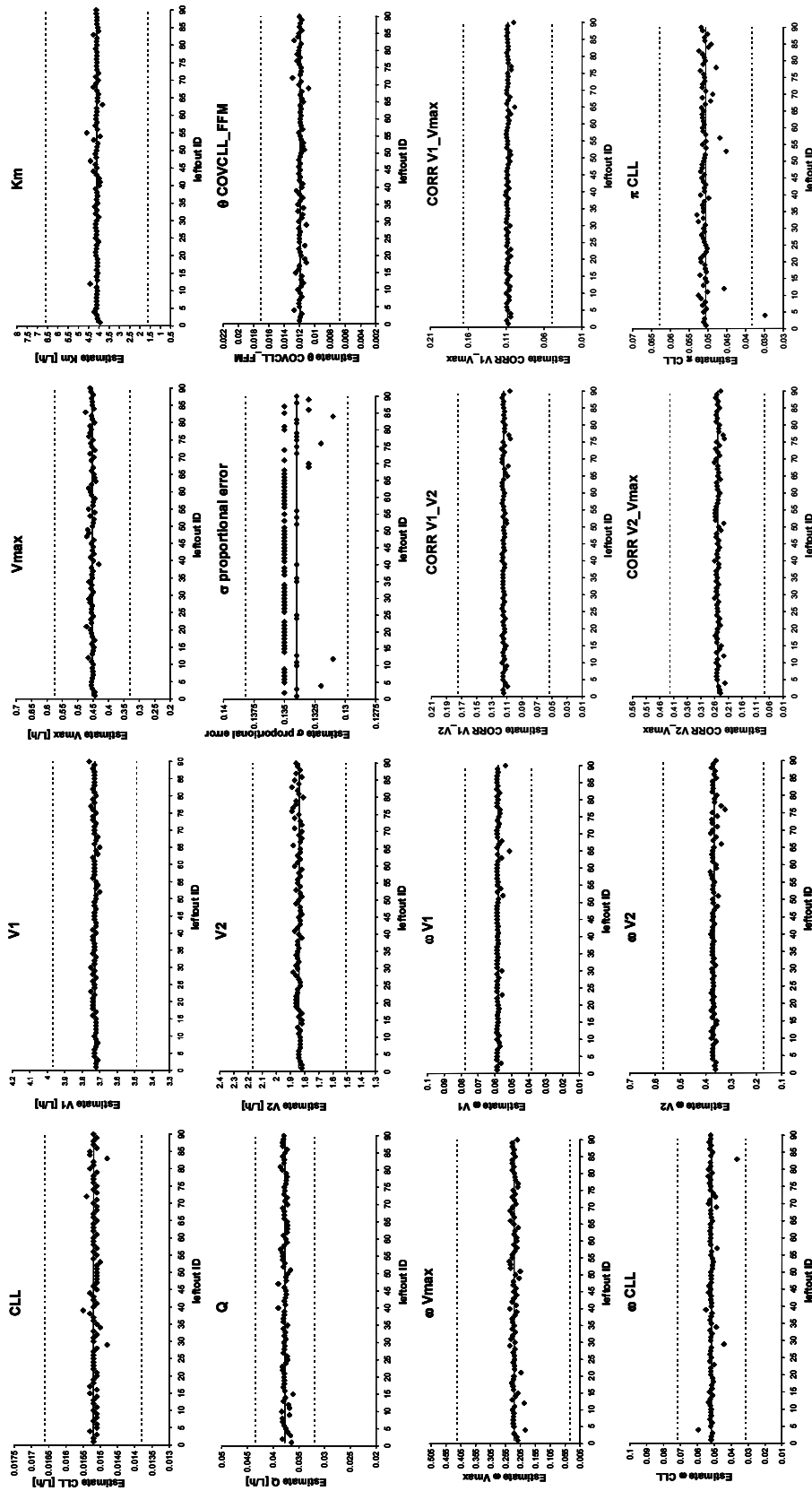
Figure 11 Case deletion diagnostics (scenario 2): deletion of one study subject; confidence intervals (dashed lines), original estimates from final model (solid lines), new parameter estimates (diamonds).
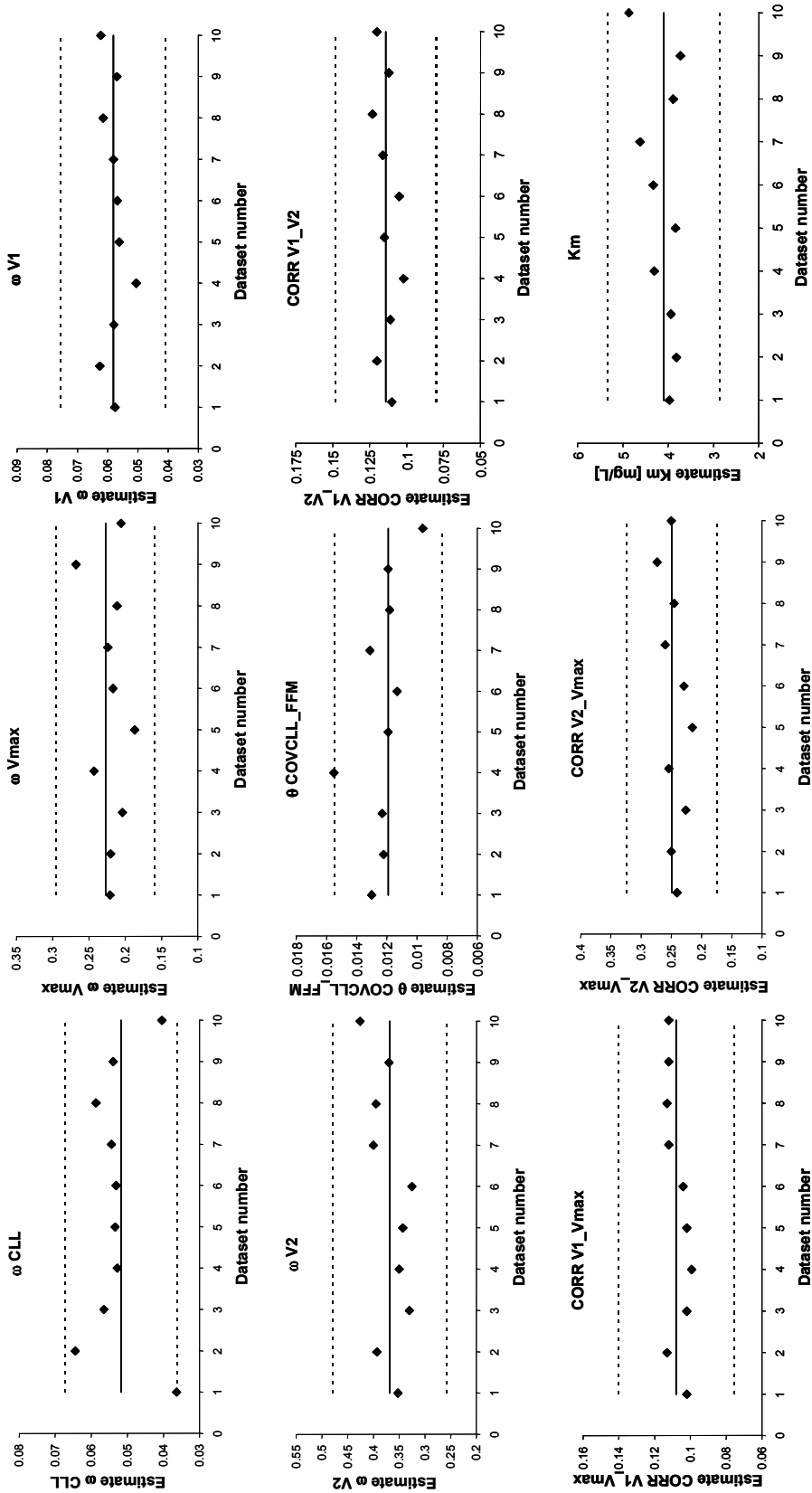
45

Figure 12 Case deletion diagnostics (scenario 3), new confidence intervals: deletion of 10% of the study population; confidence intervals (dashed lines), original estimates from final model (solid lines), new parameter estimates (diamonds).
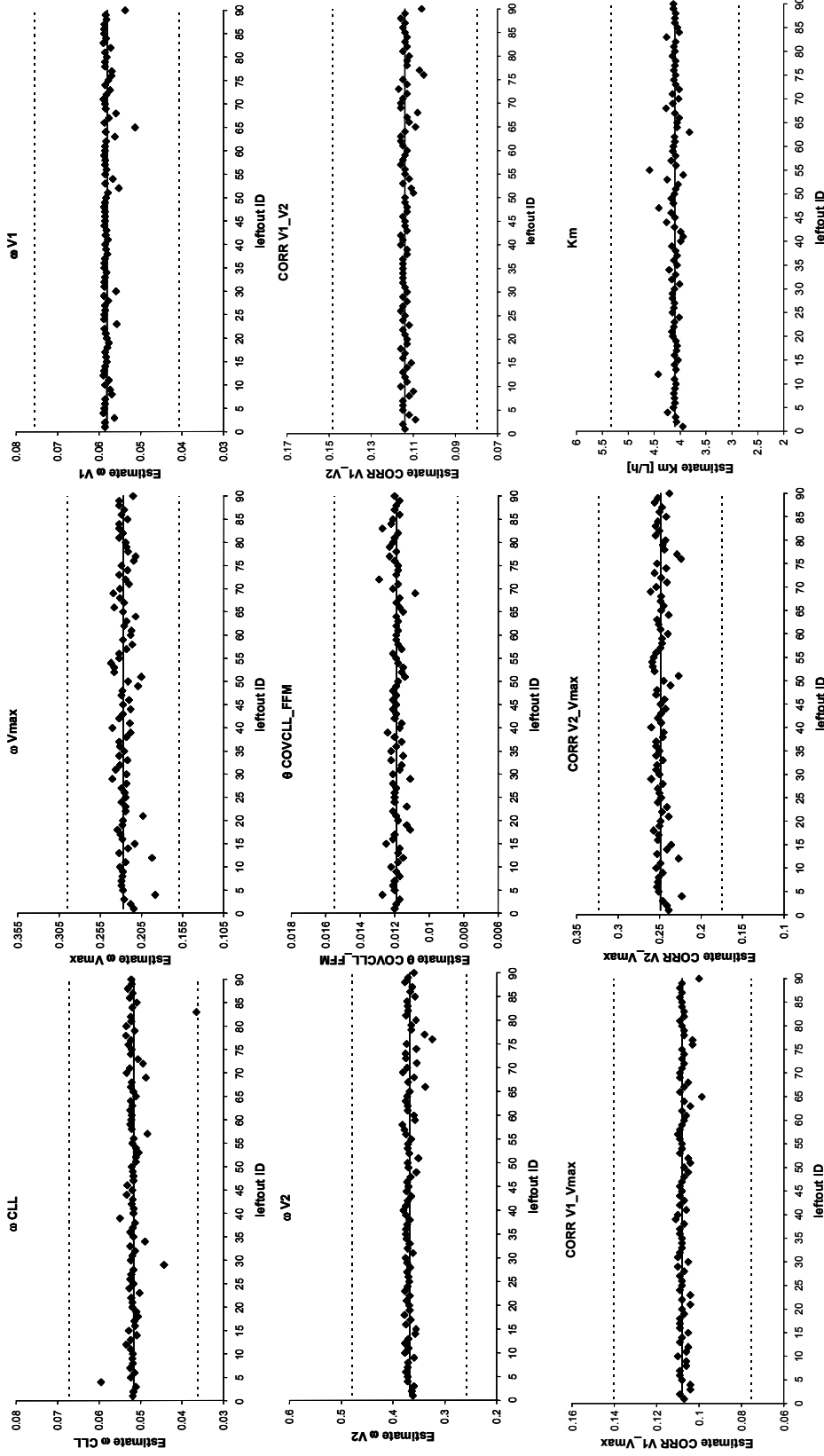
Figure 13 Case deletion diagnostics (scenario 4), new confidence intervals: deletion of one study subject; confidence intervals (dashed lines), original estimates from final model (solid lines), new parameter estimates (diamonds).

estimates were similar to the original parameters, only for the covariate relation a slight difference was observed (+/-1.2%/kg to +/-1.3%/kg). After deletion of the influential concentration value (DV) from the dataset and reestimation of all parameters with the reduced dataset, the obtained new model parameters, including the covariate relation, displayed only marginal differences to the original values and equal precision. Only the IOV value decreased from 22.5% CV to 18.3% CV (19% redcution). Model parameters obtained from the complete dataset, from the dataset reduced by the whole individual and from the dataset reduced by only the influential concentration value (Table 11, columns: Final Model, Final Model – ID 4, Final Model – ID 4, 1 DV) are presented.

Table 11 Parameter estimates after case deletion (ID 4 or ID 4, 1 DV) in comparison to the final model parameter values.

Model Parameter	Unit	Final Model Population estimate	RSE, %[a]	Final Model – ID 4 Population estimate	RSE, %[a]	Final Model – ID 4, 1 DV Population estimate	RSE, %[a]
Fixed effects							
CLL [b]	[mL/h]	15.2	4.4	15.3	4.6	15.4	4.7
V1	[L]	3.73	3.2	3.73	3.4	3.73	3.4
Q	[mL/h]	37.7	7.7	37.1	7.1	37.6	7.1
V2	[L]	1.84	9.0	1.84	9.0	1.84	8.8
Vmax	[mg/h]	0.453	13.4	0.456	12.8	0.459	12.9
Km	[mg/L]	4.1	30.2	4.2	29.2	4.3	28.7
Covariate influence							
CLL_FFM [b, c]		0.0119	21.6	0.0127	21.3	0.0120	22.8
Random effects							
Interindividual variability							
ω CLL [b]	[%CV]	22.7	19.5	24.4	19.2	24.8	19.2
ω V1	[%CV]	24.1	17.1	24.3	24.8	24.1	26.5
ω V2	[%CV]	60.7	27.0	61.0	29.8	60.5	29.8
ω Vmax	[%CV]	47.6	41.7	43.4	38.6	43.2	39.8
Correlation V1_V2		0.780	26.6	0.757	20.1	0.761	30.3
Correlation V2_Vmax		0.862	34.7	0.843	34.4	0.841	35.0
Correlation V1_Vmax		0.940	26.9	0.988	28.6	0.988	29.1
Interoccasion variability							
π CLL [b]	[%CV]	22.5	12.1	18.7	17.2	18.3	17.2
Residual error							
σ proportional	[%CV]	13.4	1.6	13.2	1.4	13.3	1.4
σ additive	[mg/L]	0.312 FIX	-	0.312 FIX	-	0.312 FIX	-

[a] relative standard error (standard error divided by population estimate*100; for random effects parameters RSE is related to the corresponding variance scale)
[b] CLL: linear clearance part; CLNL: non-linear clearance part (at concentrations<<Km); FFM: fat-free mass
[c] $CLL\_FFM_{individual} = CLL * [1 + CLL\_FFM * (FFM_{individual} - FFM_{median})] * EXP(\eta CLL_{individual} + \kappa CLL_{individual})$

3.4.3 Model evaluation by visual predictive checks

Single dosing

The results from the visual predictive checks (see section 2.4.2.3) for single dosing of matuzumab (400, 800, 1200 and 1600 mg administration) were analysed on a linear

scale and on a semi-log scale (to better visualise higher and lower concentrations). In Figure 14 the results from the 400 mg and the 1200 mg matuzumab single dosing are presented on linear scale. The area between the two blue solid lines represents the 90% prediction interval and the red solid line signifies the central tendency obtained from 1000 simulated new concentration-time profiles. The black diamonds symbolise the observed serum concentrations.
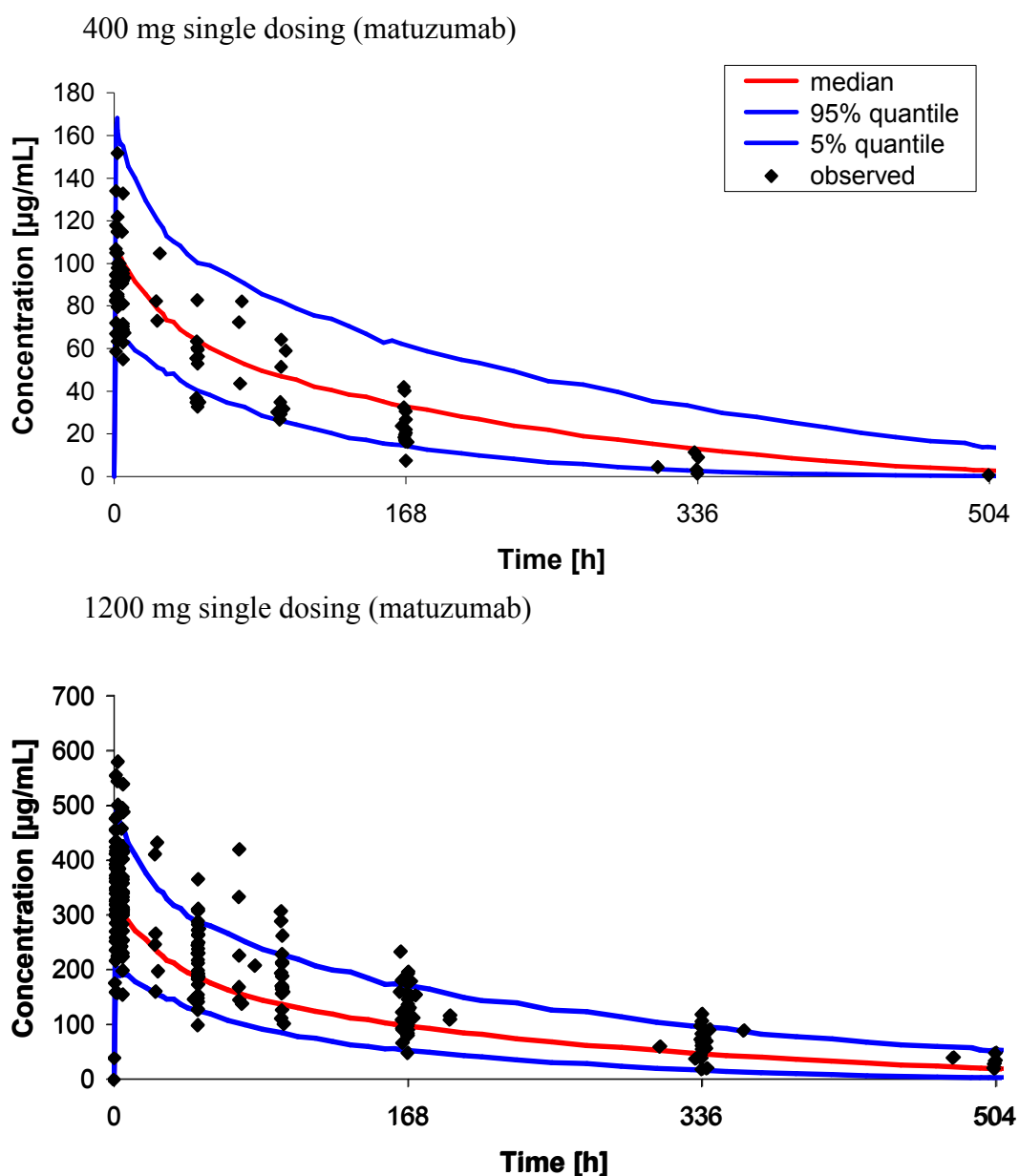
400 mg single dosing (matuzumab)

1200 mg single dosing (matuzumab)

Figure 14 Visual predictive checks for 400 mg (upper panel) and 1200 mg (lower panel) single dosing of matuzumab.

For the 400 mg single dosing VPC plot the predicted median concentration-time course was slightly higher compared to the original measured concentrations. Also, the variability seemed to be marginally higher, but for the other single dosing administrations the predictive performance was in high agreement with the observed data, because most of the original datapoints were inside the 90% prediction interval and only some outside. For the single dosing plots all available original datapoints were included into the plots, i.e. from all dosing regimens with a first dosing of 400, 800, 1200 or 1600 mg matuzumab, concentrations before the second administration were incorporated. Regarding the 1200 mg single dosing group, this plot included the largest amount of datapoints. Here, the central tendency of the median concentration-time course was marginally underpredicted compared to the observed data. For the other single dosing administrations the 90% prediction intervals and medians were in good agreement with the observed data, because most of the original datapoints were inside the prediction interval. In total, the predictive performance of the model, even including residual variability, was in good agreement with observed data for single dosing administration.

Multiple dosing

VPCs for multiple dosing were performed for each dose group separately and for the duration of 8 weeks, because for later timepoints only few original datapoints were available. From dose groups with only few original concentrations it could be anticipated that the variability and by this the 90% prediction interval was slightly larger than obtained from observed data (see Figure 15: dose group 1200 mg every two weeks), but from the plots of the dose groups where a larger number of datapoints were available, this variability was in good agreement with the observed data (see Figure 15: dose group 1200 mg every three weeks). For the visual inspection of the graphs it had to be taken into account that for the simulation of the 1000 new concentration-time profiles the planned timepoints were considered, but for the original serum concentrations the actual timepoints. Thus, a discrepancy appeared for some original datapoints lying outside the 90% prediction interval (see Figure 15: dose group 1600 mg weekly, marked datapoints). Originally these were pre-dose samples, but samples were taken later than the original 'time planned'; however, the actual timepoints were still before the next administration.

1200 mg every two weeks (matuzumab)
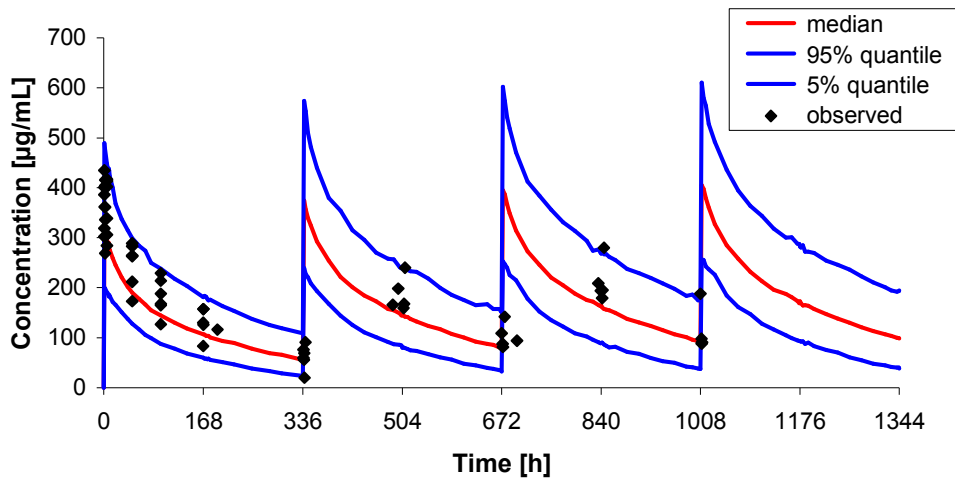
1200 mg every three weeks (matuzumab)
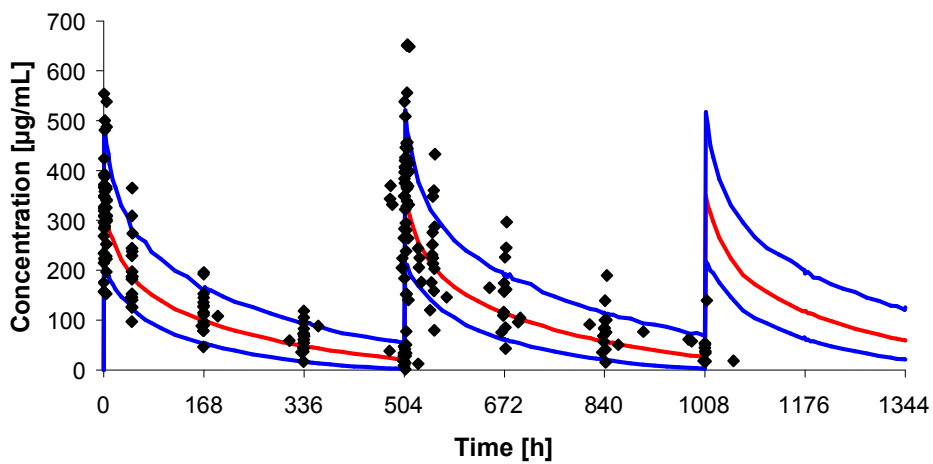
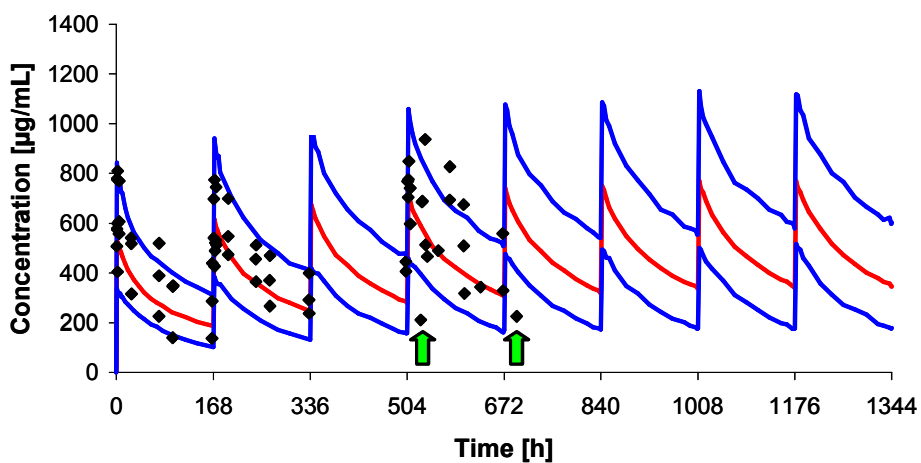2000 mg for the first week, followed by 1600 mg weekly (matuzumab)

Figure 15 Visual predictive checks for three different dosing regimens over 8 weeks; note: marked data points are examples for pre-dose samples.

Part II

3.5   Simulations

Three different simulation scenarios were performed based on the final population PK model for matuzumab:

Scenario 1a/1b: To determine the impact of dosing on the PK profiles in the central and in the peripheral compartment three subjects with the same cumulative dose of matuzumab of different dosing regimens (SIM-ID A: 400 mg weekly, SIM-ID B: 800 mg every two weeks and SIM-ID C: 1200 mg every three weeks) were simulated with the median FFM of 53 kg (i.e. differences in simulated profiles were not obtained from the covariate relation because the subjects had the same FFM value).

Simulated profiles for the central compartment (scenario 1a) are presented in Figure 16. The simulated minimum steady-state concentrations after 12 weeks (2014 hours, shortly before next infusion) were: 90 (SIM-ID A), 65 (SIM-ID B) and 44 (SIM-ID C) µg/mL. For the maximum steady-state concentrations after 2017 hours (i.e. Cmax after end of infusion) values of 196 (SIM-ID A), 277 (SIM-ID B) and 363 (SIM-ID C) µg/mL were reached. These values corresponded to a difference of Δ-51% for minimum steady-state concentrations and Δ-46% for maximum steady-state concentrations (highest values were set to 100%, respectively).

Simulated profiles for the peripheral compartment (scenario 1b) are presented in Figure 17. The simulated minimum steady-state concentrations after 12 weeks (2014 hours, shortly before next infusion) were: 107 (SIM-ID A), 78 (SIM-ID B) and 54 (SIM-ID C) µg/mL. For the maximum steady-state concentrations values of 140 (SIM-ID A, after 2070 hours), 168 (SIM-ID B, after 2090 hours) and 203 (SIM-ID C, after 2090 hours) µg/mL were reached (respective hours corresponded to Cmax after end of infusion). These values represented a difference of Δ-50% for minimum steady-state concentrations and Δ-31% for maximum steady-state concentrations (highest values were set to 100%, respectively).
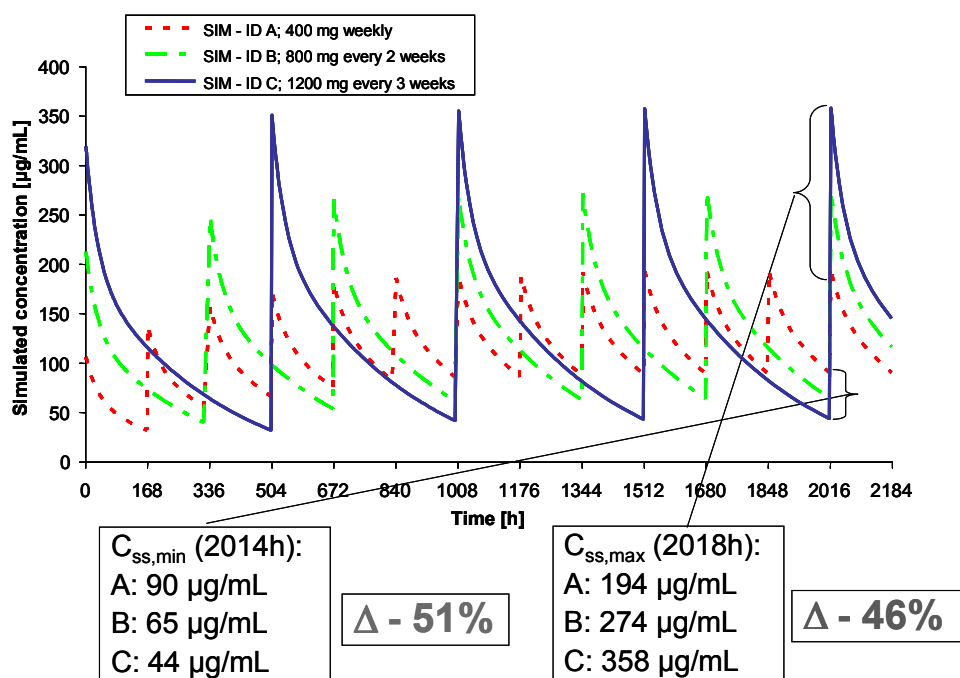
Figure 16 Simulation of concentration-time profiles of three different dosing regimens with the same mean dose amount per week in the central compartment (scenario 1a).
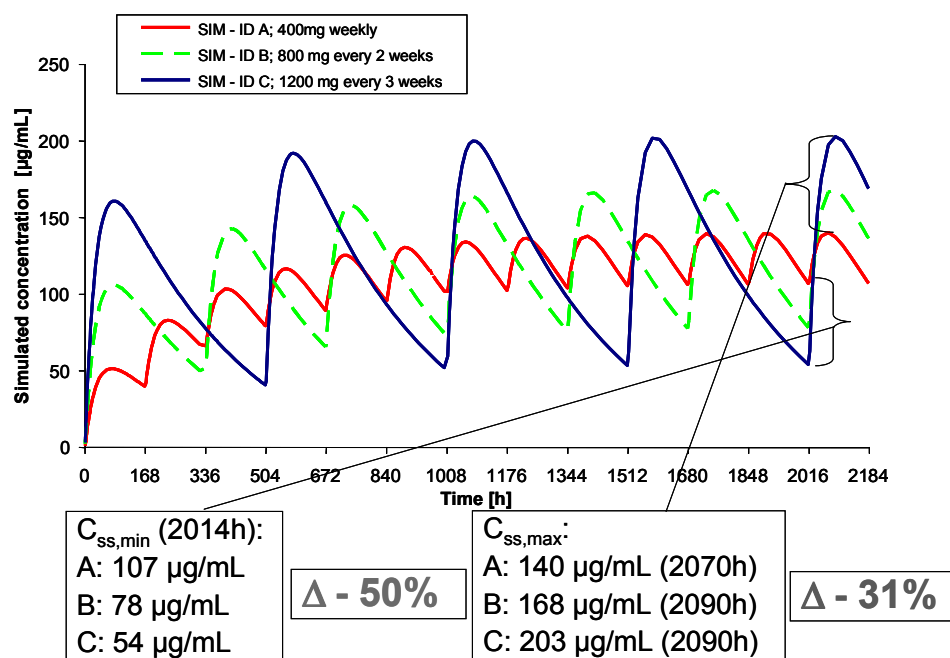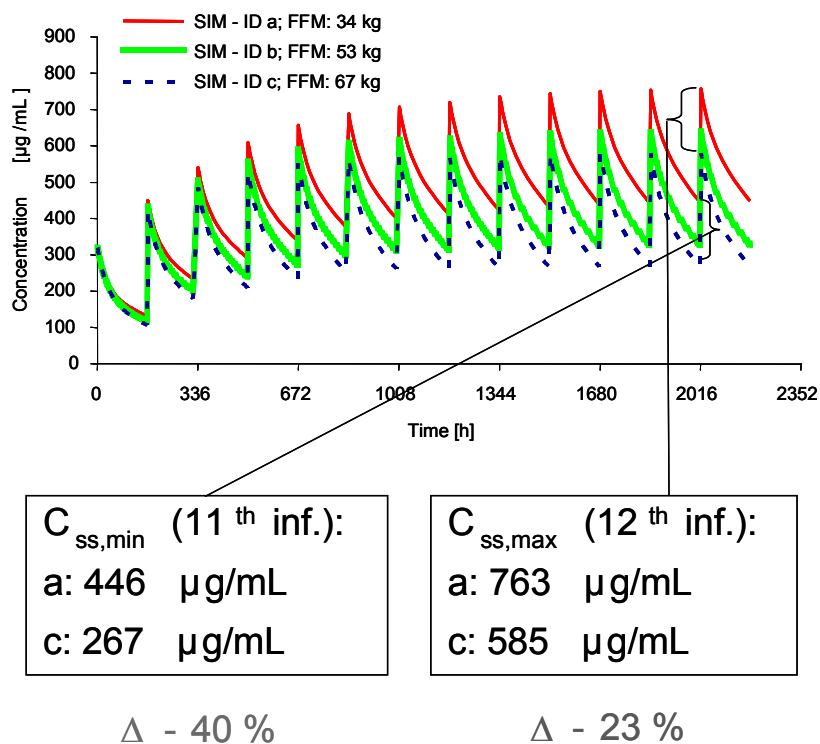

Figure 17 Simulation of concentration-time profiles of three different dosing regimens with the same mean dose amount per week in the peripherial compartment (scenario 1b).

Scenario 2: The final population PK model for matuzumab (described in sections 3.2 and 3.3; Table 9, column: Final Model) included the covariate FFM on CLL. To visualise the impact of this covariate relation on the PK profiles three subjects (representing the 5th, 50th and 95th FFM percentiles of the development study population: 34, 53 and 67 kg, respectively) were simulated with a dosing regimen of 1200 mg weekly. Simulated profiles showed a large variability in minimum (Δ-40%) and maximum (Δ-23%) steady-state concentrations, but less variability for the first infusions (Figure 18, upper panel). These observations were confirmed by the simulation of all study subjects with their original FFM values (Figure 19): the large variability in minimum and maximum steady-state concentrations was not driven by only a few subjects but by the whole study population. Additionally, to confirm these results by original data, the minimum steady-state concentrations after each occasion from each study subject from study 4 were compared and a remarkable increase of the minimum concentration range over time was assessed (Figure 20).

Scenario 3: Based on the results from scenario 2, a new dosing strategy was developed for matuzumab. Exemplarily Figure 18, lower panel, presents the resulting PK profiles simulated with a proposed adapted dosing regimen of original dosing (e.g. 1200 mg weekly) for the first four weeks (loading doses) followed by an adapted weekly dosing (based on the fractional covariate influence on total clearance, i.e.: only the linear clearance part was influenced by FFM) according to 50% of the original dosing (e.g. 600 mg) plus a proportionally adapted amount (e.g. 11.4 mg/kg FFM, because 11.4 mg * 53 kg FFM [median FFM] = 600 mg). Compared to the 1200 mg weekly simulations, the dose adaption resulted in a remarkable decrease of differences in minimum steady-state concentrations ($C_{ss,min}$) from Δ-40% (SIM-ID a to SIM-ID c) to Δ-16% (SIM-ID a* to SIM-ID c*) and for maximum steady-state concentrations ($C_{ss,max}$) from Δ-23% (SIM-ID a to SIM-ID c) to Δ-6% (SIM-ID a* to SIM-ID c*).

1200 mg weekly (matuzumab)

$C_{ss,min}$ (11th inf.):
a: 446 µg/mL
c: 267 µg/mL

$C_{ss,max}$ (12th inf.):
a: 763 µg/mL
c: 585 µg/mL

Δ - 40 %   Δ - 23 %

1200 mg weekly for the first four infusions – dose adaption from infusion 5: 600 mg + 11.4 mg/kg FFM (matuzumab)

$C_{ss,min}$ (11th inf.):
a*: 364 µg/mL
c*: 307 µg/mL

$C_{ss,max}$ (12th inf.):
a*: 624 µg/mL
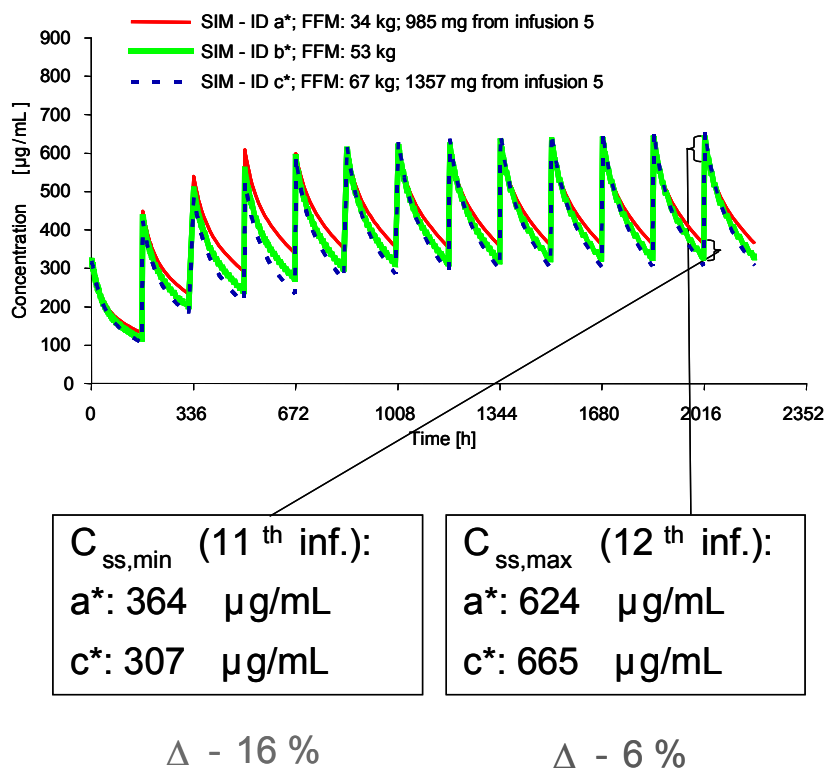c*: 665 µg/mL

Δ - 16 %   Δ - 6 %

Figure 18 Simulations of the covariate impact (upper panel, scenario 2) and of the reduction of steady-state variability by a proposed dose adaption (lower panel, scenario 3).
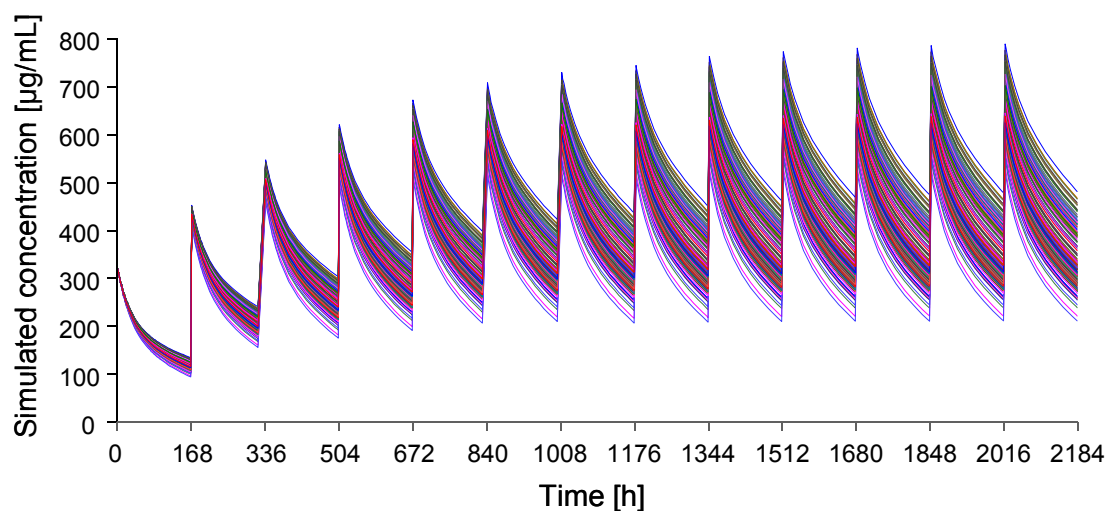
Figure 19 Simulation of the impact of the covariate relation on the pharmacokinetic profiles: simulation of all 171 study subjects receiving 1200 mg matuzumab weekly dosing.
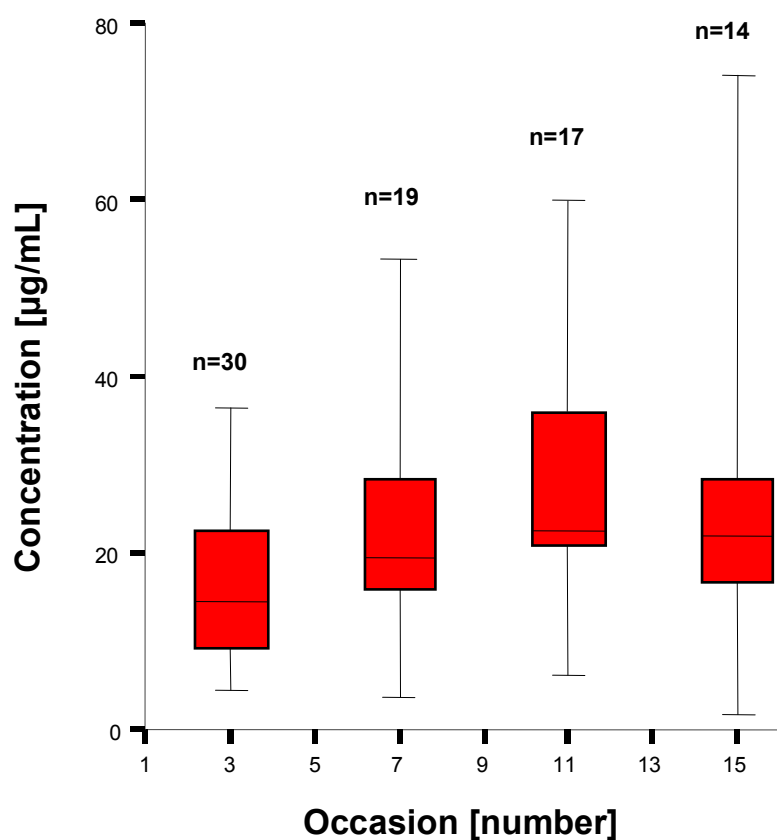

Figure 20 Box-whisker plots of minimum concentrations in study 4 at different occasions (every new occasion corresponded to another infusion).

3.6 Body size descriptors in population analyses

To derive a general conclusion for the usage of body size descriptors in population analyses for monoclonal antibodies different investigations have been performed.

Investigation 1)

In the population PK analysis for matuzumab body weight, body surface area and fat-free mass were considered and compared as body size descriptors for the covariate relation on CLL. The final model including the covariate fat-free mass on CLL served as reference. For both, the development and the evaluation dataset, the results from the different covariate models, including all model parameters, are presented in Table 12a and Table 12b, respectively. Comparing obtained objective function values, the covariate models including the fat-free mass relation reached the lowest values (for DD: 9713.56 and for ED: 7898.35). The OFV differences for DD between the FFM-based model and

      i)   the WT-based model and

      ii)   the BSA-based model

were ΔOFV-8.7 and ΔOFV-5.3, respectively. These results represented a statistically significant improvement for DD when including FFM compared to the other body size descriptors.

For ED an improvement was observed (ΔOFV-3.3 and ΔOFV-0.8) but not a significant decrease in the OFV (significant decrease: ΔOFV-3.84, $p<0.05$, df=1).

For the combined datasets the WT-based and the BSA-based model failed to converge and accordingly relative standard errors were not available. However, the estimated parameters at the last iteration were comparable to those obtained for the FFM-based model (see Table 9: Evaluation 3) and hence, it was considered to be feasible to analyse the OFV differences. The OFV differences between the FFM-based model (OFV: 17844.4) and

      i)   the WT-based model (OFV: 17851.3) and

      ii)   the BSA-based model (OFV: 17846.4)

showed a significant decrease compared to the WT-based model (ΔOFV-6.9) and a not significant decrease compared to the BSA-based model (ΔOFV-2.0).

Table 12a Parameters from different body size descriptor models (obtained for the development dataset, DD).

Model Parameter	Unit	Weight Model (DD) Population estimate	RSE, % [a]	Body Surface Model (DD) Population estimate	RSE, % [a]	Fat-free mass Model (DD) Population estimate	RSE, % [a]
Fixed effects							
CLL [b]	[mL/h]	14.5	4.0	14.7	4.2	15.2	4.4
V1	[L]	3.73	3.2	3.72	3.2	3.73	3.2
Q	[mL/h]	38.2	7.7	38.2	7.7	37.7	7.7
V2	[L]	1.85	9.1	1.84	9.0	1.84	9.0
Vmax	[mg/h]	0.465	13.4	0.462	13.5	0.453	13.4
Km	[mg/L]	4.3	29.6	4.3	29.8	4.1	30.2
Covariate influence							
CLL_WT [b,1]		0.0072	33.6	-	-	-	-
CLL_BSA [b,2]		-	-	0.5470	27.6	-	-
CLL_FFM [b,3]		-	-	-	-	0.0119	21.6
Random effects							
Interindividual variability							
ω CLL [b]	[%CV]	23.9	19.7	23.4	19.8	22.7	19.5
ω V1	[%CV]	24.1	17.1	24.1	17.1	24.1	17.1
ω V2	[%CV]	61.0	27.2	60.3	27.0	60.7	27.0
ω Vmax	[%CV]	51.1	40.6	50.0	40.8	47.6	41.7
Correlation V1_V2		0.789	26.8	0.784	27.0	0.780	26.6
Correlation V2_Vmax		0.870	33.8	0.871	33.9	0.862	34.7
Correlation V1_Vmax		0.910	28.4	0.913	28.2	0.940	26.9
Interoccasion variability							
π CLL [b]	[%CV]	22.7	12.1	22.7	11.9	22.5	12.1
Residual error							
σ proportional	[%CV]	13.4	1.5	13.4	1.5	13.4	1.6
σ additive	[mg/L]	0.312 FIX	-	0.312 FIX	-	0.312 FIX	-
Objective function value		9722.3		9718.9		9713.6	

[a] relative standard error (standard error divided by population estimate*100; for the random effects parameters RSE is related to the corresponding variance scale)
[b] CLL: linear clearance; WT: weight; BSA: body surface area; FFM: fat-free mass
[1] $CLL\_WT_{individual} = CLL * [1+ CLL\_WT * (WT-WT_{median})] * EXP(\eta CLL+\kappa CLL)$
[2] $CLL\_BSA_{individual} = CLL * [1+ CLL\_BSA * (BSA-BSA_{median})] * EXP(\eta CLL+\kappa CLL)$
[3] $CLL\_FFM_{individual} = CLL * [1+ CLL\_FFM * (FFM-FFM_{median})] * EXP(\eta CLL+\kappa CLL)$

Table 12b Parameters from different body size descriptor models (obtained for the evaluation dataset, ED).

Model Parameter	Unit	Weight Model (ED) Population estimate	RSE, % [a]	Body surface area (ED) Population estimate	RSE, % [a]	Fat-free mass Model (ED) Population estimate	RSE, % [a]
Fixed effects							
CLL [b]	[mL/h]	11.6	9.8	12.1	9.5	12.0	9.8
V1	[L]	3.89	6.4	3.87	6.3	3.88	6.4
Q	[mL/h]	21.1	12.3	21.1	12.0	21.1	12.8
V2	[L]	2.69	14.9	2.65	14.9	2.67	16.1
Vmax	[mg/h]	0.584	20.9	0.571	20.5	0.563	21.5
Km	[mg/L]	6.0	38.6	5.6	41.6	5.1	52.2
Covariate influence							
CLL_WT [b,1]		0.0103	45.6	-	-	-	-
CLL_BSA [b,2]		-	-	0.7860	36.0	-	-
CLL_FFM [b,3]		-	-	-	-	0.0150	32.3
Random effects							
Interindividual variability							
ω CLL [b]	[%CV]	31.2	50.0	29.7	52.2	29.9	49.8
ω V1	[%CV]	40.4	26.7	40.3	26.7	40.4	26.9
ω V2	[%CV]	31.9	89.8	32.7	87.4	29.9	78.1
ω Vmax	[%CV]	56.4	45.3	54.8	45.7	53.9	47.1
Correlation V1_V2		0.907	43.2	0.748	47.6	0.986	41.8
Correlation V2_Vmax		0.600	81.4	0.608	78.4	0.626	74.9
Correlation V1_Vmax		0.725	46.6	0.782	46.1	0.725	51.0
Interoccasion variability							
π CLL [b]	[%CV]	55.1	21.1	54.6	21.0	55.0	21.8
Residual error							
σ proportional	[%CV]	18.9	2.5	18.9	2.5	18.9	2.5
σ additive	[mg/L]	0.312 FIX	-	0.312 FIX	-	0.312 FIX	-
Objective function value		7901.7		7899.1		7898.3	

[a] relative standard error (standard error divided by population estimate*100; for the random effects parameters RSE is related to the corresponding variance scale)
[b] CLL: linear clearance; WT: weight; BSA: body surface area; FFM: fat-free mass
[1] $CLL\_WT_{individual} = CLL * [1+ CLL\_WT * (WT\text{-}WT_{median})] * EXP(\eta CLL + \kappa CLL)$
[2] $CLL\_BSA_{individual} = CLL * [1+ CLL\_BSA * (BSA\text{-}BSA_{median})] * EXP(\eta CLL + \kappa CLL)$
[3] $CLL\_FFM_{individual} = CLL * [1+ CLL\_FFM * (FFM\text{-}FFM_{median})] * EXP(\eta CLL + \kappa CLL)$

Overall, the values for all fixed-effects model parameters from the WT-, BSA- and FFM-based models were in the same range (except for the covariate relation) and had similar precision (except a higher RSE of 52.5% for the Km parameter in the FFM-based model). For the random-effects parameters, comparably precise values were obtained. The lowest RSE values for the covariate relation were reached with the FFM-based models (for DD: 21.6% and for ED: 32.3%) compared to the WT-based (for DD: 33.6% and for ED: 45.6%) and the BSA-based (for DD: 27.6% and for ED: 36.0%) models. These results indicated that the covariate relations including FFM were estimated with the highest precision.

Investigation 2)

Simulations were performed to visualise the impact of the covariate effects of the different body size descriptors. The simulations based on the final model for matuzumab and performed with models including in each case one of the body size covariate relations (WT, BSA or FFM) showed similar simulated concentration-time profiles, respectively (Figure 21). For the simulation scenarios, IIV and residual error parameters were fixed to zero and therefore, the simulated concentration-time profiles represented the typical population behaviour for subjects with the chosen body size values. These values corresponded to the 5th, 50th, 95th body size percentiles of the study population for the matuzumab analysis with 171 patients (for FFM: 34, 54, 69 kg; for WT: 48, 71, 96 kg; for BSA: 1.47, 1.82, 2.18 m²). The spread at steady-state levels for the simulated concentration-time profiles, reflecting the covariate effect, was calculated for each covariate model between the simulated patients representing the 5th and the 95th body size percentiles. The difference among these patients for minimum steady-state concentrations after 2014 hours (i.e. shortly before next infusion) for the FFM- (WT-, BSA-) based model was Δ-42% between SIM-IDs 1 and 3 (Δ-35% between SIM-IDs 4 and 6, Δ-39% between SIM-IDs 7 and 9). Comparing the patients representing the respective 5th percentile (50th percentile; 95th percentile) for the body size descriptors FFM and WT between SIM–IDs 1 and 4 (SIM-IDs 2 and 5; SIM-IDs 3 and 6), the difference for minimum steady-state concentrations was approximately Δ-5% (Δ-5%; Δ-6%). For maximum steady-state concentrations after 2018 hours (i.e. Cmax after end of infusion) the difference in concentration values between SIM-IDs 1 and 3 (SIM-IDs 4 and 6; SIM-IDs 7 and 9) was Δ-25% (Δ-20%; Δ-23%). Comparing

the maximum steady-state concentrations of the SIM-IDs 1 and 4 (SIM-IDs 2 and 5; SIM-IDs 3 and 6), the simulated concentration difference was Δ-3% (Δ-3%; Δ-3%). The concentration-time profiles for the BSA-based model (SIM-IDs 7-9) were located between the FFM-based and the WT-based profiles.
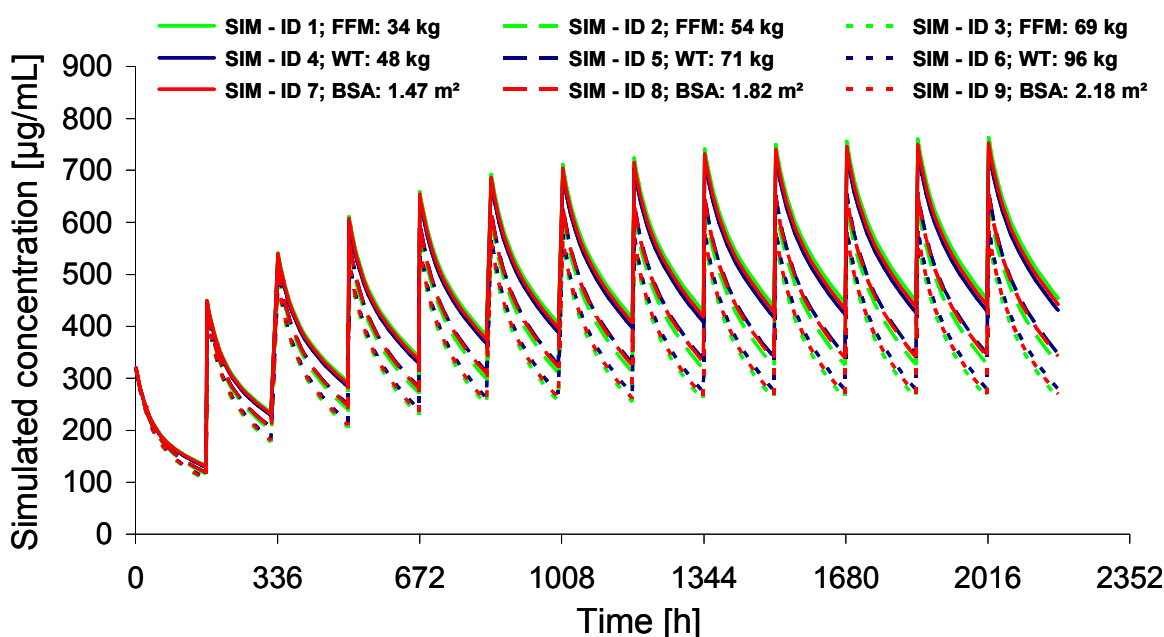

Figure 21 Simulations of concentration-time profiles based on models including as body size descriptor fat-free mass (FFM), body weight (WT) or body surface area (BSA) in the covariate relation.

Investigation 3)

To evaluate whether FFM might potentially be the most recommendable body size descriptor for monoclonal antibodies the following analysis was performed: in Figure 22, the WT, BSA and FFM distributions of the two study populations from the sibrotuzumab (A, 60 patients) and the matuzumab (B, 171 patients) dataset are presented in histograms. Whereas, after visual inspection, the WT and the BSA distributions of both populations seemed to follow a Gaussian distribution with similar median values for WT of 75 kg and for BSA of 1.87 m² (for the sibrotuzumab population) and for WT of 71 kg and for BSA of 1.83 m² (for the matuzumab population), the FFM distributions rather seemed to follow a bimodal distribution with

a 'median' FFM of 55 kg (sibrotuzumab) and of 53 kg (matuzumab). The 'median' FFM values could approximately present a mixture of two different unimodal distributions (x-y: ~30-50 kg FFM; z-a: ~50-90 kg FFM). The two local maxima for both FFM distributions were approximately around 40 and 58 kg FFM.

In the next step, to further inspect the distribution, the FFM populations of both datasets were divided into two separate groups for male and female study patients, respectively. The histograms for these groups (Figure 23) present the difference between the FFM 'median values' for men (sibrotuzumab: 60 kg, 39 patients; matuzumab: 56 kg, 109 patients) and women (sibrotuzumab: 39 kg, 21 patients, matuzumab: 42 kg, 62 patients). In the four additional histograms of the FFM distributions, the bimodal behaviour was less visible. However, the distributions did not follow a precise Gaussian distribution. Therefore, other effects apart from the sex effect seemed to influence the FFM distribution.
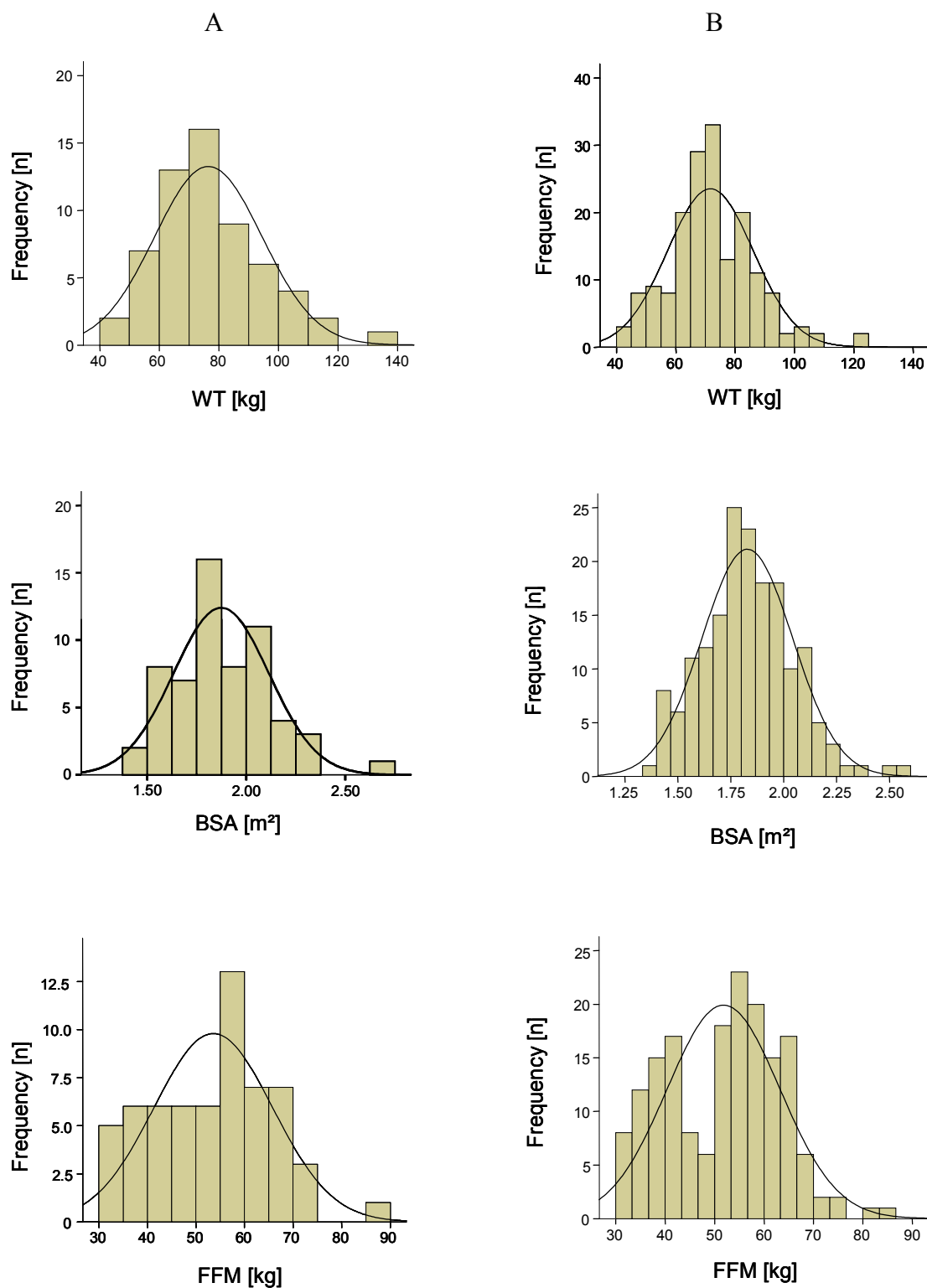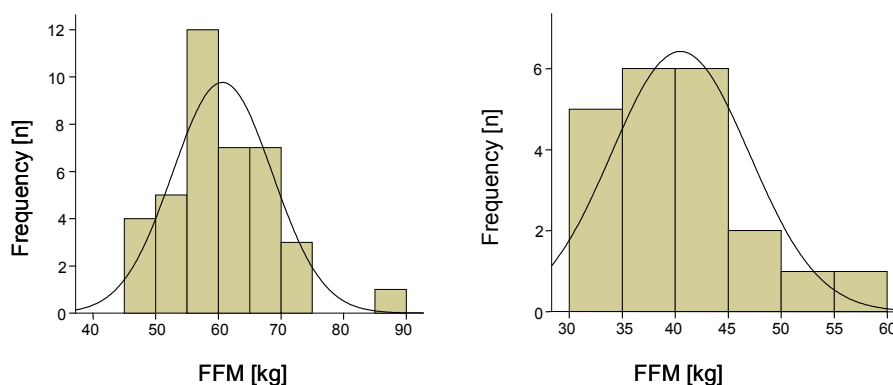
Figure 22 Histograms of the body weight (upper panel), body surface area (middle panel) and fat-free mass (lower panel) distributions of the sibrotuzumab (A) and matuzumab (B) study population. Respective curves indicate Gaussian distribution.
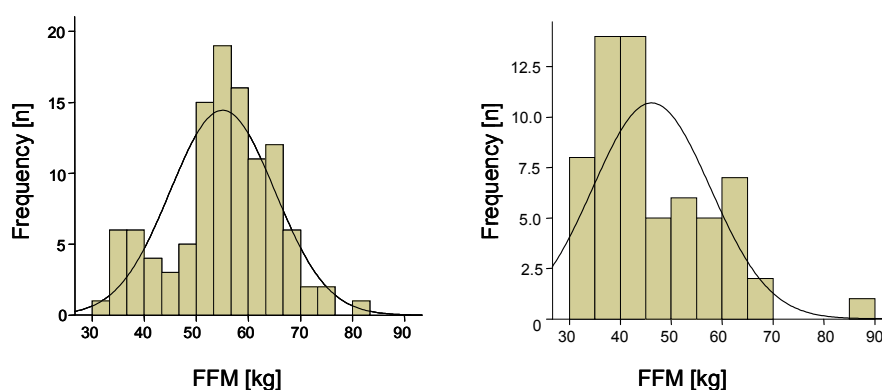
A

B

Figure 23 Histograms of the fat-free mass distribution for men (left panel) and women (right panel) of the sibrotuzumab (A) and the matuzumab (B) dataset. Respective curves indicate Gaussian distribution.

The developed population PK model for the monoclonal antibody sibrotuzumab [71] was compared with new results obtained after the substitution of the covariates including WT by covariates including FFM. Aside from the covariate exchanges, no further changes were made to the original population PK model. To compare the two different covariate models as part of the sibrotuzumab population PK model and to exclude bias differences due to unequal NONMEM^{TM} versions (WT-based model was developed with NONMEM^{TM}, version VI), all model parameters were reestimated with NONMEM^{TM}, version V. No differences in estimated parameter values and the OFV were observable between the published (NONMEM VI) and the reestimated (NONMEM V) parameter values [71]. All parameter estimates from the WT-based and the FFM-based model are presented in Table 13. By the exchange of the body size descriptor a statistical significant improvement of the previous (WT-based) model was

achieved by a decrease of Δ-12.16 in the OFV. In general, all population estimates were in the same range. IIV on V1/V2 and Vmax and the corresponding RSE values were slightly decreased. A significant decrease of the RSE for CLL (from 9.6% RSE for the WT-based model to 0.9% for the FFM-based model) and a respective higher precision for the CLL estimate also showed the improvement of the FFM-based model compared to the WT-based model. Furthermore, the covariate relations were estimated with equal or higher precision in the FFM-based model. Only the RSE for the parameter Km was higher than in the WT-based model (change from 57% to 79% RSE). Interestingly, the values for the covariate relations were approximately two times higher for the FFM-based covariates compared to the WT-based covariates (see Table 13). Compared to the FFM-based covariate relations for sibrotuzumab, the FFM-based covariate relation value for matuzumab was less than two times higher than the WT-based covariate relation (DD: WT-based covariate relation value: 0.0072, FFM-based covariate relation value: 0.0119; ED: WT-based covariate relation value: 0.0103, FFM-based covariate relation value: 0.015; combined datasets: WT-based covariate relation value: 0.0102, FFM-based covariate relation value: 0.0138). To assess the effect of the different FFM-based and WT-based relation values, median FFM and WT values had to be considered. For the sibrotuzumab median FFM value of 55 kg a ±1 kg change in FFM corresponded to a ±1.8% change in FFM. For the median WT value of 75 kg a ±1 kg change in WT corresponded to a ±1.3% change in WT. To compare changes in WT and FFM, the influence of a ±1% change of the body size was considered. Accordingly, a change of ±0.75 kg in WT and of ±0.55 kg in FFM corresponded to a ±1% change in WT and FFM, respectively. The influence of ±1% change in WT or FFM on CLL for sibrotuzumab can be calculated with the covariate relation values from Table 13:

- CLL_WT: ±1.82% change in CLL per 1 kg deviating from the median WT

→ ±1.37% change in CLL per ±1 % change in WT

- CLL_FFM: ±3.38% change in CLL per kg deviating from the median FFM

→ ±1.86% change in CLL per ±1% kg change in FFM

Hence, a change of ±1% in FFM influences the change of the typical value of CLL to a higher extent than a ±1% change in WT.

Table 13 Parameter estimates of the WT-based and the FFM-based model for sibrotuzumab.

Model Parameter	Unit	WT-based Model Population estimate	RSE[a], %	FFM-based Model Population estimate	RSE[a], %
Fixed effects					
CLL	[mL/h]	22.1	9.6	21.1	0.9
V1	[L]	4.13	3.7	4.00	3.0
Q	[mL/h]	37.6	9.6	37.5	9.7
V2	[L]	3.19	8.8	3.11	7.8
Vmax	[mg/h]	0.0338	25	0.0331	33
km	[mg/L]	0.219	57	0.212	79
Covariate influence					
CLL_WT/CLL_FFM		0.0182	19	0.0338	18
V1_WT/V1_FFM		0.0125	21	0.0247	21
V2_WT/V2_FFM		0.0105	40	0.0208	37
Vmax_WT/Vmax_FFM		0.00934	49	0.0190	43
Random effects					
Interindividual variability					
ω CLL	[%CV]	57	52	58	53
ω V1, ω V2	[%CV]	20	52	17	41
ω Vmax	[%CV]	29	50	27	48
Interoccasion variability					
π CLL	[%CV]	13	25	13	25
Residual error					
σ proportional	[%CV]	9.3	6.8	9.3	6.9
σ additive	[mg/L]	0.0491	19	0.0488	20
Objective function value		1288.265	-	1276.103	-

[a] relative standard error (standard error divided by population estimate*100; for the random effects parameters RSE is related to the corresponding variance scale)

For matuzumab the difference in percentage influence of the two body size descriptors was much smaller: the analogous examination revealed a $\pm$0.72% change of the typical CLL value per $\pm$1% change in WT and only a slightly higher change of $\pm$0.75% change of the typical value per $\pm$1% change in FFM. Hence, the influence of FFM in sibrotuzumab pharmacokinetics was more pronounced than in matuzumab.

4   Discussion

In this thesis, in Part I the pharmacokinetics of matuzumab, a humanised monoclonal antibody directed against EGFR, was thoroughly analysed. For this, a population pharmacokinetic analysis (sections 3.1, 3.2 and 3.3) and multiple evaluation techniques for the developed model for its precision, robustness and predictivity (section 3.4) were applied. In Part II of this thesis, simulations (section 3.5) on the basis of the estimated PK model parameters for matuzumab and a thorough analysis to determine, which body size descriptor is capable to best characterise covariate relations in population PK analyses for monoclonal antibodies (section 3.6) were performed. For this purpose, simulations based on the developed model for matuzumab and a covariate analysis of an already developed model for sibrotuzumab, another monoclonal antibody, were performed. Because the results from Part II were a prerequisite for the development of the final population PK model for matuzumab in Part I, the results from both parts of this thesis will be discussed together in the following.

The final PK model (Table 9, column: Final Model) was developed using over 1200 serum concentration data points from 90 cancer patients with widely differing characteristics and multiple dosing regimens. The structural model comprised two compartments with two elimination pathways from the central compartment, one linear and one non-linear (Michaelis-Menten kinetics) (Figure 4). Non-linear PK behaviour has also been reported for other mAbs, e.g. sibrotuzumab and clenoliximab [71, 103]. It has also been investigated, in addition to the linear elimination, for rituximab but the model did not perform significantly better than the simple linear model. However, goodness of fit plots suggested a misspecification for high concentrations [104].

Regarding the structural model (see section 3.1), matuzumab was initially distributed to a restricted central volume of distribution of 3.7 L and an even smaller peripheral volume of distribution of 1.8 L, which indicated that matuzumab was not (largely) distributed apart from serum volume. Beside the low peripheral volume, the inter-compartmental clearance Q also indicated a limited distribution, which was consistent with the behaviour of endogenous IgG immunoglobulins [12, 105, 106]. In total,

matuzumab showed similar PK characteristics (clearance, volumes of distribution) to other therapeutic mAbs following intravenous administration [30, 103, 107]. The long half-life for matuzumab (~10 days at concentrations of 1000 μg/mL, see Figure 6, lower panel) was shorter than half-lives of physiological immunoglobulins (IgG1, $t_{1/2}$: ~21 days) but comparable to other mAbs ($t_{1/2}$ alemtuzumab: 8 days; $t_{1/2}$ bevacizumab: 13-21 days, $t_{1/2}$ trastuzumab: 3-10 days) [12]. A reason for different half-lives among mAbs lies in the origin of the therapeutic antibodies. Degradation will be more rapid for more non-human antibodies: the lower the non-human fraction, the longer the half-life. A protective mechanism of the Fc-Rn, the Fc receptor of neonates (postulated by Brambell et al. [108]; the name originated from experiments, that have shown the influence of the receptor on the absorption of antibodies in the gastrointestinal tract of neonates), against catabolism is mainly responsible for the long terminal half-lives of therapeutic antibodies [12].

Three components of random variability (interindividual, interoccasion and residual variability) were possible to be implemented into the model for matuzumab. With the relatively small residual variability (13.4% CV for the proportional part and a fixed additive error of 0.312 mg/L) it can be suggested that the developed model describes the PK characteristics well. IOV has been rarely investigated in mAb research, but in more recent population PK analysis it has been included to improve the model [71]. The inclusion of IOV in the population PK model for matuzumab was limited to eight infusions due to insufficient data hereafter and implemented by different ways of assigning the eight infusions to a varying number of occasions. The best result (lowest OFV, smallest RSEs) was achieved with IOV on CLL, where every infusion corresponded to one occasion. The estimated IOV of matuzumab for the final model of 23% CV and a RSE of 12% (Table 9, column: Final Model) was in the range or slightly higher than that for other immunologicals: e.g. sibrotuzumab and etanercept showed 13% and 28% CV as well as RSE imprecisions of 25% for sibrotuzumab (not reported for etanercept) [71, 109]. However, after the case deletion diagnostics, which detected a lower IOV (18% CV, RSE: 17%, Table 11, column: Final Model-ID 4, 1 DV) after neglecting one specific concentration, the IOV was also in the above mentioned IOV ranges. It has to be pointed out, that, because of the results from CDD, the closest and most realistic value to represent the true value of the parameter IOV of matuzumab has to be reported as 18% CV (and not as the value from the final model in Table 9). The importance of implementing IOV in population PK analysis has been demonstrated and

the investigation of IOV avoids biased population parameter estimates [110]. In this analysis of cancer patient study data the IOV investigation was feasible, because the conditions of cancer patients could vary significantly over the study period or even from week to week.

The aim of building the covariate model (see section 3.1) was to identify patient- or study-specific characteristics, which could explain and thus reduce the variability of the base model. In the development of the primary model the inclusion of the covariates WT on V1 and WT on CLL significantly improved the model, i.e. IIV on CLL was reduced by approximately 25%. These results are in good agreement with investigations of other mAbs. Similar results have been reported for the chimeric antibody basiliximab [107]. The incorporation of WT on V1 for golimumab, a fully human mAb, also significantly improved the model [111]. The population PK analysis for trastuzumab showed a significant influence of WT on V1 and/or on clearance. However, these influences were not considered to be clinically relevant, particularly in comparison with the large interindividual variability on clearance (IIV on clearance: 43% CV) [30]. For another population pharmacokinetic study of the monoclonal antibody sibrotuzumab, clearance has been reported with a similar covariate relation of body weight on the linear clearance (typical population estimate for CLL: 22.1 mL/h; covariate relation: +/-1.8% change in the population CLL per kg body weight deviating from the median body weight value in this study, 75 kg). Moreover, the presented simulations in that work might also suggest that the design of dosage regimens should consider the influence of body weight [71].

The decision to change the body size descriptor in the covariate relations from WT to FFM was motivated by the question, which body size descriptor is best to use in population pharmacokinetic analyses for monoclonal antibodies (section 3.6). Generally, WT-based dosing suggests a continuous increase in dose with increase in body weight, i.e. degree in obesity. Especially for anticancer drugs, extensive research has been carried out to recommend individualised drug dosing instead of empirical dosing regimens. It has been demonstrated that weight or obesity may have an influence on the disposition of some anticancer drugs [112-114]. However, it has also been recommended that for each agent it has to be individually investigated, which dosing strategy is the most appropiate [101]. Lean body weight (LBW) has been proposed to be a superior predictor of drug dosage compared to other size descriptors

(e.g. body surface area and weight) [115]: in most studies in adults in which dosage based on LBW has been evaluated prospectively, LBW has been shown to be superior to other measures of body size as a predictor of drug dosage. Additionally, the volume of distribution of relatively hydrophilic drugs correlated very well with LBW, with correlation coefficients of up to 0.9. For many drugs eliminated predominantly by the liver, there was a good correlation between systemic clearance and LBW. Such a correlation could be due to a correlation between systemic clearance and liver size or liver blood flow, which has been demonstrated for a few drugs, and a correlation between LBW and liver size and blood flow [115]. LBW and FFM can be used interchangeably, but by definition LBW is the mass of the body excluding fat content other than the lipids in cellular membranes, the central nervous system and bone marrow while FFM also excludes these lipids [73, 116]. For piperacillin, it has been investigated that allometric scaling by LBW and accordingly FFM reduced the IIV in clearance [117]. However, especially for drugs with a highly complex disposition profile, such as irinotecan, it has been reported, that the importance of body size consideration in drug dosage may be completely unnecessary because of variations in other factors affecting PK [118]. In the population pharmacokinetic analysis for matuzumab, a statistically significant influence of a body size covariate was found. The decision to incorporate FFM, instead of WT, into the model for matuzumab was motivated by the study results from Janmahasatian et al., where it has been reported that body weight seemed to be inappropiate for dose scaling [73]. This is reasonable as body composition usually varies as a function of total body weight where the ratio of adipose tissue to lean body weight increases with body weight [100]. The proposed equations for FFM in Janmahasatian et al. included easily accessible patient characteristics (weight and height), which are often routinely gained in clinical practise. However, because of, e.g. limited time and/or human resources, these basic patient informations are sometimes missing. Nevertheless, a semi-mechanistic model for LBW, which quantifies the influence of body composition on drug clearance, seemed to be an ideal metric for adjusting chronic dosing in obese [119]. Although the semi-mechanistic model included empirical features, it was based on strong underlying biological mechanisms [120]: adult data from the literature suggested that if a person is smaller than ideal body weight then scaling dose to body weight is appropriate. When a person is larger than ideal body weight, dose should be scaled to ideal body weight or to ideal body weight plus some fraction of the difference between total weight and ideal

body weight [121, 122]. However, this model has recently been discussed in association with the assessment of the quantitative relations between LBW and the clearance of eight commonly used anticancer drugs: the results indicated that for six of the eight investigated drugs incorporation of the LBW size formula did not lead to a substantially improved relation with clearance (compared to conventional approaches), regardless of the model [123]. Nevertheless, in a recently published review on mechanism-based concepts of size and maturity in pharmacokinetics, Anderson and Holford expressed their opinion that FFM is perhaps the size descriptor that is closest to capturing the concept of body mass that is used in allometric theory [120]. This theory for endotherm species was based on the link between structure and function [124]. Additionally, the authors concluded that FFM might be expected to be better than total body weight when there are wide variations in fat affecting body composition. Furthermore, they supposed that FFM alone is a good predictor of clearance because fat is not a clearance organ and is unlikely to be a determinant of elimination function [120].

In this population analysis, including covariate investigations, it was demonstrated that the covariate relation FFM on CLL, compared with the covariate relations WT on CLL and BSA on CLL, provided very comparable results for matuzumab, e.g. simulations were performed, which showed similar simulated concentration-time profiles and a similar spread in concentrations for the analysed body size descriptors (see section 3.6 and Figure 21). Furthermore, the physiological background supported the exchange. Additionally, and especially to demonstrate that only the fat-free mass fraction of the whole body weight was responsible for the influence on CLL, the model was analysed by deleting the FFM-based relation and including a covariate relation incorporating only the fat mass (FM, obtained by the difference between WT and FFM). The model parameters were similarly estimated to the developed model but the covariate relation was not (at all) supported (value of 0.000004 and RSE ~ 10000%).

Regarding to a general recommendation for the best body size descriptor, which should be used for monoclonal antibody analyses, the special physico-chemical properties (high molecular mass of ~150 kD; high hydrophilicity) and disposition characteristics (limited distribution; residence confined to plasma and interstitial space fluid) have to be considered. With respect to these properties it can be suggested, that distribution is

better related to FFM than related to WT, which in many cases neglects body composition.

After it has been shown that the developed model with the FFM-based covariate relation was superior to the WT-based covariate relation for characterising the PK of matuzumab (see Table 12), a second mAb dataset was analysed: a covariate analysis of the already published population PK model for sibrotuzumab was performed to evaluate the previous results and to elucidate whether FFM might be the recommendable body size descriptor for the population PK analyses for monoclonal antibodies. In this analysis, the exchange of the covariate relations including WT by covariate relations including FFM showed a significant improvement of the previous population PK model for sibrotuzumab (see Table 13). On the basis of these two analyses it might be suggested, that, in general, FFM might be a superior body size descriptor compared to e.g. WT or BSA for covariate relations included in population PK models for monoclonal antibodies. Several developed models for this class of biologicals already included WT-based covariates [30, 57, 111, 125] or allometric WT-based models [126]. If FFM has not been considered during model development, these models should be reanalysed including FFM relations to support the proposed hypothesis in future. A developed population pharmacokinetic model for rituximab included BSA- and sex-related covariate relations [104]. BSA was calculated based on the Du Bois and Du Bois equation, which takes weight and height into account [75]. The FFM-based model, which has been used in this thesis, considered on the one hand weight and height but also - by the different calculation of FFM for men and women - sex. The influence of sex on FFM was shown by the histograms of the sex separated FFM distributions (Figure 23): women generally had lower FFM values (median FFM ~ 40 kg) than men (median FFM ~ 58 kg). If FFM is included in a covariate relation in a population PK model, sex will also be considered indirectly. For the rituximab model it should be reanalysed, if FFM-based covariates can reduce the quantity of covariate relations without loosing any influence of WT, HT and sex. In general, dosing of therapeutic components against cancer based on BSA is a current practice in clinical oncology [127]. However, there are investigations, which concluded no rationale for BSA-based dosing: this dosing strategy did not increase the accuracy of predicted exposure of cisplatin [128]. Also, results demonstrated that flat-fixed dosing did not typically lead to higher pharmacokinetic variability [129]. Another investigation has determined correlation coefficients for 306 courses of antineoplastic treatment in 287

patients between morphometric measures (HT, WT and BSA) and PK parameters (clearance, central volume of distribution and steady-state volume of distribution): only five of 96 correlation coefficients were 0.707 or larger, the point where the variability in body size explains 50% of the variability in drug disposition [130]. It was concluded that normalisation of doses to BSA, WT or HT would be of minimal clinical value for the studied components (no mAb was included in the analysis).

Hempel et al. reported, that it has to be considered that most classical cytotoxic drugs have a narrow therapeutic range and are often administered at a dose close to the maximum-tolerated dose, because for many tumours increasing systemic drug exposure often results in higher response rates. The authors finally concluded, that using well-designed population pharmacokinetic studies with sufficient patient numbers representing the entire population should enable to find parameters to precisely predict the clearance of cytostatic drugs and to adjust the dose better than using flat-fixed dosing or BSA-based dosing regimens [131]. In conclusion to these aspects and in particular because mAbs have specific characteristics (e.g. in their PK behaviour) with significant advantages but also risks in their therapeutic use, the analysis of body size-related covariates (accompanied by a resulting potential impact on proposed dosing regimens) has to be performed very thoroughly. Based on the results revealed in this thesis, where FFM was the superior body size descritor for the covariate relation in the population PK model for matuzumab, a supplementary analysis including FFM-based covariates should be performed for all previously developed population PK models for monoclonal antibodies including body size covariate relations, and in prospective population PK analyses FFM should be included in the covariate analysis from the beginning of the investigation.

During the last years, population pharmacokinetic and/or pharmacodynamic models were developed and presented in the literature to a higher extent than in the past. The implementation of the non-linear mixed effects modelling approach has substantially improved the quality and impact of these analyses [56], but evaluation analyses comparable to the one performed in this thesis (see sections 3.2 and 3.4) were frequently missing. For this purpose, also the regulatory official agencies (FDA and EMEA) increasingly demand in their guidelines not only for appropriate model development methods but also for qualified model evaluation approaches. However, especially for monoclonal antibodies, recommendations are still missing, but there are

attempts to provide structural components for determining model appropriateness of population pharmacokinetic models in general [132]. A systematic review of published population analyses from 2002 to 2004 surveying different evaluation methods, which are currently used, and assessing, whether those reviewed models were adequately evaluated, revealed an unsatisfying result: only 28% of the (for the review analysed) developed PK models and 26% of the developed PD models were judged to be sufficiently evaluated [88].

For this purpose, besides model development, one main objective of this thesis was the profound and reliable evaluation of the developed model for the monoclonal antibody matuzumab by external and internal (basic and advanced) evaluation techniques. Thereby, it was to be adressed whether internal evaluation techniques and especially their combination and the combination with an external evaluation are applicable for the evaluation of population pharmacokinetic models for monoclonal antibodies in general.

Since internal techniques use data solely from the development dataset [87, 98], external evaluation is considered to be the most plausible and strongest evaluation method, because the developed model has to demonstrate its predictivity for completely new data. This evaluation technique provides the most stringent method, however, it has rarely been reported for developed models in the literature and often the lack of a second (evaluation) dataset or insufficient data for data splitting prohibits its application [133]. The obtained results from the performed external evaluation investigation for the population PK model for matuzumab showed the appropriateness of this technique for model refinement analysis (see section 3.2). Based on the results from the ED, the exclusion of the unsupported covariate relation FFM on V1 improved the model and, despite one less covariate, equally precise parameter estimates were obtained.

In addition to the basic internal evaluation with mainly visual graphical diagnostics (e.g. goodness of fit plots, Figure 7) and analysing parameter uncertainty by consideration of relative standard errors, a further aim was to present an advanced internal evaluation, which involved more complex techniques.

It has been demonstrated that the bootstrap method is a reliable evaluation tool: In Ng et al. a developed model for the recombinant human monoclonal antibody pertuzumab

was shown to be stable by the performance of 1000 successful bootstrap runs [134]. The obtained bootstrap results in this thesis, including relatively very low bias values ($\leq +/-4.3\%$ relative bias, see Table 10; section 3.4.1), confirmed the excellent precision and accuracy of the proposed model.

The results from the second performed internal evaluation technique, the case deletion diagnostic (see section 3.4.2), showed the influence of one observed and confirmed concentration data point on the IOV on CLL (Table 11). However, this observation had no impact on the entire model: all other model parameters were similar to those, which were previously obtained (for the final model). Even though the spurious concentration data point was re-checked in the original study data and although the concentration in the sample had been analysed twice, an error in sample or analysis handling or data management cannot be completely excluded. Parameter estimation without this observation resulted in a lower interocassion variability (18.3% CV). The lower IOV value better reflected the population estimate for this parameter because the concentration at this observation was implausible and hence, the exclusion of this data point was eligible. Finally, this CDD investigation provided a more realistic insight into the interoccasion variability and visualised the robustness of all other PK parameters despite the inclusion of the spurious concentration. CDD with similar scenarios were used for the evaluation of the population PK model for the monoclonal antibody sibrotuzumab: the reduced datasets did not reveal any marked differences in parameter estimates and standard errors when compared with the final model parameters of the full dataset [71]. For the population PK model for the anticancer agent topotecan, CDD were performed to show that deletion of individual patients, which may have had a significant influence on the covariate model, did not alter the final covariate structure [135].

As a further technique of advanced internal evaluation methods, visual predictive checks were performed (see section 3.4.3). This method has been used as a diagnostic tool in a population pharmacokinetic approach for two monoclonal antibodies (one humanised and one murine) to support the developed model [126]. It was shown that the median and the variability of the concentrations of both antibodies were well predicted and that this evaluation method obtained characteristic information for a predicted surgery time after antibody administration. Additionally, it was demonstrated that by this technique useful information were obtained to clearly indicate the best

model. The superiority of a visual predictive check evaluation compared to standard diagnostic plots, e.g. goodness of fit plots, has been presented. It was demonstrated that VPC is a diagnostic tool for the fixed- AND the random-effects parts of a model and does not neglect one dimension (time or prediction) such as standard plots [92].

Overall, the results from the external and the internal model evaluation confirmed that the developed population PK model for matuzumab provided an authentic and predictable tool for further investigations. Additionally, the combination of external evaluation and the three internal evaluation methods can highly be recommended for the evaluation of developed population PK models for mAbs.

After the successful model development and evaluation, simulations on the basis of the model parameters were performed to visualise the impact of the covariate relation on the PK profiles (see section 3.5). In general, simulations are used to investigate concentration-time profiles in a large patient population, using the estimated parameter values from the developed model. This technique provides information for decision making and is beneficial for different situations: sparse data situations, predictions from single dosing to multiple dosing, formulation changes or simulation of further clinical trials [30, 60, 136, 137]. Simulation tools have been used more frequently in the last years [138-140]. Especially for specific populations (e.g. in paediatric studies, studies with obese patients) it is recommended to use simulations to replace empirically based dose selection [141]. In addition, experts agree that modelling and simulation methods are very useful in the development and use of anti-cancer drugs [137]. For example, dose individualisation by dose adjustment based on concentration-time data related to pharmacodynamic factors was demonstrated for the monoclonal antibody trastuzumab [30, 142]. The aim of the performed simulations in this thesis was to analyse the possible impact of the defined covariate relation and the influence of different dosing regimens on the concentration-time profile of matuzumab. The presented results showed the differences in minimum and maximum steady-state concentrations (see Figure 18), which were obtained as a result of the covariate relation. These differences were also confirmed by original data: in study 4 the minimum steady-state concentrations after each occasion from each study subject were compared and a remarkable increase of the minimum concentration range over time was assessed (see Figure 20). In another published PBPK/PD model simulations were performed to obtain population predicted time courses of neutrophil concentrations based on the

developed model. The simulated individual profiles did not show an uniform distribution of the concentrations over the entire range and accordingly subgroups were able to be identified [143]. This behaviour was not observed for the simulation scenarios in this thesis: simulated concentration-time profiles from subjects with matuzumab administration revealed that the variability in matuzumab concentration-time curves was present throughout the whole study population (uniform distribution of profiles, see Figure 19).

The presented simulations might give advice in decision making for dosing regimens, e.g. whether a certain dosing regimen would result in maximum concentrations possibly associated with toxic events. The comparison of simulated concentration-time data between different dosing regimens of weekly matuzumab dosing of 400 mg, a dosing of 800 mg every two weeks and a dosing of 1200 mg every three weeks might guide the decision for the preferred effective dosing regimen for further clinical trials (see Figures 16 and 17).

The proposed adapted dosing regimen included the FFM-adaption only for 50% of the total dose amount because FFM influenced only the linear clearance fraction. At the reached steady-state concentrations the linear clearance was approximately 50% of the total clearance. In consequence, the adaption of these 50% was considered to be a plausible dosing strategy. The low variability in the first weeks of administration observed in real (Figure 20) and simulated (Figure 19) data was considered by adapting the dose only from the 5th administration onwards (i.e from the 2nd month). Less variability in the first weeks could be explained by not completely utilised distribution and/or clearance processes at these time points. The presented simulations demonstrated a possible reduction of the variability in the pharmacokinetic behaviour of matuzumab. The simulations are a guide to clinical trial design, and there may be other information available, which has to be considered. Additionally, it should be noticed that in all simulations the 'typical' patients (IIV and IOV parameters were set to a value of zero) were simulated, leading to a considerable reduction in variability among the real patient population. Taking the final estimates of these random-effects parameters also into consideration would even further increase the variability between patients.

Monoclonal antibodies, such as matuzumab, comprise specific and sometimes unique characteristics, especially in their PK behaviour. Compared to the PK of small

molecule drugs, which usually have linear kinetics in therapeutic doses, mAbs often show non-linear or combined (linear and non-linear) PK, which can also be influenced by the development of anti-idiotype antibodies against the therapeutic antibody [12, 144]. For the modelling and simulation of the PK data these specific characteristics have to be considered. Beside model development, it has been demonstrated in this thesis, that advanced internal evaluation techniques, which are normally used to evaluate small molecule PK models, and also the combination with an external evaluation technique, were also applicable for the monoclonal antibody matuzumab and that they additionally produced reliable results.

In the developed population PK model for matuzumab a non-linear elimination process has been incorporated (see Figure 4 and Table 9: parameters Vmax and Km). Different hypotheses can be discussed to ascertain the source for the non-linear PK behaviour for matuzumab (and, in general, for monoclonal antibodies because non-linear PK has also been observed for several other mAbs [71, 103]). Sources for the non-linear PK of matuzumab might be:

- steric hindrance (at high mAb concentrations)

- downregulation of the EGF-receptor production (at high mAb concentrations)

- delay of EGF-receptor recycling (at high mAb concentrations)

- receptor-mediated endocytosis (pinocytosis) and binding to the Fc-Rn (at low mAb concentrations).

The hypothesis of the steric hindrance is a potential source for the non-linearity because if high mAb concentrations are present, not all EGF-receptors could be reached and for this purpose, unbound mAbs could be saved from degradation inside the cell. The downregulation of the EGF-receptor also presents a possible mechanism to explain non-linearity if a high concentration of mAb causes high receptor internalisation and for this purpose receptor production could be downregulated. The delay of EGF-receptor recycling might occur in the cell recycling processes at high mAb concentrations (for specific processes see next paragraph) and hence, internalised receptors could be available on the cell surface after a specific time delay. The idea that receptor-mediated endocytosis and binding to the Fc-Rn might be responsible for the non-linear PK originated from investigations, which had identified that the Fc-Rn is

responsible for the extraordinarily long half-lives of three immunoglobulin subclasses by protecting them from proteolysis [145]. Further experiments revealed that the higher the serum IgG concentration, the shorter the half-life: at low concentrations IgG is bound to the receptor and protected from proteolysis. At high concentrations, however, the receptor binding sites are saturated much more rapidly and more unbound IgG molecules are digested.

To analyse these potential explanations for the non-linearity in the PK of matuzumab the complex processes of mAb binding to the receptor, internalisation of the receptor-mAb complex, receptor and mAb degradation, receptor recycling and receptor synthesis should be included into the developed and evaluated population PK model for matuzumab, which has to be considered an empirical model. In general, the development of empirical models is data-driven: the primary aim (of the 'black box' models) is e.g. to describe the data and to explain observed variability by the investigation of covariate relations [146]. However, population pharmacokinetic models can also be (semi)-mechanistic. Nevertheless, another model approach, the physiologically based pharmacokinetic (PBPK) modelling is able to gain a more thorough mechanistic understanding of the underlying processes by incorporating additional knowledge (e.g. blood flow, saturable receptor binding, transport to tissues) into a model. For this purpose, two types of input data are required: physiological parameters (e.g. blood flows, organ volumes) and compound-related parameters (e.g. hydrophilicity) [147]. Besides population PK modelling, PBPK modelling is an additional supporting method in drug discovery, drug development and therapeutic use [148-152]. Whole body PBPK models simulate PK or PD at an organism level where the idea is to characterise drug disposition on the basis of relevant anatomical and physiological parameters. This approach generally requires more parameters, which might result in a poorer performance of these models in the process of model selection, since models containing more parameters are usually penalised in modelling procedures. However, physiologically based models have the advantage of a mechanistic interpretation of the parameters and, for this purpose, might generate a better understanding of the underlying processes taking place. Investigations initialised in collaboration with the Hamilton Institute, Maynooth, Ireland and the DFG Research Center MATHEON, Berlin, Germany, aim to analyse the potential explanations for the observed non-linearity in the population PK model for matuzumab and to support the developed empirical model for matuzumab by PBPK modelling. The objective of this

research is to ascertain the source for the non-linear PK behaviour of protein drugs in general (and of monoclonal antibodies as an example for protein drugs). First attempts have been investigated to incorporate mechanistic modelling into the NLME model for matuzumab. However, these preliminary attempts have not been successful so far and in the future, further investigations have to be performed to support and to expand the developed empirical population PK model for matuzumab by the successful implementation of mechanistic modelling into the NLME model. The ultimate goal should be to incorporate the results from the PBPK modelling into the empirical modelling, to compare then obtained results with those presented in this thesis, to gain a more mechanistical understanding of the clinical data of matuzumab and furthermore, to explain the source of non-linearity PK behaviour of matuzumab.

Additionally, appropriate pharmacodynamic data from matuzumab should be combined with the results from this thesis in future investigations. For example, the identification of molecular tumour markers, which should have a strong exposure-response relation, is considered to be an essential prerequisite in order to link the PK results in a PK/PD model. This could lead to a better prediction of the response for this new class agent and maximise the patients' benefit. Information about an achievable target serum level at steady-state for efficacy, a defined time over a target serum concentration or a desired area under the curve might ultimately provide a comprehensive understanding of especially the simulation results. Additionally, simulations have documented the ability of the model to predict matuzumab concentrations for different dosing regimens. This is another prerequisite to investigate exposure-response or exposure-toxicity relations in future clinical trials and modelling approaches. Implementation of and relation to appropriate pharmacodynamic or efficacy data could expand the final population PK model as a tool that could guide selection of optimal dose regimens for matuzumab, a highly promising 'targeted' cancer therapy.

5   Conclusions

In this thesis, a population pharmacokinetic model including linear and non-linear elimination processes for the humanised monoclonal antibody matuzumab was developed and evaluated by external and internal evaluation techniques. In the model, interindividual, interoccasion and residual variability were incorporated and the covariate relation fat-free mass on the linear clearance significantly improved the model. The combination of internal evaluation techniques and their combination with an external evaluation can be recommended for the evaluation of developed population PK models for monoclonal antibodies. By a performed covariate analysis, a dose adjustment based on sex, age or organ functions such as liver or kidney did not seem to be necessary. A simulated dose adaption incorporating the impact of fat-free mass on the PK profiles significantly reduced observed variability at steady-state concentrations among subjects. The model showed the ability to accurately, precisely, robustly and reproducably estimate all model parameters by different evaluation techniques (bootstrap method, case deletion diagnostics, visual predictive checks). The observed influence of one concentration on the IOV had no impact on the final model and, based on model evaluations, did not bias the obtained results. In addition, the model was able to describe a second (external) dataset with completely new data. The inclusion of the body size descriptor fat-free mass in the covariate relation showed its superiority compared to other body size descriptors (BSA, WT). By the covariate analysis including exchanged FFM covariate relations a population PK model for sibrotuzumab was significantly improved. Hence, FFM as body size descriptor for covariate relations in population PK analyses for mAbs was supported. From these results and the biological background of FFM it can be proposed that FFM could be a better body size descriptor in population pharmacokinetic modelling for mAbs than BSA or WT.

The results from this thesis present the basis for following pharmacokinetic and pharmacodynamic investigations and for further clinical trials. Implementation of and relation to pharmacodynamic or efficacy data might expand the final model. This way, it might be used as a tool to guide selection of optimal dose regimens for matuzumab.

6 Comments on my contribution

In paper I, II and IV, I performed the population pharmacokinetic analysis for matuzumab, the model evaluation investigations for the developed model and the simulation scenarios and I wrote the manuscripts.

In paper III, I contributed my knowledge about the EGFR system and monoclonal antibodies in general and to the manuskript.

In paper V, I performed the body size descriptor investigations and simulations for matuzumab and sibrotuzumab and I wrote the manuscript.

7 Acknowledgements

Ich möchte allen, die zu der Erstellung dieser Doktorarbeit beigetragen haben, danken und im Besonderen:

Mein besonderer Dank gilt Frau Professor Charlotte Kloft für die Betreuung meiner Arbeit, bei der sie mir immer mit Engagement, Enthusiasmus und inspirierender Hilfe zur Seite gestanden hat. Ich möchte mich auch für die Überlassung meines Dissertationsthemas bedanken, die mir die Gelegenheit gegeben hat, auf diesem interessanten Forschungsgebiet zu arbeiten. Außerdem habe ich die fördernden Diskussionen über meine Arbeit und die umfassende Unterstützung sehr geschätzt und ebenso die Möglichkeit, mit Experten auf dem Gebiet in Kontakt und Austausch treten zu können. Zusätzlich war es eine interessante Aufgabe, an dem Graduate Research Training Programm an der Universität in Halle teilnehmen zu können und es teilweise mitzugestalten.

Herrn Professor Hans-Hubert Borchert danke ich für seinen besonderen Einsatz für die Klinische Pharmazie in Berlin und die Vertretung der Doktorandenanliegen gegenüber höheren Stellen.

Herrn Professor Karsten Mäder danke ich für die Begutachtung meiner Arbeit.

Meinem Kooperationspartner Merck Serono danke ich für die Überlassung der klinischen Studiendaten. Stellvertretend gilt mein besonderer Dank Herrn Dr. Andreas Kovar, Herrn Dr. Christian Lüpfert und Frau Brigitte Brockhaus.

Allen meinen früheren und jetzigen Kollegen aus den Arbeitskreisen der Klinischen Pharmazie in Berlin und Halle danke ich für die schöne gemeinsame Zeit. Im speziellen danke ich Frau Dr. Nele Plock für die Hilfe, Kollegialität und Freundschaft – ich habe Dich im Labor sehr vermisst und der Platz mir gegenüber war nach Deinem Verlassen so leer! Außerdem möchte ich Frau Monika Frank danken für die vielen Skype-Unterhaltungen – Du bist auf jeden Fall einer der witzigsten Menschen, die ich kenne!

Herrn Oliver Schwalbe und Herrn Christian Scheerans danke ich für den guten Zusammenhalt im Restbestand der Berliner Klinischen Pharmazie und ihre Hilfsbereitschaft. Besonders möchte ich mich auch bei Frau Dr. Anna-Katharina Manzer bedanken für die Begleitung über die gesamte Zeit des Doktoranden-Daseins, die gemeinsamen Erfahrungen und Erlebnisse, die wir seit der Zeit in Florida immer wieder zusammen erleben durften.

Zusammenfassend möchte ich auch der Mittagscrew und meinen „nicht-pharmazeutischen" Freunden danken, die mich in so vieler Hinsicht in meiner Doktorandenzeit begleitet und unterstützt haben.

Für den technischen Support und der Hilfe bei jedem noch so kleinen Computerproblem danke ich im Besonderen Herrn Mike Nürnberg.

Meiner Familie und vor allem meinen Eltern, die ich letztendlich von dem Sinn einer Doktorarbeit überzeugen konnte, danke ich für ihre immerwährende Unterstützung mit Liebe, Rat und Beistand.

Nicht zuletzt gilt mein ganz besonderer Dank Herrn Fabian Flügge für seine liebevolle Aufmunterung, Unterstützung und Geduld, die mir eine unermässliche Hilfe besonders in der letzten Phase waren.

8   References

1.   WHO Cancer. World Health Organisation. Available from http://www.who.int/mediacentre/factsheets/fs297/en/ [Accessed 2008 May 20] (2006)

2.   Li Z, Zhao R, Wu X, Sun Y, Yao M, Li J, Xu Y, Gu J Identification and characterization of a novel peptide ligand of epidermal growth factor receptor for targeted delivery of therapeutics. Faseb J 19:1978-1985 (2005)

3.   Cancer in Germany, 2003 – 2004. Incidence and Trends. Sixth edition. Berlin: Robert Koch Institute and the Association of Population-Based Cancer Registries in Germany (2008)

4.   Breitscheidel L, Sahakyan A Modeling The Probability Of Developing Cancer in Germany. The Internet Journal of Epidemiology. Volume 3 Number 2 (2006)

5.   Tamburini M, Gangeri L, Brunelli C, Boeri P, Borreani C, Bosisio M, Karmann CF, Greco M, Miccinesi G, Murru L, Trimigno P Cancer patients' needs during hospitalisation: a quantitative and qualitative study. BMC Cancer 3:12 (2003)

6.   Goel S, Mani S, Perez-Soler R Tyrosine kinase inhibitors: a clinical perspective. Curr Oncol Rep 4:9-19 (2002)

7.   Traxler P Tyrosine kinases as targets in cancer therapy - successes and failures. Expert Opin Ther Targets 7:215-234 (2003)

8.   Croom KF, Perry CM Imatinib mesylate: in the treatment of gastrointestinal stromal tumours. Drugs 63:513-522; discussion 523-514 (2003)

9.   Nadler LM, Stashenko P, Hardy R, Kaplan WD, Button LN, Kufe DW, Antman KH, Schlossman SF Serotherapy of a patient with a monoclonal antibody directed against a human lymphoma-associated antigen. Cancer Res 40:3147-3154 (1980)

10.   Emens LA, Davidson NE Trastuzumab in breast cancer. Oncology (Williston Park) 18:1117-1128; discussion 1131-1112, 1137-1118 (2004)

11.   Leget GA, Czuczman MS Use of rituximab, the new FDA-approved antibody. Curr Opin Oncol 10:548-551 (1998)

12. Kuester K, Kloft C Pharmacokinetics of monoclonal antibodies. In: Meibohm B (ed) Pharmacokinetics and Pharmacodynamics of Biotech Drugs. 1 ed. Wiley-VCH Verlag, Weinheim, 45-91 (2006)

13. Kohler G, Milstein C Continuous cultures of fused cells secreting antibody of predefined specificity. Nature 256:495-497 (1975)

14. Handbook of Therapeutic Antibodies, Volume III: Approved Therapeutics. Wiley-VCH Verlag, Weinheim (2007)

15. Stern M, Herrmann R Overview of monoclonal antibodies in cancer therapy: present and promise. Crit Rev Oncol Hematol 54:11-29 (2005)

16. McCormack PL, Keam SJ Bevacizumab: a review of its use in metastatic colorectal cancer. Drugs 68:487-506 (2008)

17. McCormack PL, Keam SJ Spotlight on bevacizumab in metastatic colorectal cancer. BioDrugs 22:339-341 (2008)

18. Ternant D, Paintaud G Pharmacokinetics and concentration-effect relationships of therapeutic monoclonal antibodies and fusion proteins. Expert Opin Biol Ther 5:37-47 (2005)

19. Kollmannsberger C, Schittenhelm M, Honecker F, Tillner J, Weber D, Oechsle K, Kanz L, Bokemeyer C A phase I study of the humanized monoclonal anti-epidermal growth factor receptor (EGFR) antibody EMD 72000 (matuzumab) in combination with paclitaxel in patients with EGFR-positive advanced non-small-cell lung cancer (NSCLC). Ann Oncol 17:1007-1013 (2006)

20. Rivera F, Vega-Villegas ME, Lopez-Brea MF, Marquez R Current situation of Panitumumab, Matuzumab, Nimotuzumab and Zalutumumab. Acta Oncol 47:9-19 (2008)

21. Wells A EGF receptor. Int J Biochem Cell Biol 31:637-643 (1999)

22. Harari PM Epidermal growth factor receptor inhibition strategies in oncology. Endocr Relat Cancer 11:689-708 (2004)

23. Watanabe T, Shintani A, Nakata M, Shing Y, Folkman J, Igarashi K, Sasada R Recombinant human betacellulin. Molecular structure, biological activities, and receptor interaction. J Biol Chem 269:9966-9973 (1994)

24. Lee JJ, Chu E First-line use of anti-epidermal growth factor receptor monoclonal antibodies in metastatic colorectal cancer. Clin Colorectal Cancer 6:42-46 (2007)

25. Sibilia M, Kroismayr R, Lichtenberger BM, Natarajan A, Hecking M, Holcmann M The epidermal growth factor receptor: from development to tumorigenesis. Differentiation 75:770-787 (2007)

26. Carteni G, Fiorentino R, Vecchione L, Chiurazzi B, Battista C Panitumumab a novel drug in cancer treatment. Ann Oncol 18 Suppl 6:vi16-21 (2007)

27. Walker RA, Dearing SJ Expression of epidermal growth factor receptor mRNA and protein in primary breast carcinomas. Breast Cancer Res Treat 53:167-176 (1999)

28. Brabender J, Danenberg KD, Metzger R, Schneider PM, Park J, Salonga D, Holscher AH, Danenberg PV Epidermal growth factor receptor and HER2-neu mRNA expression in non-small cell lung cancer Is correlated with survival. Clin Cancer Res 7:1850-1855 (2001)

29. Ohsaki Y, Tanno S, Fujita Y, Toyoshima E, Fujiuchi S, Nishigaki Y, Ishida S, Nagase A, Miyokawa N, Hirata S, Kikuchi K Epidermal growth factor receptor expression correlates with poor prognosis in non-small cell lung cancer patients with p53 overexpression. Oncol Rep 7:603-607 (2000)

30. Bruno R, Washington CB, Lu JF, Lieberman G, Banken L, Klein P Population pharmacokinetics of trastuzumab in patients with HER2+ metastatic breast cancer. Cancer Chemother Pharmacol 56:361-369 (2005)

31. Ritter CA, Arteaga CL The epidermal growth factor receptor-tyrosine kinase: a promising therapeutic target in solid tumors. Semin Oncol 30:3-11 (2003)

32. De Luca A, Carotenuto A, Rachiglio A, Gallo M, Maiello MR, Aldinucci D, Pinto A, Normanno N The role of the EGFR signaling in tumor microenvironment. J Cell Physiol 214:559-567 (2008)

33. Herbst RS, Shin DM Monoclonal antibodies to target epidermal growth factor receptor-positive tumors: a new paradigm for cancer therapy. Cancer 94:1593-1611 (2002)

34. Dassonville O, Formento JL, Francoual M, Ramaioli A, Santini J, Schneider M, Demard F, Milano G Expression of epidermal growth factor receptor and survival in upper aerodigestive tract cancer. J Clin Oncol 11:1873-1878 (1993)

35. Rusch V, Baselga J, Cordon-Cardo C, Orazem J, Zaman M, Hoda S, McIntosh J, Kurie J, Dmitrovsky E Differential expression of the epidermal growth factor receptor and its ligands in primary non-small cell lung cancers and adjacent benign lung. Cancer Res 53:2379-2385 (1993)

36. Salomon DS, Brandt R, Ciardiello F, Normanno N Epidermal growth factor-related peptides and their receptors in human malignancies. Crit Rev Oncol Hematol 19:183-232 (1995)

37. Murthy U, Basu A, Rodeck U, Herlyn M, Ross AH, Das M Binding of an antagonistic monoclonal antibody to an intact and fragmented EGF-receptor polypeptide. Arch Biochem Biophys 252:549-560 (1987)

38. Rodeck U, Williams N, Murthy U, Herlyn M Monoclonal antibody 425 inhibits growth stimulation of carcinoma cells by exogenous EGF and tumor-derived EGF/TGF-alpha. J Cell Biochem 44:69-79 (1990)

39. Cunningham D, Humblet Y, Siena S, Khayat D, Bleiberg H, Santoro A, Bets D, Mueser M, Harstrick A, Verslype C, Chau I, Van Cutsem E Cetuximab monotherapy and cetuximab plus irinotecan in irinotecan-refractory metastatic colorectal cancer. N Engl J Med 351:337-345 (2004)

40. Harding J, Burtness B Cetuximab: an epidermal growth factor receptor chemeric human-murine monoclonal antibody. Drugs Today (Barc) 41:107-127 (2005)

41. Baselga J The EGFR as a target for anticancer therapy--focus on cetuximab. Eur J Cancer 37:16-22 (2001)

42. Kettleborough CA, Saldanha J, Heath VJ, Morrison CJ, Bendig MM Humanization of a mouse monoclonal antibody by CDR-grafting: the importance of framework residues on loop conformation. Protein Eng 4:773-783 (1991)

43. Vanhoefer U, Tewes M, Rojo F, Dirsch O, Schleucher N, Rosen O, Tillner J, Kovar A, Braun AH, Trarbach T, Seeber S, Harstrick A, Baselga J Phase I study of the humanized antiepidermal growth factor receptor monoclonal antibody EMD72000 in patients with advanced solid tumors that express the epidermal growth factor receptor. J Clin Oncol 22:175-184 (2004)

44. Socinski MA Antibodies to the epidermal growth factor receptor in non small cell lung cancer: current status of matuzumab and panitumumab. Clin Cancer Res 13:4597-4601 (2007)

45. Vallbohmer D, Lenz HJ Epidermal growth factor receptor as a target for chemotherapy. Clin Colorectal Cancer 5:19-27 (2005)

46. Graeven U, Kremer B, Sudhoff T, Killing B, Rojo F, Weber D, Tillner J, Unal C, Schmiegel W Phase I study of the humanised anti-EGFR monoclonal

antibody matuzumab (EMD 72000) combined with gemcitabine in advanced pancreatic cancer. Br J Cancer 94:1293-1299 (2006)

47. Derendorf H, Gramatté T, Schäfer HG Pharmakokinetik. 2 ed. Wissenschaftliche Verlagsgesellschaft mbH, Stuttgart (2002)

48. Aarons L Population pharmacokinetics: theory and practice. Br J Clin Pharmacol 32:669-670 (1991)

49. FDA Guidance for Industry: Population Pharmacokinetics (1999)

50. EMEA Guideline on reporting the results of population pharmacokinetic analyses (2007)

51. Sheiner LB, Beal SL Evaluation of methods for estimating population pharmacokinetics parameters. I. Michaelis-Menten model: routine clinical pharmacokinetic data. J Pharmacokinet Biopharm 8:553-571 (1980)

52. Sheiner BL, Beal SL Evaluation of methods for estimating population pharmacokinetic parameters. II. Biexponential model and experimental pharmacokinetic data. J Pharmacokinet Biopharm 9:635-651 (1981)

53. Sheiner LB, Beal SL Evaluation of methods for estimating population pharmacokinetic parameters. III. Monoexponential model: routine clinical pharmacokinetic data. J Pharmacokinet Biopharm 11:303-319 (1983)

54. Plock N, Buerger C, Joukhadar C, Kljucar S, Kloft C Does linezolid inhibit its own metabolism? Population pharmacokinetics as a tool to explain the observed nonlinearity in both healthy volunteers and septic patients. Drug Metab Dispos 35:1816-1823 (2007)

55. Fliss G, Staab A, Tillmann C, Trommeshauser D, Schaefer HG, Kloft C Population Pharmacokinetic Data Analysis of Cilobradine, an I(f) Channel Blocker. Pharm Res 25:359-368 (2008)

56. Dartois C, Brendel K, Comets E, Laffont CM, Laveille C, Tranchand B, Mentre F, Lemenuel-Diot A, Girard P Overview of model-building strategies in population PK/PD analyses: 2002-2004 literature survey. Br J Clin Pharmacol 64:603-612 (2007)

57. Dirks NL, Nolting A, Kovar A, Meibohm B Population pharmacokinetics of cetuximab in patients with squamous cell carcinoma of the head and neck. J Clin Pharmacol 48:267-278 (2008)

58. Lehr T, Staab A, Tillmann C, Trommeshauser D, Raschig A, Schaefer HG, Kloft C Population pharmacokinetic modelling of NS2330 (tesofensine) and its

major metabolite in patients with Alzheimer's disease. Br J Clin Pharmacol 64:36-48 (2007)

59. Vozeh S, Steimer JL, Rowland M, Morselli P, Mentre F, Balant LP, Aarons L The use of population pharmacokinetics in drug development. Clin Pharmacokinet 30:81-93 (1996)

60. Aarons L, Karlsson MO, Mentre F, Rombout F, Steimer JL, van Peer A Role of modelling and simulation in Phase I drug development. Eur J Pharm Sci 13:115-122 (2001)

61. Holford NH, Kimko HC, Monteleone JP, Peck CC Simulation of clinical trials. Annu Rev Pharmacol Toxicol 40:209-234 (2000)

62. Sheiner LB, Steimer JL Pharmacokinetic/pharmacodynamic modeling in drug development. Annu Rev Pharmacol Toxicol 40:67-95 (2000)

63. Sheiner LB, Beal SL Bayesian individualization of pharmacokinetics: simple implementation and comparison with non-Bayesian methods. J Pharm Sci 71:1344-1348 (1982)

64. Sun H, Fadiran EO, Jones CD, Lesko L, Huang SM, Higgins K, Hu C, Machado S, Maldonado S, Williams R, Hossain M, Ette EI Population pharmacokinetics. A regulatory perspective. Clin Pharmacokinet 37:41-58 (1999)

65. Sheiner LB, Beal S, Rosenberg B, Marathe VV Forecasting individual pharmacokinetics. Clin Pharmacol Ther 26:294-305 (1979)

66. Grasela TH, Sheiner BL Pharmacostatistical modeling for observational data. J Pharmacokinet Biopharm: 19:25-36 (1991)

67. Racine-Poon A, Wakefield J Statistical methods for population pharmacokinetic modelling. Stat Methods Med Res 7:63-84 (1998)

68. Wahlby U, Matolcsi K, Karlsson MO, Jonsson EN Evaluation of type I error rates when modeling ordered categorical data in NONMEM. J Pharmacokinet Pharmacodyn 31:61-74 (2004)

69. Aarons L, Balant LP, Mentre F, Morselli PL, Rowland M, Steimer JL, Vozeh S Population approaches in drug development. Report on an expert meeting to discuss population pharmacokinetic/pharmacodynamic software. Eur J Clin Pharmacol 46:389-391 (1994)

70. Aarons L Software for population pharmacokinetics and pharmacodynamics. Clin Pharmacokinet 36:255-264 (1999)

71. Kloft C, Graefe EU, Tanswell P, Scott AM, Hofheinz R, Amelsberg A, Karlsson MO Population pharmacokinetics of sibrotuzumab, a novel therapeutic monoclonal antibody, in cancer patients. Invest New Drugs 22:39-52 (2004)

72. DeSilva B, Smith W, Weiner R, Kelley M, Smolec J, Lee B, Khan M, Tacey R, Hill H, Celniker A Recommendations for the bioanalytical method validation of ligand-binding assays to support pharmacokinetic assessments of macromolecules. Pharm Res 20:1885-1900 (2003)

73. Janmahasatian S, Duffull SB, Ash S, Ward LC, Byrne NM, Green B Quantification of lean bodyweight. Clin Pharmacokinet 44:1051-1065 (2005)

74. Cockcroft DW, Gault MH Prediction of creatinine clearance from serum creatinine. Nephron 16:31-41 (1976)

75. Du Bois D, Du Bois EF A formula to estimate the approximate surface area if height and weight be known. Arch Intern Med 17:863-871 (1916)

76. Wood AM, White IR, Thompson SG Are missing outcome data adequately handled? A review of published randomized controlled trials in major medical journals. Clin Trials 1:368-376 (2004)

77. Beal SL, Sheiner BL NONMEM Users Guide. San Fransicso, CA: NONMEM project group, University of California (1998)

78. Sheiner LB Analysis of pharmacokinetic data using parametric models--1: Regression models. J Pharmacokinet Biopharm 12:93-117 (1984)

79. Plock N Target Site Pharmacokinetics of Antiinfectives in the Treatment of Serious Grampositive Infections - Linezolid and Vancomyzin. 1 ed. WiKu-Verlag Verlag für Wissenschaft und Kultur, Köln (2007)

80. Mandema JW, Verotta D, Sheiner LB Building population pharmacokinetic--pharmacodynamic models. I. Models for covariate effects. J Pharmacokinet Biopharm 20:511-528 (1992)

81. Jonsson EN, Karlsson MO Xpose--an S-PLUS based population pharmacokinetic/pharmacodynamic model building aid for NONMEM. Comput Methods Programs Biomed 58:51-64 (1999)

82. Pan W Akaike's information criterion in generalized estimating equations. Biometrics 57:120-125 (2001)

83. Jonsson EN, Karlsson MO Xpose 2.0 User's Manual. Department of Pharmacy, Uppsala University, Sweden (1998)

84. Jonsson EN, Karlsson MO Automated covariate model building within NONMEM. Pharm Res 15:1463-1468 (1998)

85. Maitre PO, Buhrer M, Thomson D, Stanski DR A three-step approach combining Bayesian regression and NONMEM population analysis: application to midazolam. J Pharmacokinet Biopharm 19:377-384 (1991)

86. Kowalski KG, Hutmacher MM Design evaluation for a population pharmacokinetic study using clinical trial simulations: a case study. Stat Med 20:75-91 (2001)

87. Bonate PL Pharmacokinetic-Pharmacodynamic Modeling and Simulation. 1 ed. Springer Science and Business Media, New York (2006)

88. Brendel K, Dartois C, Comets E, Lemenuel-Diot A, Laveille C, Tranchand B, Girard P, Laffont CM, Mentre F Are population pharmacokinetic and/or pharmacodynamic models adequately evaluated? A survey of the literature from 2002 to 2004. Clin Pharmacokinet 46:221-234 (2007)

89. Akins RB, Tolson H, Cole BR Stability of response characteristics of a Delphi panel: application of bootstrap data expansion. BMC Med Res Methodol 5:37 (2005)

90. Efron B Bootstrap methods: Another look at the jackknife. Ann Stat 7:1-26 (1979)

91. Post TM, Freijer JI, Ploeger BA, Danhof M Extensions to the Visual Predictive Check to facilitate model performance evaluation. J Pharmacokinet Pharmacodyn 35:185-202 (2008)

92. Holford N The Visual Predictive Check - Superiority to Standard Diagnostics (Rorschach) Plots. PAGE 14, Abstr 738. Available from www.page-meeting.org/?abstract=972 [Accessed 2008 May 20]. (2005)

93. Ette EI Stability and performance of a population pharmacokinetic model. J Clin Pharmacol 37:486-495 (1997)

94. Holford NH Wings for NOMEM. Available from URL: http://wfn.sourceforge.net/ [Accessed 2008 May 13] (2003)

95. Lindbom L, Pihlgren P, Jonsson EN PsN-Toolkit--a collection of computer intensive statistical methods for non-linear mixed effect modeling using NONMEM. Comput Methods Programs Biomed 79:241-257 (2005)

96. Wang HM, Jones MP, Storer BE Comparison of case-deletion diagnostic methods for Cox regression. Stat Med 25:669-683 (2006)

97. FDA Bioanalytical Method Validation. Guidance for Industry. (2001)

98. Yano Y, Beal SL, Sheiner LB Evaluating pharmacokinetic/pharmacodynamic models using the posterior predictive check. J Pharmacokinet Pharmacodyn 28:171-192 (2001)

99. Van Buskirk P Saving corporations milliones:The benefits of modeling. PC AI 14:38 (2000)

100. Green B, Duffull SB What is the best size descriptor to use for pharmacokinetic studies in the obese? Br J Clin Pharmacol 58:119-133 (2004)

101. Sparreboom A, Wolff AC, Mathijssen RH, Chatelut E, Rowinsky EK, Verweij J, Baker SD Evaluation of alternate size descriptors for dose calculation of anticancer drugs in the obese. J Clin Oncol 25:4707-4713 (2007)

102. Holford NH A size standard for pharmacokinetics. Clin Pharmacokinet 30:329-332 (1996)

103. Mould DR, Davis CB, Minthorn EA, Kwok DC, Elliott MJ, Luggen ME, Totoritis MC A population pharmacokinetic-pharmacodynamic analysis of single doses of clenoliximab in patients with rheumatoid arthritis. Clin Pharmacol Ther 66:246-257 (1999)

104. Ng CM, Bruno R, Combs D, Davies B Population pharmacokinetics of rituximab (anti-CD20 monoclonal antibody) in rheumatoid arthritis patients during a phase II clinical trial. J Clin Pharmacol 45:792-801 (2005)

105. Morell A, Terry WD, Waldmann TA Metabolic properties of IgG subclasses in man. J Clin Invest 49:673-680 (1970)

106. Koleba T, Ensom MH Pharmacokinetics of intravenous immunoglobulin: a systematic review. Pharmacotherapy 26:813-827 (2006)

107. Kovarik JM, Nashan B, Neuhaus P, Clavien PA, Gerbeau C, Hall ML, Korn A A population pharmacokinetic screen to identify demographic-clinical covariates of basiliximab in liver transplantation. Clin Pharmacol Ther 69:201-209 (2001)

108. Brambell FW, Hemmings WA, Morris IG A Theoretical Model of Gamma-Globulin Catabolism. Nature 203:1352-1354 (1964)

109. Lee H, Kimko HC, Rogge M, Wang D, Nestorov I, Peck CC Population pharmacokinetic and pharmacodynamic modeling of etanercept using logistic regression analysis. Clin Pharmacol Ther 73:348-365 (2003)

110. Karlsson MO, Sheiner LB The importance of modeling interoccasion variability in population pharmacokinetic analyses. J Pharmacokinet Biopharm 21:735-750 (1993)

111. Zhou H, Jang H, Fleischmann RM, Bouman-Thio E, Xu Z, Marini JC, Pendley C, Jiao Q, Shankar G, Marciniak SJ, Cohen SB, Rahman MU, Baker D, Mascelli MA, Davis HM, Everitt DE Pharmacokinetics and safety of golimumab, a fully human anti-TNF-alpha monoclonal antibody, in subjects with rheumatoid arthritis. J Clin Pharmacol 47:383-396 (2007)

112. Powis G, Reece P, Ahmann DL, Ingle JN Effect of body weight on the pharmacokinetics of cyclophosphamide in breast cancer patients. Cancer Chemother Pharmacol 20:219-222 (1987)

113. Lind MJ, Margison JM, Cerny T, Thatcher N, Wilkinson PM Prolongation of ifosfamide elimination half-life in obese patients due to altered drug distribution. Cancer Chemother Pharmacol 25:139-142 (1989)

114. Rodvold KA, Rushing DA, Tewksbury DA Doxorubicin clearance in the obese. J Clin Oncol 6:1321-1327 (1988)

115. Morgan DJ, Bray KM Lean body mass as a predictor of drug dosage. Implications for drug therapy. Clin Pharmacokinet 26:292-307 (1994)

116. Roubenoff R, Kehayias JJ The meaning and measurement of lean body mass. Nutr Rev 49:163-175 (1991)

117. Bulitta JB, Duffull SB, Kinzig-Schippers M, Holzgrabe U, Stephan U, Drusano GL, Sorgel F Systematic comparison of the population pharmacokinetics and pharmacodynamics of piperacillin in cystic fibrosis patients and healthy volunteers. Antimicrob Agents Chemother 51:2497-2507 (2007)

118. Mathijssen RH, Verweij J, de Jonge MJ, Nooter K, Stoter G, Sparreboom A Impact of body-size measures on irinotecan clearance: alternative dosing recommendations. J Clin Oncol 20:81-87 (2002)

119. Han PY, Duffull SB, Kirkpatrick CM, Green B Dosing in obesity: a simple solution to a big problem. Clin Pharmacol Ther 82:505-508 (2007)

120. Anderson BJ, Holford NH Mechanism-based concepts of size and maturity in pharmacokinetics. Annu Rev Pharmacol Toxicol 48:303-332 (2008)

121. Bouillon T, Shafer SL Does size matter? Anesthesiology 89:557-560 (1998)

122. Anastasio P, Spitali L, Frangiosa A, Molino D, Stellato D, Cirillo E, Pollastro RM, Capodicasa L, Sepe J, Federico P, Gaspare De Santo N Glomerular

filtration rate in severely overweight normotensive humans. Am J Kidney Dis 35:1144-1148 (2000)

123. Mathijssen R, Sparreboom A Influence of Lean Body Weight on Anticancer Drug Clearance. Clin Pharmacol Ther (2008)

124. West GB, Brown JH, Enquist BJ A general model for the origin of allometric scaling laws in biology. Science 276:122-126 (1997)

125. Sun YN, Lu JF, Joshi A, Compton P, Kwon P, Bruno RA Population pharmacokinetics of efalizumab (humanized monoclonal anti-CD11a antibody) following long-term subcutaneous weekly dosing in psoriasis subjects. J Clin Pharmacol 45:468-476 (2005)

126. Fang L, Holford NH, Hinkle G, Cao X, Xiao JJ, Bloomston M, Gibbs S, Saif OH, Dalton JT, Chan KK, Schlom J, Martin EW, Jr., Sun D Population pharmacokinetics of humanized monoclonal antibody HuCC49deltaCH2 and murine antibody CC49 in colorectal cancer patients. J Clin Pharmacol 47:227-237 (2007)

127. Sawyer M, Ratain MJ Body surface area as a determinant of pharmacokinetics and drug dosing. Invest New Drugs 19:171-177 (2001)

128. de Jongh FE, Verweij J, Loos WJ, de Wit R, de Jonge MJ, Planting AS, Nooter K, Stoter G, Sparreboom A Body-surface area-based dosing does not increase accuracy of predicting cisplatin exposure. J Clin Oncol 19:3733-3739 (2001)

129. Mathijssen RH, de Jong FA, Loos WJ, van der Bol JM, Verweij J, Sparreboom A Flat-fixed dosing versus body surface area based dosing of anticancer drugs in adults: does it make a difference? Oncologist 12:913-923 (2007)

130. Grochow LB, Baraldi C, Noe D Is dose normalization to weight or body surface area useful in adults? J Natl Cancer Inst 82:323-325 (1990)

131. Hempel G, Boos J Flat-fixed dosing versus body surface area based dosing of anticancer drugs: there is a difference. Oncologist 12:924-926 (2007)

132. Ette EI, Williams PJ, Kim YH, Lane JR, Liu MJ, Capparelli EV Model appropriateness and population pharmacokinetic modeling. J Clin Pharmacol 43:610-623 (2003)

133. Mentre F, Escolano S Prediction discrepancies for the evaluation of nonlinear mixed-effects models. J Pharmacokinet Pharmacodyn 33:345-367 (2006)

134. Ng CM, Lum BL, Gimenez V, Kelsey S, Allison D Rationale for fixed dosing of pertuzumab in cancer patients based on population pharmacokinetic analysis. Pharm Res 23:1275-1284 (2006)

135. Gallo JM, Laub PB, Rowinsky EK, Grochow LB, Baker SD Population pharmacokinetic model for topotecan derived from phase I clinical trials. J Clin Oncol 18:2459-2467 (2000)

136. Hing JP, Piotrovsky V, Kimko H, Brashear HR, Zhao Q Pharmacokinetic simulation for switching from galantamine immediate-release to extended-release formulation. Curr Med Res Opin 21:483-488 (2005)

137. Rombout F, Aarons L, Karlsson M, Man A, Mentre F, Nygren P, Racine A, Schaefer H, Steimer JL, Troconiz I, van Peer A Modelling and simulation in the development and use of anti-cancer agents: an underused tool? J Pharmacokinet Pharmacodyn 31:419-440 (2004)

138. Bauer RJ, Guzy S, Ng C A survey of population analysis methods and software for complex pharmacokinetic and pharmacodynamic models with examples. AAPS J 9:E60-83 (2007)

139. Dingemanse J, Appel-Dingemanse S Integrated pharmacokinetics and pharmacodynamics in drug development. Clin Pharmacokinet 46:713-737 (2007)

140. Gieschke R, Steimer JL Pharmacometrics: modelling and simulation tools to improve decision making in clinical drug development. Eur J Drug Metab Pharmacokinet 25:49-58 (2000)

141. Anderson BJ, Allegaert K, Holford NH Population clinical pharmacology of children: general principles. Eur J Pediatr 165:741-746 (2006)

142. Hortobagyi GN Overview of treatment results with trastuzumab (Herceptin) in metastatic breast cancer. Semin Oncol 28:43-47 (2001)

143. Kloft C, Wallin J, Henningsson A, Chatelut E, Karlsson MO Population pharmacokinetic-pharmacodynamic model for neutropenia with patient subgroup identification: comparison across anticancer drugs. Clin Cancer Res 12:5481-5490 (2006)

144. Lobo ED, Hansen RJ, Balthasar JP Antibody pharmacokinetics and pharmacodynamics. J Pharm Sci 93:2645-2668 (2004)

145. Ghetie V, Popov S, Borvak J, Radu C, Matesoi D, Medesan C, Ober RJ, Ward ES Increasing the serum persistence of an IgG fragment by random mutagenesis. Nat Biotechnol 15:637-640 (1997)

146. Ette EI, Williams PJ Pharmacometrics: The Science of Quantitative Pharmacology. 1 ed. John Wiley & Sons, Inc., Hoboken, New Jersey (2007)

147. von Kleist M, Huisinga W Physiologically based pharmacokinetic modelling: a sub-compartmentalized model of tissue distribution. J Pharmacokinet Pharmacodyn 34:789-806 (2007)

148. Theil FP, Guentert TW, Haddad S, Poulin P Utility of physiologically based pharmacokinetic models to drug development and rational drug discovery candidate selection. Toxicol Lett 138:29-49 (2003)

149. Jones HM, Parrott N, Jorga K, Lave T A novel strategy for physiologically based predictions of human pharmacokinetics. Clin Pharmacokinet 45:511-542 (2006)

150. Parrott N, Paquereau N, Coassolo P, Lave T An evaluation of the utility of physiologically based models of pharmacokinetics in early drug discovery. J Pharm Sci 94:2327-2343 (2005)

151. Grass GM, Sinko PJ Physiologically-based pharmacokinetic simulation modelling. Adv Drug Deliv Rev 54:433-451 (2002)

152. Blesch KS, Gieschke R, Tsukamoto Y, Reigner BG, Burger HU, Steimer JL Clinical pharmacokinetic/pharmacodynamic and physiologically based pharmacokinetic modeling in new drug development: the capecitabine experience. Invest New Drugs 21:195-223 (2003)

9 Curriculum Vitae

Name	Katharina Küster
Date of birth	16 January 1979
Place of birth	Bremen
Nationality	German

Education and Qualifications

10/2004 – 11/2008	Doctoral thesis under the supervision of Prof. Charlotte Kloft Department Clinical Pharmacy, Freie Universität Berlin and Martin-Luther-Universität Halle-Wittenberg *'Population Pharmacokinetic Analysis for the Therapeutic anti-EGFR Humanised Monoclonal Antibody Matuzumab'*
08/2004	Registration as a pharmacist in Germany
04/1999 – 05/2003	Degree in Pharmacy (2. Staatsexamen: 1.5) Christian-Albrechts-Universität Kiel, Germany
08/1991 – 06/1998	High school degree (Allgemeine Hochschulreife) Gymnasium an der Max-Planck-Strasse, Delmenhorst, Germany

Professional Experience

04/2007 – 11/2008	Employment as pharmacist • Nord-Apotheke, Berlin, Germany
10/2006 – 04/2007	Employment as pharmacist • Cornelia-Apotheke, Berlin, Germany
04/2005 – 10/2006	Employment as pharmacist • Apotheke im Ring-Center, Berlin, Germany
10/2004 – 03/2005	Employment as pharmacist • Kurfürsten-Apotheke, Berlin, Germany
01/2004 – 06/2004	Pre-registration pharmacist • Heidemarkt-Apotheke, München, Germany
07/2003 – 12/2003	Pre-registration pharmacist • Research project (Phase II metabolism) under the supervision of Prof. Margaret O. James, College of Pharmacy, University of Florida, USA

Awards/Grants

06/2008	Travel award Population Approach Group Europe
06/2007	Travel award Population Approach Group Europe

Member of Scientific Societies

German Pharmaceutical Society (DPhG)
German Cancer Society (DKG)

10 Publications

Original papers

K. Kuester, A. Kovar, C. Lüpfert, B. Brockhaus, C. Kloft
Population pharmacokinetic data analysis of three phase I studies of matuzumab, a humanised anti-EGFR monoclonal antibody in clinical cancer development.
Br J Cancer., 2008; 98(5): 900-906.

K. Kuester, A. Kovar, C. Lüpfert, B. Brockhaus, C. Kloft
Refinement of the population pharmacokinetic model for the monoclonal antibody matuzumab: external model evaluation and simulations.
Clin Pharmacokinet., accepted (2008).

B. Krippendorff, **K. Kuester**, C. Kloft, W. Huisinga
Nonlinear pharmacokinetics of therapeutic proteins resulting from receptor mediated endocytosis.
J Pharmacokinet Pharmacodyn., submitted 2008.

K. Kuester, A. Kovar, C. Lüpfert, B. Brockhaus, C. Kloft
Population pharmacokinetic evaluation techniques for a monoclonal antibody in clinical development for cancer therapy.
In manuscript.

K. Kuester and C. Kloft
Body size descriptors in population pharmacokinetic analyses for monoclonal antibodies.
In preparation.

Book chapter

K. Kuester, C. Kloft.
Pharmacokinetics of monoclonal antibodies.
In: B. Meibohm (Hrsg.): Pharmacokinetics and pharmacodynamics of biotech drugs, Wiley-VCH Verlag, Weinheim: 45-91(2006).

Oral and poster presentations

K. Kuester, J. Tillner, B. Brockhaus, A. Kovar, C. Kloft. (Poster)
Population pharmacokinetic approach for matuzumab – a humanised monoclonal antibody.
Annual Meeting of the German Pharmaceutical Society (DPhG) 2005, Mainz, 05.-08.10.2005. Abstract book 94 (2005).

K. Kuester, A. Kovar, B. Brockhaus, C. Kloft. (Poster)
Population pharmacokinetic analysis for matuzumab (EMD 72000) – a humanised EGFR-targeted monoclonal antibody.
15th Annual Meeting Population Approach Group Europe (PAGE), Brugge, Belgium, 14.-16.06.2006. Abstract book 971 (2006) [www.page-meeting.org/?abstract=971].
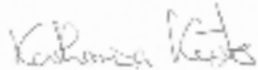
N. Plock, C. Buerger, **K. Kuester**, C. Joukhadar, S. Kljucar, C. Kloft. (Poster)
A population pharmacokinetic model for the simultaneous description of linezolid tissue and plasma disposition in healthy volunteers and septic patients.
15th Annual Meeting Population Approach Group Europe (PAGE), Brügge, Belgien, 14.-16.06.2006. Abstract book 886 (2006) [www.page-meeting.org/?abstract=886].

K. Kuester, A. Kovar, B. Brockhaus, C. Kloft. (Poster)
Matuzumab – a population pharmacokinetic analysis.
Annual Meeting of the German Pharmaceutical Society (DPhG) 2006, Marburg, 04.-07.10.2006. Abstract book 95 (2006).

K. Kuester, A. Kovar, B. Brockhaus, C. Kloft. (Presentation)
A population pharmacokinetic model for the monoclonal antibody matuzumab.
Pre-Satellite Meeting of the 3rd Pharmaceutical Sciences World Congress (PSWC), Amsterdam, The Netherlands, 20.-21.04.2007. Abstract book 26 (2007) [http://www.parthen-impact.com/eventure/publicAbstractView.do?id=32252].

K. Kuester, A. Kovar, B. Brockhaus, C. Kloft. (Poster)
A population pharmacokinetic model for the monoclonal antibody matuzumab.
3rd Pharmaceutical Sciences World Congress (PSWC), Amsterdam, The Netherlands, 22.-25.04.2007. Abstract book 48 (2007) [www.parthen-impact.com/eventure/publicAbstractView.do?id=32255].

K. Kuester, A. Kovar, B. Brockhaus, C. Kloft. (Poster)
Matuzumab – a population pharmacokinetic model and its evaluation.
16th Annual Meeting Population Approach Group Europe (PAGE), Copenhagen, Denmark, 13.-15.06.2007. Abstract book (2007) [www.page-meeting.org/?abstract=1090].

K. Kuester, A. Kovar, C. Lüpfert, B. Brockhaus, C. Kloft. (Poster)
Population pharmacokinetics of matuzumab – a monoclonal antibody with complex elimination.
Annual Meeting of the German Pharmaceutical Society (DPhG) 2007, Erlangen, 10.-13.10.2007. Abstract book 50 (2007).

K. Kuester, A. Kovar, C. Lüpfert, B. Brockhaus, C. Kloft. (Poster)
The pharmacokinetics of matuzumab – a novel monoclonal antibody.
28th Annual German Cancer Congress, Berlin, 20.-23.02.2008. Proceedings Journal 136 (2008).

K. Kuester, A. Kovar, C. Lüpfert, B. Brockhaus, C. Kloft. (Poster)
Matuzumab – evaluation of the population pharmacokinetic model and analyses of the covariate impact on the pharmacokinetic profile.
17th Annual Meeting Population Approach Group Europe (PAGE), Marseille, France, 18.-20.06.2008. [www.page-meeting.org/?abstract=1244] (2008).

K. Kuester, A. Kovar, C. Lüpfert, B. Brockhaus, C. Kloft. (Poster)
Population pharmacokinetic model for matuzumab – evaluation and simulation.
Annual Meeting of the German Pharmaceutical Society (DPhG) 2008, Bonn, 08.-11.10.2008. Abstract book 277 (2008).

Eidesstaatliche Erklärung

Hiermit erkläre ich, dass ich mich mit der vorliegenden Dissertation erstmals um die Erlangung eines Doktorgrades bewerbe.

Ferner erkläre ich, dass ich die vorliegende Arbeit selbständig und ohne fremde Hilfe angefertigt, andere als die von mir angegebenen Quellen und Hilfsmittel nicht benutzt und die den verwendeten Werken wörtlich oder inhaltlich entnommenen Stellen als solche kenntlich gemacht habe.

Halle, 30.01.2009

Katharina Küster